

BLAST FURNACE OIL INJECTION.

by

Anthony G. Storey

A thesis submitted to the Faculty of Graduate Studies and
Research in partial fulfillment of the requirements for
the degree of Master of Science.

Department of Mining & Metallurgical Eng.,
McGill University,
Montreal, Canada.

August, 1973.

ABSTRACT.

The optimisation of the process of oil injection was studied, using Mobilwax 2305 as a 'substitute fluid' for Bunker 'C' Oil. Injection of this molten wax into high velocity air streams was effected using two types of lances, one where there was no atomisation prior to injection (simple or straight-through nozzle), and one where primary atomisation was achieved by a two-spiral corkscrew inserted into the lance (corkscrew nozzle).

It was seen that the particle mean diameter of the wax spray was smaller with injection through the corkscrew nozzle at all air velocities, but injection of wax through both nozzles into an air stream of 450 feet per second velocity produced particles of sufficiently small diameter as to effect efficient combustion.

Also, the importance of injection angle and fluid flow rate were examined. It was found that an angle of injection of 15° gave the best results for injection through both types of lance, and that at the higher air stream velocities, the flow rate of the fluid was not critical in producing a uniform droplet size.

Finally, with a knowledge of the particle mean diameter of the wax at any air stream velocity, particle trajectories within the blow pipe were computed.

RÉSUMÉ

L'optimisation du procédé d'injection d'huile a été étudié en utilisant la cire Mobil 2305 comme "fluide de substitution" à l'huile Bunker 'C'. L'injection de cette cire liquide dans les courants d'air à vitesse élevée a été effectuée à l'aide de deux lances, l'une ne produisant pas d'atomisation avant injection (buse directe - ou simple), l'autre réalisant une atomisation préalable grâce à un tire-bouchon à deux spirales inséré dans la lance (buse tire-bouchon)

On a observé que le diamètre moyen des particules de cire vapourée est plus petit lorsque l'injection est réalisée avec la buse tire-bouchon, quelle que soit la vitesse de l'air. Cependant, pour la courant d'air de 150 m/s., les particules sont d'un diamètre suffisamment petit pour qu'une combustion efficace soit réalisée, que l'une ou l'autre des buses soit employée.

L'importance de l'angle d'injection du fluide et de sa vitesse d'écoulement a également été déterminée. On a observé que les meilleures performances étaient réalisées sous un angle de 15° , pour les deux types de lance, et qu'aux plus hautes vitesses de l'air, l'uniformité de la taille des gouttelettes ne dépendait pas de la vitesse d'écoulement.

Finalement, la connaissance du diamètre moyen des particules en fonction de la vitesse de l'air a permis de calculer les trajectoires des particules à l'intérieur de la conduite d'air.

ACKNOWLEDGEMENTS.

I should like to take this opportunity to thank Professor R.I.L. Guthrie for his constant encouragement and assistance throughout this work.

Thanks are due to Professor W.M. Williams, Chairman of the Department of Mining & Metallurgical Engineering, Professor J.G. Gruzleski and other staff and students, particularly Mr. M. Knoepfel, Mr. G. Deep and Mr. H. Henein.

I extend my gratitude to Wayne Edwards, who assisted me in the experimental work, and to my wife Alison, who tempered my imagination with much needed common sense.

TABLE OF CONTENTS.

Chapter 1. Introduction.

1.1 Problem Facing Blast Furnace Operators.	1
1.2 What is Fuel Injection.	1
1.3 Historical Review of Fuel Injection, 1800-1956.	2
1.4 Review of Work from 1957 to the Present.	3
1.5 Problems Associated with Fuel Oil Injection.	4
1.6 Previous Work.	4
1.7 Atomisation of Fuel Oil for Combustion.	5
1.8 Combustion of Fuels.	6
1.9 Present Work.	7

Chapter 2. The Art and Practice of Fuel Injection.

2.0 Introduction.	9
2.1 Reasons for Injecting Fuel into the Blast Furnace.	9
2.2 Limits to the Rate of Fuel Oil Injection.	10
2.3 Fuels Injected into the Blast Furnace.	11
2.4 Means of Injecting Fuel into the Blast Furnace.	18
2.5 Future Trends in Fuel Injection.	21

Chapter 3. Combustion.

3.0 Introduction.	23
3.1 Mechanisms of Combustion.	23
3.2 Previous Work on Combustion of Oil Droplets.	24
3.3 Combustion with Pressure Atomisation.	27

3.4 Combustion with Twin-Fluid Atomisation.	27
3.5 Combustion of Fuel Oil in Blast Furnaces.	28

Chapter 4. Atomisation.

4.0 Introduction.	30
4.1 Pressure Atomisation.	30
4.2 Pneumatic Atomisers (or Twin-Fluid Atomisers).	31
4.3 Theory of Atomisation.	32
4.4 Atomisation in an Air Stream.	34

Chapter 5. Injection of Wax into Still Air.

5.0 Introduction.	38
5.1 Theory of Nozzle Design.	38
5.2 Investigation of Initial Nozzle Design.	39
5.3 Current Nozzle Design.	39
5.4 Modelling - Experimental Apparatus for Still Air Atomisation Studies.	40
5.5 Droplet Size Analysis of Water Injection.	41
5.6 Injection of Molten Wax into Still Air.	41
5.7 Analysis of Wax Spray.	43
5.8 Droplet Size Analysis.	44
5.9 Experimental Results and Discussion of Results.	44
5.9.1 Nozzle Spray Characteristics.	44
5.9.2 Determination of Flow Rates and Cone Angle as a Function of Injection Pressure.	45
5.9.3 Drop Size Analysis of Wax Particles.	47

5.9.4 Drop Size as a Function of Flow Rate.	49
5.9.5 Drop Size as a Function of Viscosity.	50
5.9.6 Drop Size Distribution of the Spray.	51
5.9.7 Reproducibility of Results.	52
5.10 Effectiveness of Wax for Injection Studies.	52

Chapter 6. Injection of Molten Wax into High Velocity Air Streams.

6.0 Introduction.	54
6.1 Experimental Modelling of Blast Furnace Blow Pipe.	54
6.2 Experimental Technique for Injection into High Velocity Air Streams.	55
6.2.1 Measurement of Air Velocity.	55
6.2.2 Water Injection into High Velocity Air Streams.	57
6.2.3 Wax Injection into High Velocity Air Streams.	57
6.2.4 Particle Collection after Injection.	60
6.2.5 Particle Sizes and Calculation on Particle Mean Diameter.	60
6.3 Experimental Results and Discussion of Results.	61
6.3.1 Photographic Study of Water Injection into High Velocity Air Streams.	61
6.3.2 Spray Sheet Velocity.	64
6.3.3 Injection of Molten Wax into High Velocity Air Streams.	66
6.3.4 Spray Distribution and Spray Pattern.	75
6.3.5 Distribution of Particle Sizes.	78
6.3.6 Particle Trajectories.	79

6.4 Optimum Conditions for Blast Furnace Oil Injection.

81

Chapter 7. Conclusions.

84

Appendix.

Chapter 1

INTRODUCTION.

INTRODUCTION.

1.1 PROBLEM FACING BLAST FURNACE OPERATORS.

Owing to the relative scarcity and cost of good coking coals, it has been a constant objective of blast furnace operators to minimise the amount of coke required to reduce iron oxide to iron. Early solutions were to preheat the incoming air blast to the furnace by burning the off-gases in a heat exchange system (Cowper Stoves), and to use uniformly sized burdens.

Since the early 1950's, this quest for decreased coke rates has been stepped up and current blast furnace practice can now include:

- (a) Improved burden preparation
- (b) High top pressure
- (c) Increased blast temperature
- (d) Humidity control of the blast
- (e) Oxygen enrichment of the blast
- (f) Fuel injection at the tuyeres.

All these procedures have been tried and have been successful to varying degrees in lowering coke rates. Each has been the subject of extensive investigation, and undoubtedly will continue to be so. The work presently described is concerned with fuel injection at the tuyeres (item f). Items (c), (d), and (e) are however generally associated with fuel injection and are discussed where appropriate.

1.2 WHAT IS FUEL INJECTION.

Simply stated, it is the practice of introducing a hydrocarbon fuel into the tuyere region of the blast furnace, where the fuel

combusts to form the reducing gases, CO and H_2 , (with the hot air blast).

The types of fuel that have been injected into the blast furnace include tar, pitch, heavy and light fuel oils, natural gas and coke-oven gas.

1.3 HISTORICAL REVIEW OF FUEL INJECTION, 1800-1956.

The concept of fuel injection is not new. During the nineteenth century, at least two British patents were issued on this topic, one to Barnett (1) in 1838, who suggested the injection of gaseous hydrocarbons and tar as a means of reducing the coke rate, and one to Banks, who favoured the injection of solid fuels.

Other early patents of note are those of Weber (2) in 1885 and Fleming (3) in 1934.

Spasmodic attempts to inject fuel into the blast furnace were made throughout the 1940's and early 1950's. Coche (4), in a historical review, lists trials in France in 1947, where 80 kgs. of fuel oil/NTHM were injected into the tuyere region, trials in the Soviet Union in 1948, where powdered coal was used as the injectant, and trials at the Lone Star Steel Company in 1951, in the U.S.A., where natural gas was injected. All were unsuccessful due to:

- (a) Too low an air blast temperature
- (b) Incomplete combustion of the fuel, giving rise to soot formation
- (c) Inexperience and lack of expertise.

1.4 REVIEW OF WORK FROM 1957 TO THE PRESENT.

During this period, renewed investigations of fuel injection were undertaken. The first of these were in 1957 in France, where reformed fuel oil (i.e. CO and H₂) was injected into the tuyere region of the furnace. The experimenters first conducted their trials with natural gas due to the relative ease of introduction of the gas, into the main air blast, and the subsequent good mixing of both gaseous mediums, prior to combustion. Such trials were conducted at the Bureau of Mines Experimental Furnace at Bruceton, Penn. in 1957. The following year, similar trials were conducted both at Bruceton, and at Ougree, in Belgium, where fuel oil was injected. Reports of these trials are well documented (5-11). In 1961, Dominion Foundries and Steel Company Limited (Dofasco), in Hamilton, Canada, in conjunction with Imperial Oil, were the first operators in North America to use oil injection on full-scale furnaces (12), while the year previously, France had some ten blast furnaces using fuel oil as a replacement fuel. The practice of fuel injection grew rapidly and today about 70-75% of all North American furnaces use some form of fuel injection (see Fig. 1).

Advancing technology has also enabled current maximum oil rates of approximately 250 lbs./NTHM to be achieved, compared with initial oil rates of some 50-80 lbs./NTHM a decade or so ago. Table 1-1 lists some of these furnaces which employ the highest oil rates in the world.

1.5 PROBLEMS ASSOCIATED WITH FUEL OIL INJECTION.

The most important problem associated with fuel oil injection is that of incomplete combustion at high oil rates. This results in formation of soot, which ascends through the furnace, to be collected in the gas-cleaning system. Fig. 2 shows the result of incomplete combustion of fuel oil on the gas-cleaning equipment, where the efficiency of this plant is reduced. Although this soot is generally formed wherever fuel oil is combusted (13-16), there are also reports of soot resulting from natural gas injection (17). Finally, it has been reported that soot formation can lead to a decrease in burden permeability.

1.6 PREVIOUS WORK.

As indicated in section 1.4, most of the previous experimental work in this field has been committed to proving the benefit of fuel injection on experimental furnaces. Some operators have been dissatisfied with their injection practice and have sought to change them (19-21). Heynert (21), for example, cites work done at August-Thyssen, West Germany, where homogenisation of the oil with water prior to injection allows injection rates of over 250 lbs./VHM. Other plants (19, 20) report trials with complex hydraulic nozzles in an effort to reduce soot formation.

It is generally accepted that the problem of soot is due to the inefficient combustion of the injectant.

1.7 ATOMISATION OF FUEL OIL FOR COMBUSTION.

A pre-requisite for combustion is to cause the stream of fuel to be disrupted into droplets which are small enough to maintain a stable flame in the tuyere region of the furnace. Good atomisation is therefore needed.

There are two classes of atomisation, (a) Primary and (b) Secondary.

Primary refers to the atomisation caused prior to injection, either by passing the stream of fuel through a complicated nozzle, as is the case in pressure atomisation, or by causing a high-velocity 'sheet' of air to converge onto the fuel stream, as in pneumatic atomisation. In both cases, the original stream of fuel will be disrupted to either a 'fan' Fig. 3, or more probably, a 'hollow-cone', Fig. 4. In both cases, the thickness of the sheet will be very small.

Secondary atomisation is that caused by the impact of the high-velocity air blast in the blow-pipe, on the stream of fuel. In the case where primary atomisation is practiced prior to injection, the thin sheet of fuel is easily disrupted into droplets by the air blast, which can then be reduced in size by the secondary atomisation. Where secondary atomisation is used as the only disruptive force for the fuel stream, the 'ignition lag', i.e. the time needed for the stream to break into droplets, is longer than the case when primary atomisation is used.

Most of the experimental work involving mechanisms of atomisation has been undertaken in the field of Aero-space research. Nevertheless, the conditions prevailing in this field can be applied to blast furnace technology, since in both cases, a liquid fuel is being



injected into a high-velocity air stream.

1.8 COMBUSTION OF FUELS.

As indicated by Von Bogdandy (22), replacement fuels display their greatest effectiveness when completely gasified to CO and H_2 by the oxygen in the air blast in front of the tuyere. The atomised fuel should combust in the oxidising zone of the blow-pipe, and thus the hot blast and auxiliary fuel must be conveyed separately to the blow-pipe, wherewith efficient atomisation, the fuel can be combined with the incoming blast with maximum intensity.

It is widely known that during the evaporation and combustion of a fuel-oil droplet, the droplet diameter decreases as

$$D_0^2 - D^2 = K(t - t_0)$$

where

D_0 = initial droplet diameter (at $t = t_0$)

D = droplet diameter (at $t = t$)

It can thus be seen that for efficient combustion, the initial particle size, D_0 , is of great importance, since a smaller D_0 leads to more rapid rates of evaporation and combustion. Good atomisation of the liquid fuel stream is thus mandatory.

In all cases of combustion, the proportion of big droplets that can be tolerated is dependent upon the relative proportion of very small droplets, since the flame-sustaining capacity of the latter will effect the burning of the former. This is of importance because the size distribution of droplets produced by any injection system will be such that there will always be large droplets (about 200 microns)

present in the blow-pipe. A big droplet burns away progressively in its turbulent flight through the air in the combustion region, the vapour envelope being continuously replenished from the residual liquid of the diminishing droplet until the supply is exhausted. Very big droplets (100 - 200 microns) may not be completely consumed and may pass out in the exhaust gases, to be thermally degraded in the stack and cause decreasing permeability of the charge.

1.9 PRESENT WORK.

The present work was initiated following fuel oil injection trials conducted on No. 3 furnace at Dofasco's plant in Hamilton. At that time, this furnace had the highest oil injection rates in the world, at 200 lbs/NTHM and it was desired to obtain still higher oil rates in view of the favourable economics. However, soot was appearing in undesirable quantities in the gas-cleaning plant, indicating that further increases in oil rates could not be achieved without some process improvement. At that time, Dofasco's injection practice was to simply pump the oil into the centre of the blow-pipe via a heavy gauge mild steel tube (or lance), $\frac{1}{4}$ " I.D. The fuel oil was then injected into the hot air blast without any prior atomisation. It was thought that the large amount of soot resulting from:

- (i) Oxygen starvation in the area of atomisation, evaporation and combustion, and/or
- (ii) Too large a particle size.

On the first count, it can be calculated that there is some 8 times the stoichiometric volume of oxygen present in the air blast

for efficient combustion (20). However, if the 'zone of atomisation' of the oil, prior to subsequent evaporation and combustion, is small, then there will be insufficient time for all the oil droplets to react with the oxygen. Also if the droplet size resulting from atomisation of the oil by the air blast is large, then there will again be insufficient time for efficient combustion.

It was on these premises that a nozzle was designed for the trials. It was simply a corkscrew insert of known pitch set into the lance, whereby a radial velocity component was imparted to the fuel oil, the issuing stream existing as a hollow-cone.

In the short space of time allotted for research, the amount of soot collected at the gas-cleaning plant was reduced, though only slightly. However, it was decided to continue the research at McGill University to obtain fundamental design data on droplet size distributions and mixing characteristics as a function of pertinent parameters (e.g. lance design, injection angle, oil rate, wind velocity etc.).

An experimental system was designed whereby full-scale trials could be conducted. Wax was used as a 'substitute fluid' since this material exhibits similar properties to fuel oil when liquid, yet solidifies in flight after atomisation to allow further analysis to be done regarding droplet size and size distribution produced.

The wax was injected into high-velocity air streams, and the effect of relative velocity, injection angle, and liquid flow rate investigated for both the straight-through lance (simple nozzle) and the nozzle with the corkscrew insert.

BIBLIOGRAPHY.

- (1) Barnett W. English Patent No. 7727 1838.
- (2) Weber F.C. U.S. Patent No. 325 293 1885.
- (3) Fleming E.P. and Labbe A.L. U.S. Patent No 1964 727 1934.
- (4) Coche L. Blast Furnace Fuel Injection Symposium, Australia 1972.
- (5) Ostrowski E.J. et al AIME Blast Furnace, Coke Oven,
and Raw Materials Conference 1960
- (6) Bonnaure E.P. and Halbrechq M.L. Journal of Metals 37-40 1961.
- (7) Decker A.M. ibid 41-44 1961.
- (8) Trense R.V. and Rosbough D.F. I.S.I. Special Report 72 53-58.
- (9) Malvaux J. et al ibid 59-71.
- (10) Rombough W.R. Blast Furnace, Coke Oven and Raw Materials Conf.
573-578 1961.
- (11) Knepper W.A. et al Blast Furnace and Steel Plant 1189-1196 1961.
- (12) Rombough W.R. Journal of Metals 743-745 1961.
- (13) Sharp K.C. I.S.I. Special Report 72 31-37
- (14) Penny W.C.R. ibid 38-46
- (15) Hirase M. Blast Furnace and Steel Plant 23-31 1963.
- (16) Rombough W.R. 30th. Ironmaking Conference, Pittsburgh 1971.
- (17) Kornev V. et al Steel in the U.S.S.R. 592-594 1971.
- (18) Decker A. and Poos A. Fuel Injection Symposium, Australia
21-1 - 21-8 1972.
- (19) Mayer H. and Mitter G. ibid 20-1 - 20-6 1972.
- (20) Guthrie R.I.L. Dofasco Report 1970.
- (21) Heynert G. Fuel Injection Symposium, Australia 26-5 - 26-6 1972.
- (22) Von Bogdandy B. Reduction of Iron Ores 448-524

Table 1-1

INDICATION OF PLANTS USING HIGH OIL INJECTION RATES.

<u>COMPANY.</u>	<u>OIL RATE.</u>	<u>OXYGEN IN BLAST.</u>	<u>HOT BLAST TEMPERATURE.</u>
Dofasco, Canada.	240 lbs/NTHM.	21%	1850°F
August Thyssen-Hutten, West Germany.	280-300 lbs/NTHM.	21%	1850°F
Inland Steel Co., U.S.A.	240 lbs/NTHM.	27%	2000°F
Chiba Works, Kawasaki Steel, Japan.	220 lbs/NTHM.	25%	2100°F
Yawata Works, Nippon Steel, Japan.	215 lbs/NTHM.	25%	2120°F
Usinor - Dunkerque, France.	200 lbs/NTHM.	21%	2200°F
Hoogovens - IJmuiden, Netherlands.	190 lbs/NTHM.	24%	1900°F

Fig. 1

INCREASE IN POPULARITY OF NORTH AMERICAN BLAST FURNACES
USING FUEL INJECTION.

NUMBER OF FURNACES USING OIL INJECTION

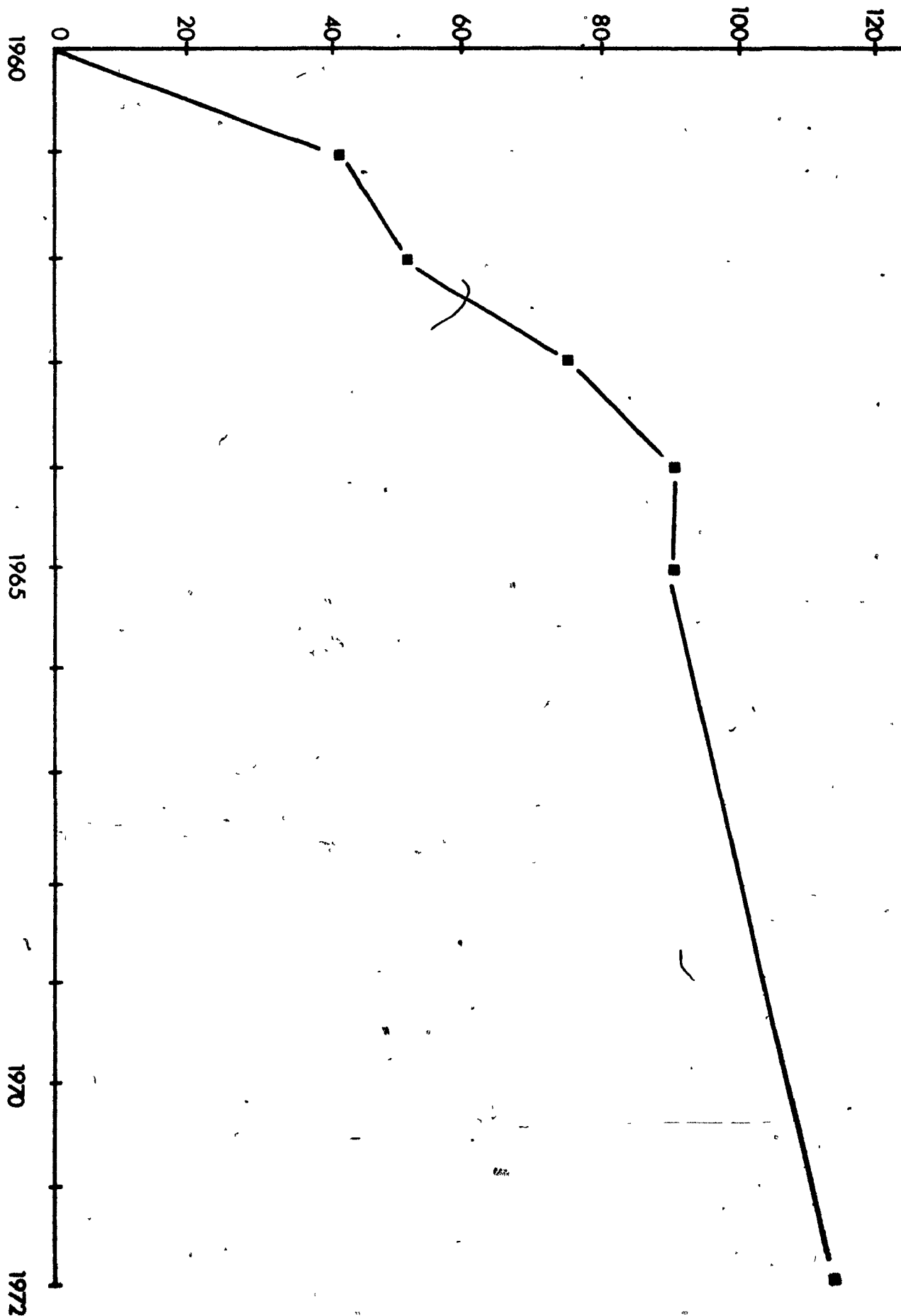


Fig. 2

EFFECT OF INCOMPLETE COMBUSTION OF OIL IN GAS-CLEANING PLANT (13, 14)

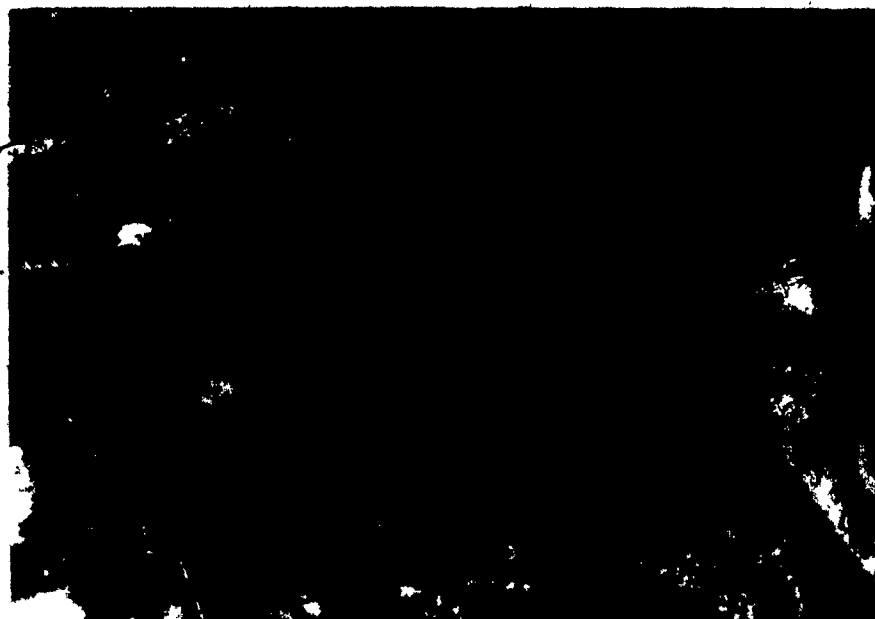
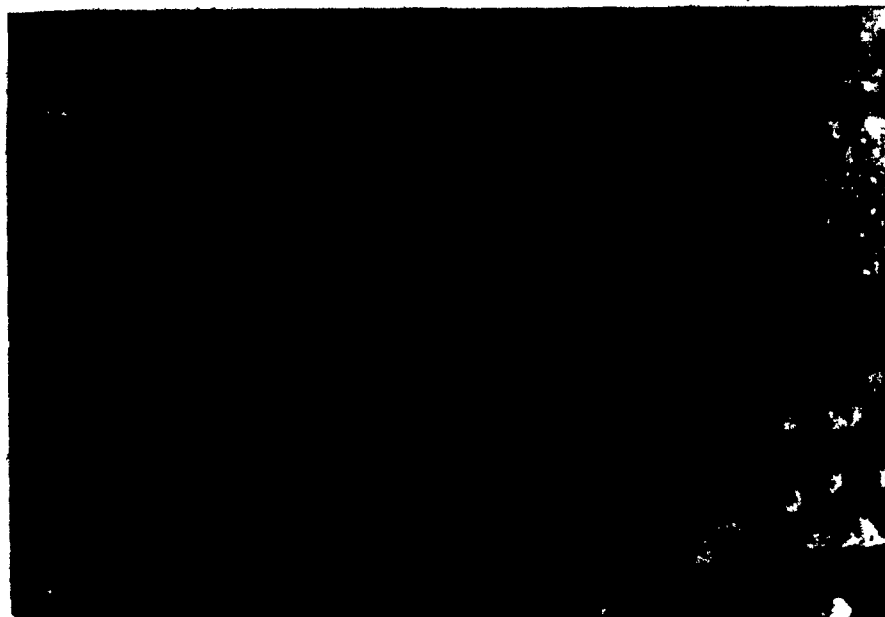
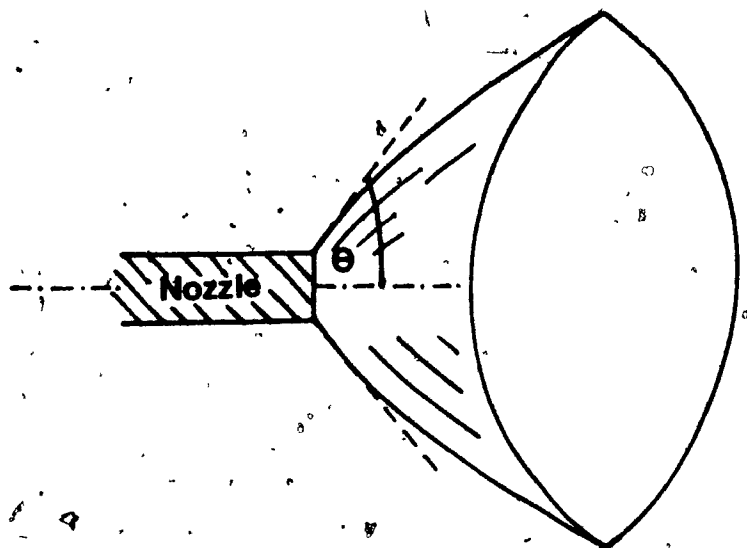


Fig. 3

DIAGRAMMATIC REPRESENTATION OF FAN SPRAY.

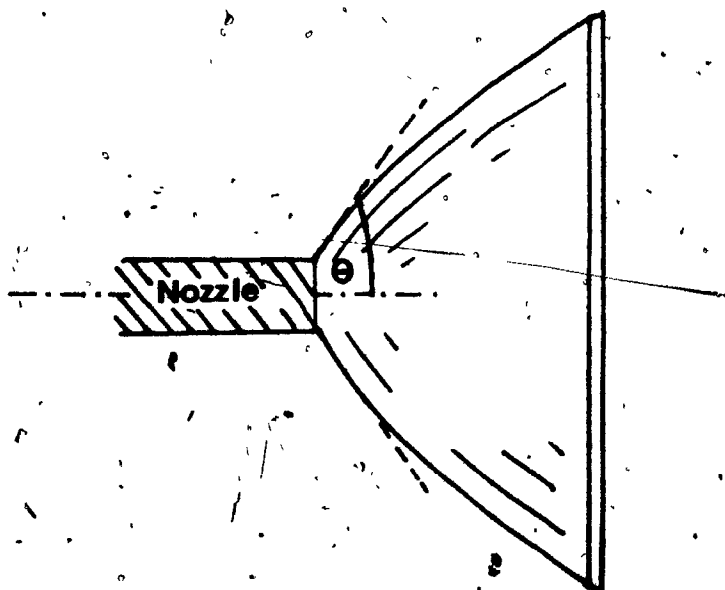
Fig. 4

DIAGRAMMATIC REPRESENTATION OF HOLLOW CONE SPRAY.



HOLLOW CONE SPRAY

SPRAY ANGLE = 2θ



FAN SPRAY

Chapter 2

"THE ART AND PRACTICE OF FUEL INJECTION"

2.0 INTRODUCTION.


This chapter discusses reasons for injecting auxiliary fuels into blast furnaces, the types of fuel injected and their mode of injection. Finally, an indication of future trends in auxiliary fuel injection is given.

2.1 REASONS FOR INJECTING FUEL INTO THE BLAST FURNACE.

The chief reason for injecting auxiliary fuels is one of economics, since a proportion of the coke normally charged to the furnace can be replaced by a less expensive fuel. Fig. 5 shows approximate cost savings involved when heavy fuel oil is used as a replacement for coke in the blast furnace. The economics are impressive, the optimum saving being about one million dollars per year, for a large blast furnace in North America. This hypothetical case pre-supposes a replacement ratio of 1.8 at low injection rates to 1.0 at high injection rates (23).

Another reason is the enormous capital costs involved in the installation of a new battery of coke ovens. Since coke ovens do have a limited life, the decrease in coke rate in the blast furnace will enable current installations to be used for a longer time, and hence new batteries can be delayed and interest charges avoided.

Another advantage of fuel injection is the speed with which variations in furnace performance can be adjusted, i.e. the injectant can be turned off immediately, should the need arise, whereas any changes in coke rate have no practical consequences for the following twelve hours or so, on account of the slow descent of the burden.



It is also known that blast furnaces using fuel injection, with high blast temperatures, tend to run more smoothly, with fewer instances of 'hanging' or 'slipping'.

2.2 LIMITS TO THE RATE OF FUEL OIL INJECTION.

Both economic and physical factors limit injection rates. On the economic side, it is found that as the rate of injection is increased, so the replacement ratio decreases, see Fig. 6. This has the effect of eliminating any cost savings, since beyond a critical limit, the coke rate can increase from its optimum, with increase of injectant rate, Fig. 7, thereby increasing the overall fuel rate and costs.

The chief physical limit on high oil injectant rates is the incomplete combustion of the injectant in the combustion zone of the tuyere. The effects of this have been discussed previously in section 1.8.

Although fuel injection rates in excess of optimum rates are technically possible, they result in a reduction in the combustion-zone flame temperature, which in turn leads to lower driving rates and increased energy losses in the top gas.

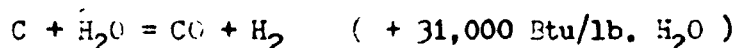
According to Raick (24), in 1962, "with a well-prepared burden, the economic limit to fuel-oil injection will be about 220 - 370 lbs./ton of metal." While these figures may have seemed outstanding a decade ago, they are now being achieved easily, and the upper limit should soon be passed.

2.3 FUELS INJECTED INTO THE BLAST FURNACE.

(1) Steam.

Although steam is not a fuel, it is appropriate to record that it was the first injectant to gain popularity. Humidity control of the blast allowed higher air blast temperatures to be used without concomitant increases in temperatures in the combustion zone. Previous to this, hanging problems associated with too high a flame temperature (R.A.F.T.) in the bosch, had limited air blast temperatures.

When water vapour is added to the blast, it reacts endothermically with coke in the combustion zone:



The added water vapour has a beneficial effect on the quality of the bosh gas, because it increases the amount of hydrogen in the gas, which has a greater potential for the reduction of iron oxide than has CO.

However, although humidity control of the blast allowed higher blast temperatures to be used, it was found that a 1% moisture addition to the blast required a 65°C increase in blast temperature. Coke savings, although lower than expected because of indirect reduction of coke by steam, amounted to 2.7 - 3.2% for each 1% increase in moisture, while the production rate increased by 4 - 6% (25).

The Bureau of Mines (5) reported that with a moisture addition of 13 grains/cubic foot of air (1 grain of moisture/cubic foot of air = 0.30% of air blast), the coke consumption in their experimental blast furnace decreased by 103 lbs. (with a blast temperature of 2475°F) and the production rate increased by 174 lbs./hour, whilst

with a moisture addition of 26 grains/cubic foot of air, the coke rate decreased by 88 lbs. and the metal production increased by 280 lbs./hour.

Decker (26) has shown that the best figures obtained from a European experimental furnace were with a moisture addition of 4.37 grains/cubic foot of air. This is illustrated in Fig. 8. The reported blast temperature was 900°C.

The practice of injecting various amounts of moisture into the air blast is widely used by blast furnace operators to control hot metal temperatures on account of the relatively rapid response of the furnace to any operating change made in the bosch zone.

(ii) Natural Gas.

As with steam, the injection of natural gas (CH_4) into the raceway causes a considerable decrease in flame temperatures, necessitating an increase in blast temperature, comparable to that of steam, to compensate for the decrease in the R.A.F.T.. Initial tests (27) indicated that with a 7% natural gas injection rate (based on wind rate), a 475°C increase in blast temperature was needed to maintain the furnace driving rate constant. At the same time, the coke rate was decreased by 256 kgs./NTHM, and the hot metal production rate was increased by 30%.

When natural gas burns in the oxidation zone, it produces CO and H_2 , and only one third as much heat as coke; consequently, it has about the same cooling effect as an equal volume of water vapour. Although the heat produced by burning coke with the hot air blast is 6,600 Btu/lb. of carbon, that produced by burning natural gas is only 2150 Btu/lb. of carbon.

It should be noted that oxygen enrichment of the blast is now generally utilised with fuel injection, and in the case of natural gas, the increased flame temperature, due to combustion with more oxygen, offsets to some extent, necessary compensating increases in blast temperatures.

The effect on the replacement ratio with increase in natural gas (and other injectant) rates can be seen in Fig. 9.

(iii) Fuel Oil.

Because of its high carbon/hydrogen ratio, and low cracking temperature, oil has only a relatively moderate cooling effect. Consequently, larger quantities of fuel oil versus natural gas can be used to produce an equivalent decrease in adiabatic flame temperatures.

Although the amount of coke saved for each pound of oil is less than that of natural gas, more coke can be saved in total with these fuels, in view of the preceding comments.

As reported by Bell and Taylor (28), if oil is added without temperature compensation, then 1.2 units of oil carbon replaces 1 unit of coke carbon. With temperature compensation, this ratio drops to 0.62. These figures illustrate the fact that the principal advantage to be derived from fuel oil is the ability to use higher blast temperatures. In fact, some 60% of the coke replacement is due to this effect. However, where there is a limited hot blast available, heavy oil, with its carbon/hydrogen ratio of 7:1, would replace some coke by direct substitution of coke carbon by oil carbon.

An addition of 115 lbs. of oil saved 100 lbs. of coke without temperature compensation, yet with a 200°F rise in blast temperature,

the saving was 173 lbs. of coke (29).

A 'rule of thumb' value for the benefit of oil injection was given by Taylor and Rombough (30). They quote an air blast temperature increase of 150°F per pound of oil injected per 1000 cubic feet of wind blown. Under these conditions, about 65 pounds of oil will replace 100 pounds of coke.

Decker et al (31) have shown that improved combustion, either by better atomisation or oxygen enrichment, has made it possible to add nearly 30% of the total fuel requirements as fuel oil injected at the tuyeres.

(iv) Coal.

The changes to be expected from the injection of powdered coal can be evaluated in precisely the same way as has been done for oil. Coal is much more variable in composition than oil and, as examples, the composition of anthracite and low-grade coal are compared;

	<u>%C</u>	<u>%H</u>	<u>%O</u>
anthracite	93	3.5	2.0
low grade coal	77	5.5	15.0

Since the chemical composition of anthracite is so similar to that of coke, it can be taken as being equivalent i.e. the replacement ratio is 1. The effect on the combustion temperature is small, (so the required increase in blast temperature is also small). Fully temperature-compensated, the replacement ratio for anthracite is 1.3 (28).

Coal, with its higher carbon/hydrogen ratio, should allow more coke to be saved for a particular change in blast moisture content

or in hot blast temperature than either natural gas or fuel oil.

Strassburger (32) has stated that:

"The full potential of solid fuel injection can be realised when using high blast-temperatures and oxygen enrichments".

The main differences compared with oil additions are that the hydrogen content of the gas is lower, and the top gas volumes are rather higher. Any improvement in gaseous reduction due to hydrogen will therefore be less and the limiting effect of top gas volume on production rates will be greater.

Complete combustion of coal particles to CO in the limited space of a tuyere raceway is only possible by an extremely fine grinding of the coal.

However, as the reserves of coal suitable for blast furnace injection are much more important than those of fuel oil and natural gas, it is possible that coal injection will be applied on a wider basis and that the effort and expenses necessary to fully develop its technology will be made in spite of initial difficulties and set-backs.

(v) Coal Tar and Pitch.

Since the injection of these fuels uses a similar technology to that used for Bunker 'C' oil, and also have a higher carbon content, indications are that their use would be preferable to that of oil. They also bring the additional benefit of a low sulphur input to the furnace.

Schmauch (33) has indicated a replacement ratio of 1.25 kgs./kg. of pitch, which agrees with the value of 1.2 quoted by Van Keuren

(34), although Stolnacker (35) reports a higher value of 1.54.

(vi) Coke Oven Gas.

This has attractions as a blast furnace additive because it is readily available. However, apart from the relatively small methane content, coke oven gas has little value as a fuel in the blast furnace. Hydrogen and carbon monoxide can take part in the reduction of iron oxide, but only at the expense of the combustion of coke, unless the proportion of gaseous reduction is increased. It is as a compensating addition enabling use of higher blast temperatures that it promises to be most useful.

A replacement ratio of 1.2 was quoted by Dean (36) on a Shenago (U.S.A.) furnace.

(vii) Slurries of Coal in Liquid.

Injection of slurries has only been done on an experimental basis, since its use has not been as economically favourable as that of other fuel available. Trials have been recorded on fuel-oil slurries (37), and also on coal-water slurries.

(viii) Oxygen Enrichment of the Air Blast.

The result of oxygen enrichment of the combustion medium is to decrease the volume of combustion gases produced per NTHM, to therefore raise the instantaneous combustion temperature and to increase the proportion of the energy of these gases, which is useful in the melting zone.

Oxygen enrichment of the blast requires an increase in the level of either blast humidification or fuel injection, either of which will increase the hydrogen content of the bosch gas.

Increasing the percentage of oxygen in the blast permits a furnace to accept a proportional increase in oil injection rate at a constant blast temperature. One result of the combined use of oil and oxygen is a decrease in coke rate, although the expected coke savings may not be as large as those achieved at the same oil rate using high blast temperature and no oxygen. These smaller coke savings are due to a decrease in the volume of bosch gas with increased oxygen usage, resulting in less efficient pre-heating of the burden. Another result of combined fuel and oxygen usage is a much greater production increase than would be achieved with fuel injection alone. A faster rate of stock descent is achieved as a result of the increase in the coke consumption rate corresponding to the level of oxygen enrichment in the blast. The flame temperature at the tuyeres is increased by the use of oxygen enrichment, which in this sense, can function as a substitute for an increase in the hot blast temperatures. The value of oxygen enrichment as a temporary substitute for hot blast temperature was clearly demonstrated by Ostrowski (38).

With supplemental oxygen enrichment, the problem of uncombusted carbon carry-over to the gas cleaning plant is decreased, when high oil injection rates are practiced. (39)

Work with oxygen and natural gas, 8% and 11% respectively, showed that a proper balance of oxygen and natural gas is maintained, replacement rates of coke and natural gas is maintained, replacement rates of coke by natural gas are equivalent to non-oxygen fuel injection with production increasing about 4% for each 1% oxygen added.

From Fig. 10, the effect of oxygen compensation for oil, gas and

coal can be seen. It is evident that as the level of oxygen enrichment is increased, so the level of fuel injection can be increased, for all fuels surveyed.

2.4 MEANS OF INJECTING FUEL INTO THE BLAST FURNACE.

This section will illustrate the different systems of injecting the different fuels into the furnace.

In order to fully understand the mechanics of injection, Fig. 11 illustrates a schematic flow-sheet of the blast furnace. It can be seen that the fuel is injected at the tuyere level, Fig. 12, so it may be incorporated in the air blast.

(1) Natural Gas and Coke-Oven Gas.

Since the gaseous injectants mix thoroughly with the air blast prior to combustion, the injection distance from the nose of the tuyere is only small. This is illustrated in Fig. 13a & b.

The gas is injected cold, at a pressure of 60 - 75 psig, and entry of the gas into the tuyere is effected by passage through a lance, inserted through the water-cooled tuyere wall.

According to Stephenson (40), the gas does not mix completely with the air, (at high gas injection rates through the tuyere), and does not reform completely. Consequently, unburnt gas escapes from the combustion zone, and hence there is a smaller proportion of reducing gas available for direct reduction, (i.e. reduction of iron oxide at lower temperatures, by $\text{FeO} + \text{CO} = \text{Fe} + \text{CO}_2$). This has necessitated some study of injection methods through the blow-pipe to produce a better mixing of the gas and air before combustion.

(ii) Fuel Oil.

Since oil is a viscous fluid, to inject it cold into the furnace would require a great deal of pumping energy. However, as seen in Fig. 14, with increasing temperature, its viscosity increases rapidly. Consequently, it is common practice to pre-heat the oil to a temperature between 150°F - 200°F . This has a two-fold benefit since it lowers the energy required for pumping and also improves the atomisation characteristics. It has been calculated (20) that the temperature of the oil increases by some 30°F in passing through the lance into the blow-pipe. Since oil tends to 'crack' at temperatures over 260°F , a 'margin of error' should be allowed in the oil pre-heat temperatures.

The oil is injected into the blow-pipe behind the tuyere to allow time for the oil to reform to CO and H_2 . The distance from the tuyere and injection angle into the blow-pipe generally depend on individual plant practice. In some plants, exact centring of the lance in the air blast is thought to be essential. Some practices can be seen in Fig. 15.

The lance through which the oil passes may or may not have an atomising device at the exit orifice. Dofasco, based on computer analysis, opted for a simple lance, with no insert, Fig. 16a, whilst other plants have used an atomiser. Atomisation of the oil can be achieved by either pressure atomisation, where the stream of oil is caused to disintegrate by a number of methods, such as inserts, Fig. 16b & c, or by pneumatic atomisation, where the stream of fluid is disrupted and atomised by a high-velocity air stream impinging on

it, Figs. 16d & e. Steam has been found favourable as the break-up medium in at least one plant (39).

In all cases of oil injection, the system is fitted with a purging stream of steam so as to clear any blockages and expel any oil remaining when the system is turned off.

Problems with oil injection can sometimes arise due to 'coking' of the oil at the lance tip, causing accretions to build up and cut off the fuel supply.

Bunker 'C' oil, a heavy residual oil, is most commonly used as an injectant, although light fuel oils have been injected in French furnaces. A typical analysis of 'C' oil is given in Table 2-1. As can be seen this oil has a high sulphur content, though no problems have been reported with high sulphur in the metal.

(iii) Tar.

Tar is also a viscous liquid, and also requires pre-heating prior to injection. Van Keuren (34) records a pre-heat temperature of 220°F. It appears that injection of tar necessitates a form of screen through which the tar passes before injection (41), to remove any suspended material that may cause a blockage in the system. No atomising is done prior to injection, although it is considered that air atomisation could help, due to the ability of such a system to atomise viscous liquids. Injection rates are generally lower than oil, in the range 40 - 75 kgs./NTHM.

A typical injection system is shown in Fig. 17.

(iv) Coal.

Generally the coal is first pulverised and dried and then stored

in bunkers from which it is transferred to a high pressure stream of air that carries it into the blast furnace combustion zone.

Moisture was a problem initially in the storage bins and the pulverised coal tended to pelletise. This was checked first by the use of screens to prevent these pellets entering the furnace, and then by pre-heating the air blast to eliminate moisture from the coal.

The rate of combustion of coal is less than that of either gas or oil, and consequently, the coal must enter the air blast about two or three feet in front of the tuyere.

The size of the coal is also important because it affects the rate of combustion. In one system, the coal is pulverised down to -200 mesh in order to effect good combustion.

A coal injection system is shown in Fig. 18.

2.5 FUTURE TRENDS IN FUEL INJECTION.

Because of the increased cost of coke and replacement fuels, it is evident that injection practice must be optimized. The injected fuel must be combusted at a rate approaching maximum efficiency, which necessitates study of the present practice.

Heynert (21) has indicated that homogenisation of oil with water has alleviated most of the problem of 'soot formation' at a West German plant, and has led to higher injection rates.

Much research has been directed towards the injection of reformed gas into the area of the furnace above the tuyeres. Any hydrocarbon fuel could be considered for reforming into CO and H_2 . Raick and Brassert (42) studied the feasibility of such a system and found it

theoretically feasible. In the Soviet Union and Japan, plans are underway to inject reformed gas into the blast furnace.

Schweitz (43) briefly comments on the F.T.G. process now being employed by Nippon Steel in Japan, where reducing gas is injected through the tuyeres. The gas is made from oil by Texaco's partial oxidation method, and is considered to give a better replacement ratio. A diagrammatic flow-sheet is shown in Fig. 19.

Other processes use natural gas and reform it with steam. One company has indicated a process which yields a higher purity gas with lower CO_2 and H_2O content.

However, Standish (44) has intimated that the full potential of injection of reducing gas has not yet been realised due to the fundamental difficulty of mixing it with the rapidly ascending furnace gases.

Finally, in the Soviet Union, nuclear energy has been considered as a source of power for the furnace, to replace some of the coke, but no meaningful reports have, as yet, been received.

BIBLIOGRAPHY.

- (23) Harries D.B. and Thomas R. Chem. Eng. Symp. in Iron & Steel Ind.
1-22, 1967.
- (24) Raick J.O. Iron and Steel Eng. Yearbook. 693-699 1962.
- (25) Burnside H.E.W. et al 6th. World Petroleum Congress. 377-384 1963.
- (26) Decker A.M. Blast Furnace, Coke Oven & Raw Materials Conf.
174-186 1961.
- (27) Melcher N.B. ibid. 69-74 1959.
- (28) Bell H.B. and Taylor J. I.S.I. Special Report 72. 10-23
- (29) Melcher N.B. et al Proc. Brit. I.S.I. Annual Meeting. 47-52 1961.
- (30) Taylor H.C. and Rombough W. Blast Furnace and Steel Plant. 35-39
- (31) Strassburger J.H. ibid. 447-457 1963. 1962.
- (32) Decker A. et al AIRBO. 1963.
- (33) Schmauch H. Stahl Und Eisen. 861-864 1971.
- (34) Van Keuren J.W. 30th. Ironmaking Vonference, Pittsburgh 1971.
- (35) Stolnacker W.J. AIME Ironmaking Proceedings. 168-179 1970.
- (36) Dean E.R. Blast Furnace and Steel Plant. 417-423 1961.
- (37) Stephenson R.L. ibid. 389-392 1965.
- (38) Ostrowski E.J. Blast Furnace Research Incorp., Final Report.
11-13 1966-7.
- (39) Quigley J.J. et al 31st. Ironmaking Conference, Cleveland. 1973.
- (40) Stephenson R.L. 30th. Ironmaking Conference, Pittsburgh 1971.
- (41) Gearge D. Private Communication. 1973.
- (42) Raick J.O. and Brassert J.E. Iron and Steel Eng. 75-80 1952.
- (43) Schwartz N.B. Iron Age. 58-59 Feb. 1971.
- (44) Standish N. Private Communication. 1973.

Table 2-1

TYPICAL ANALYSIS RANGE OF BUNKER 'C' OIL.

BUNKER 'C' OIL.

Carbon %	83.7 - 87.0
Hydrogen %	10.2 - 14.8
Sulphur %	0.06 - 4.15
Oxygen & Nitrogen %	0.00 - 2.9
Ash %	Trace.
Moisture %	-
Gross Heating Value, Btu/lb	19,000
Specific Weight lb/ft ³	54.1

Referenced from North American Combustion Handbook, 1965.

Fig. 5

COMPUTED COST SAVINGS WITH INJECTION OF OIL AS A
PARTIAL REPLACEMENT FOR COKE IN A LARGE BLAST FURNACE.
Based on replacement ratios of Harries and Thomas (23),
and cost of coke and oil being \$1.18 and \$0.78 respectively.

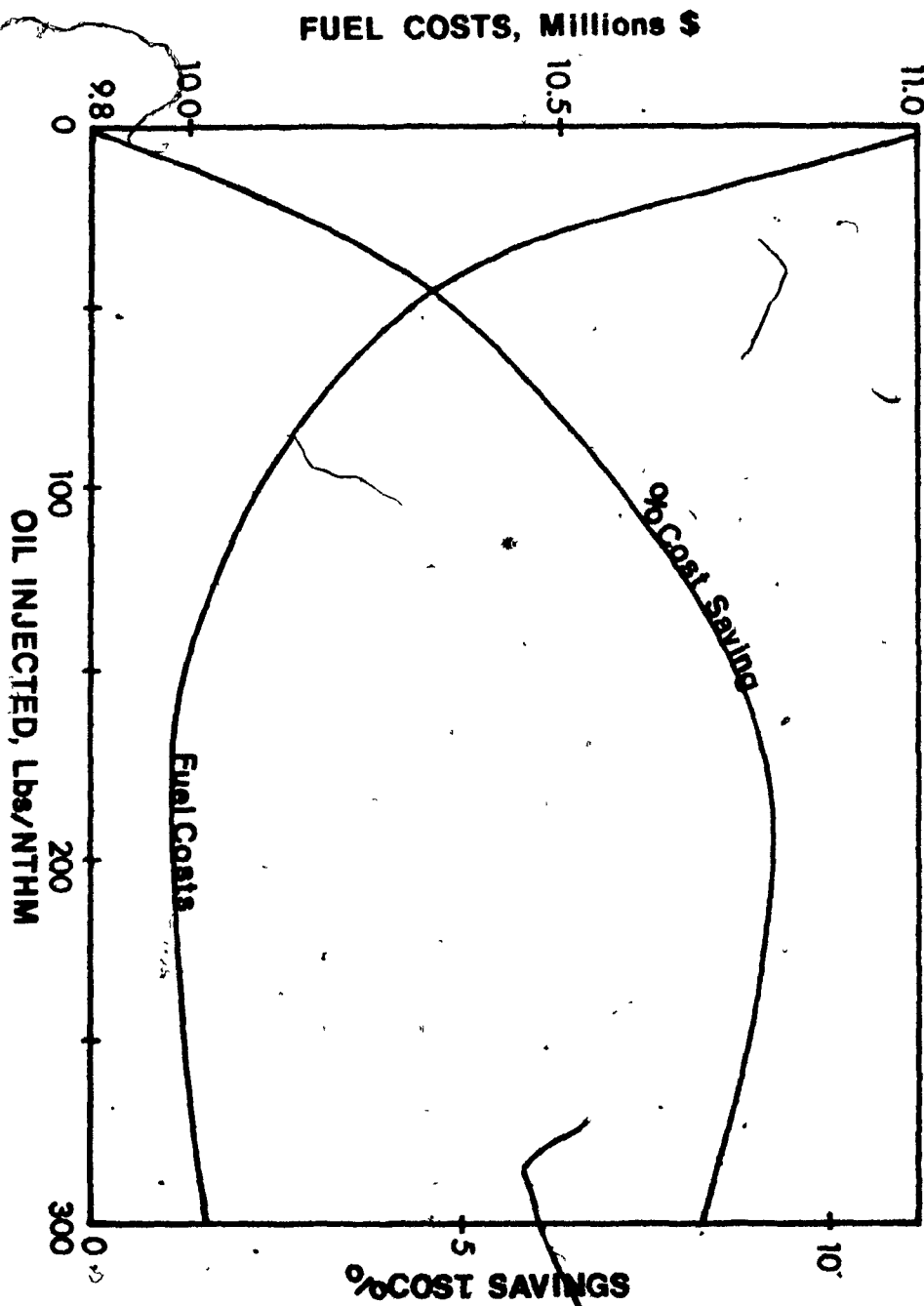


Fig. 6

EFFECT OF INCREASING OIL RATE ON COKE REPLACEMENT RATIO.

After Harries and Thomas (23). (

COKE REPLACEMENT RATIO

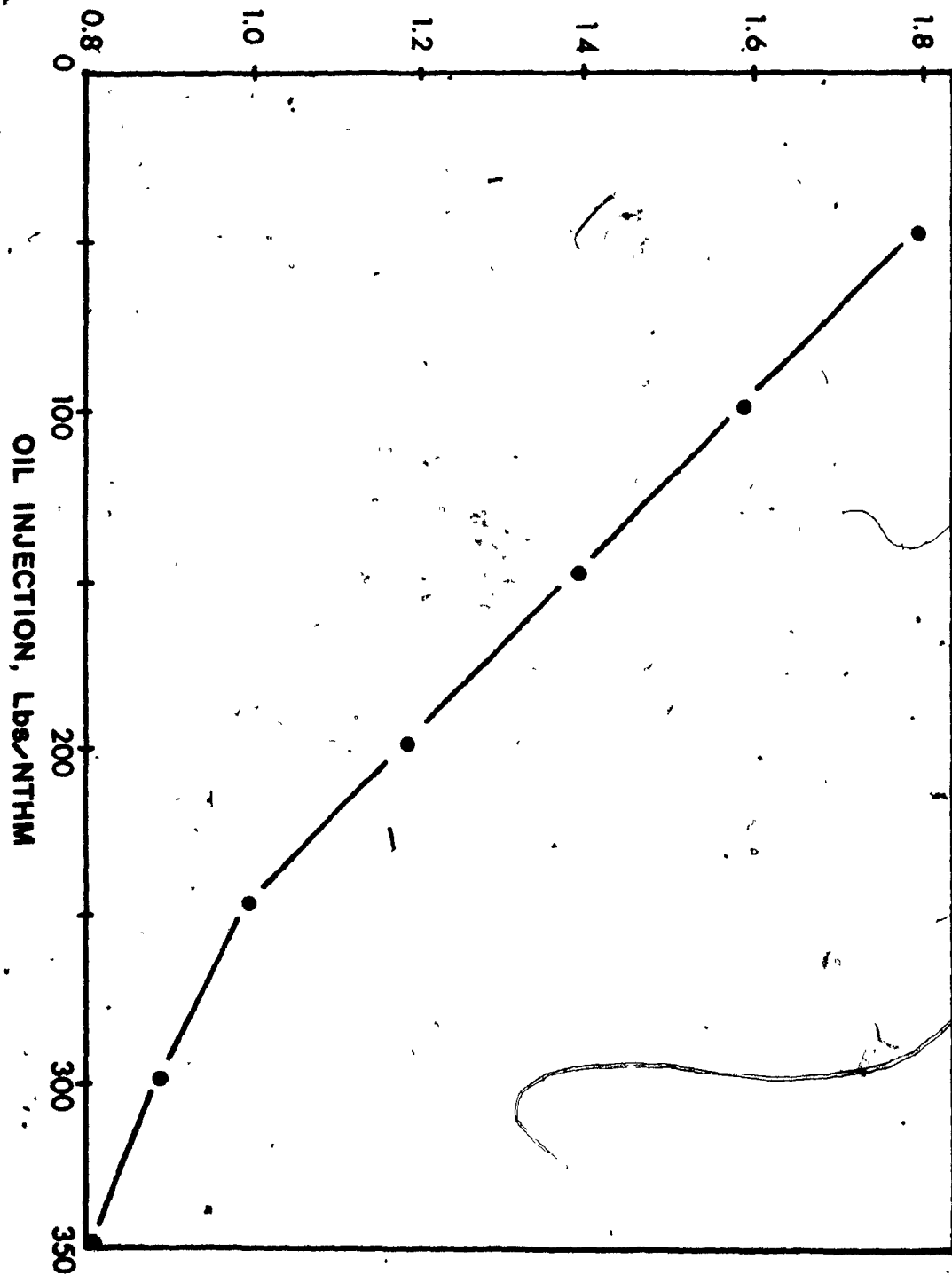
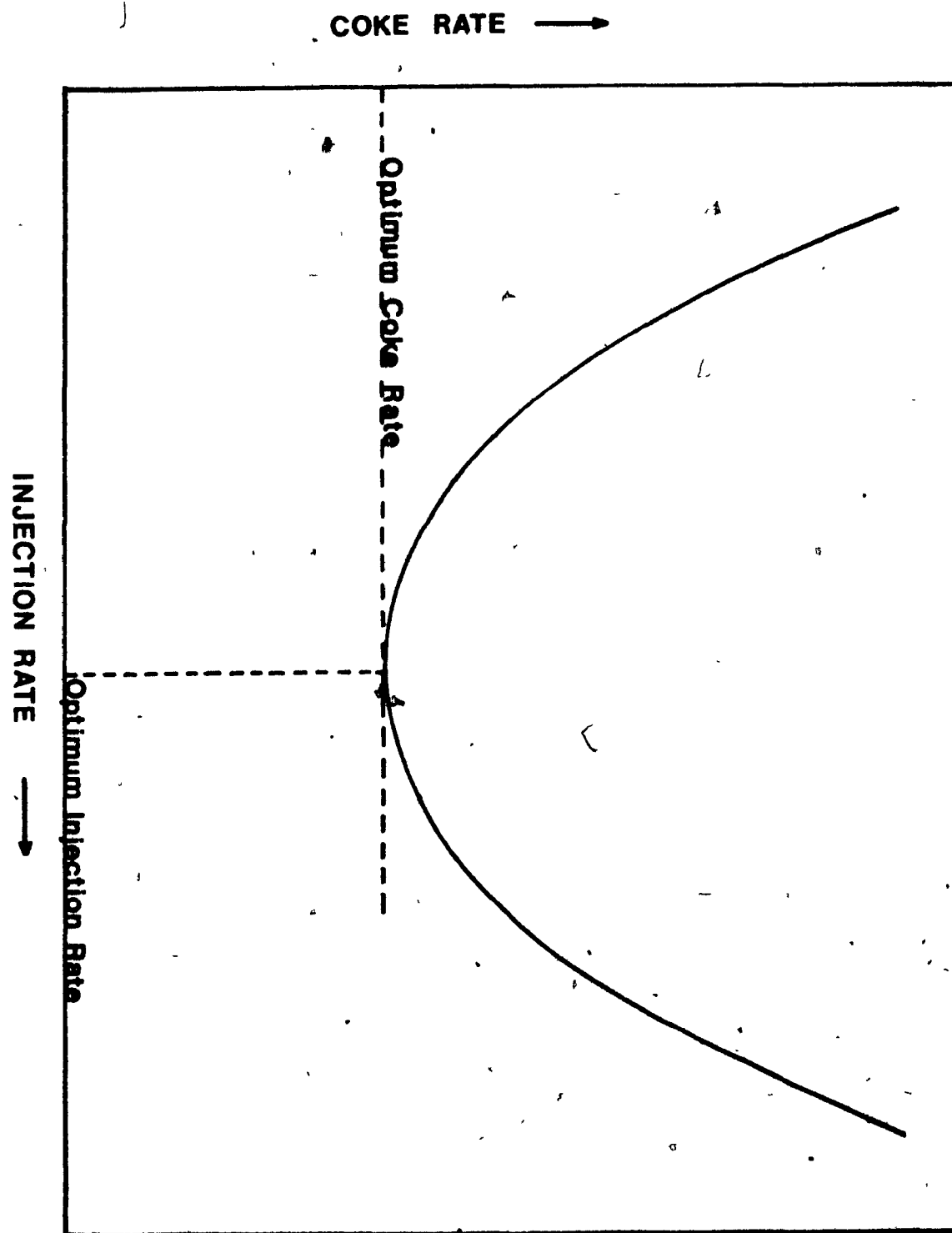


Fig. 7

EFFECT OF INCREASING INJECTION RATE ON COKE RATE



23



Fig. 8

EFFECT OF STEAM INJECTION ON COKE RATE. (26)

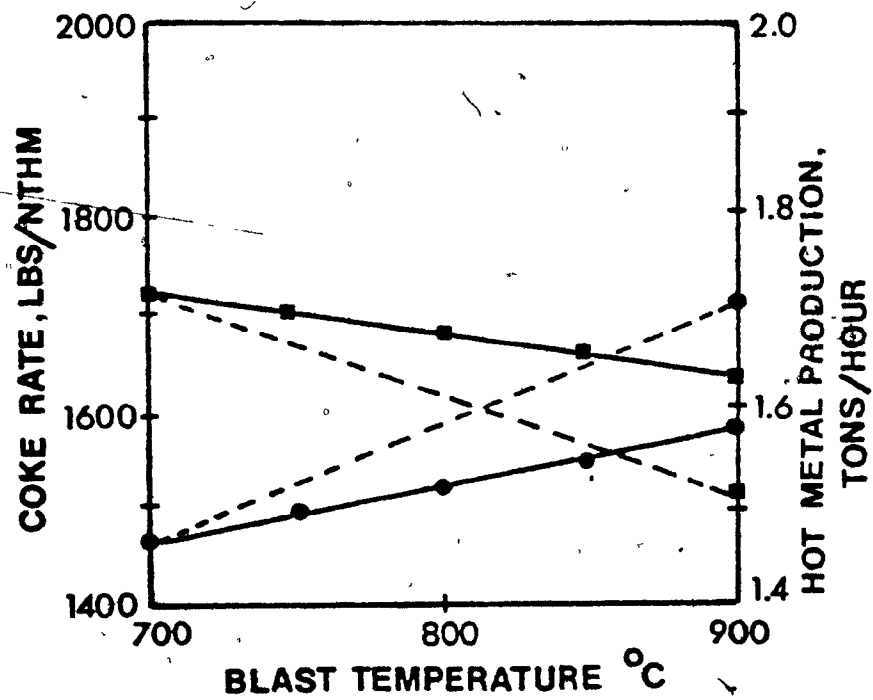


Fig. 9

EFFECT OF FUEL INJECTION ON COKE REPLACEMENT RATIO. (28)

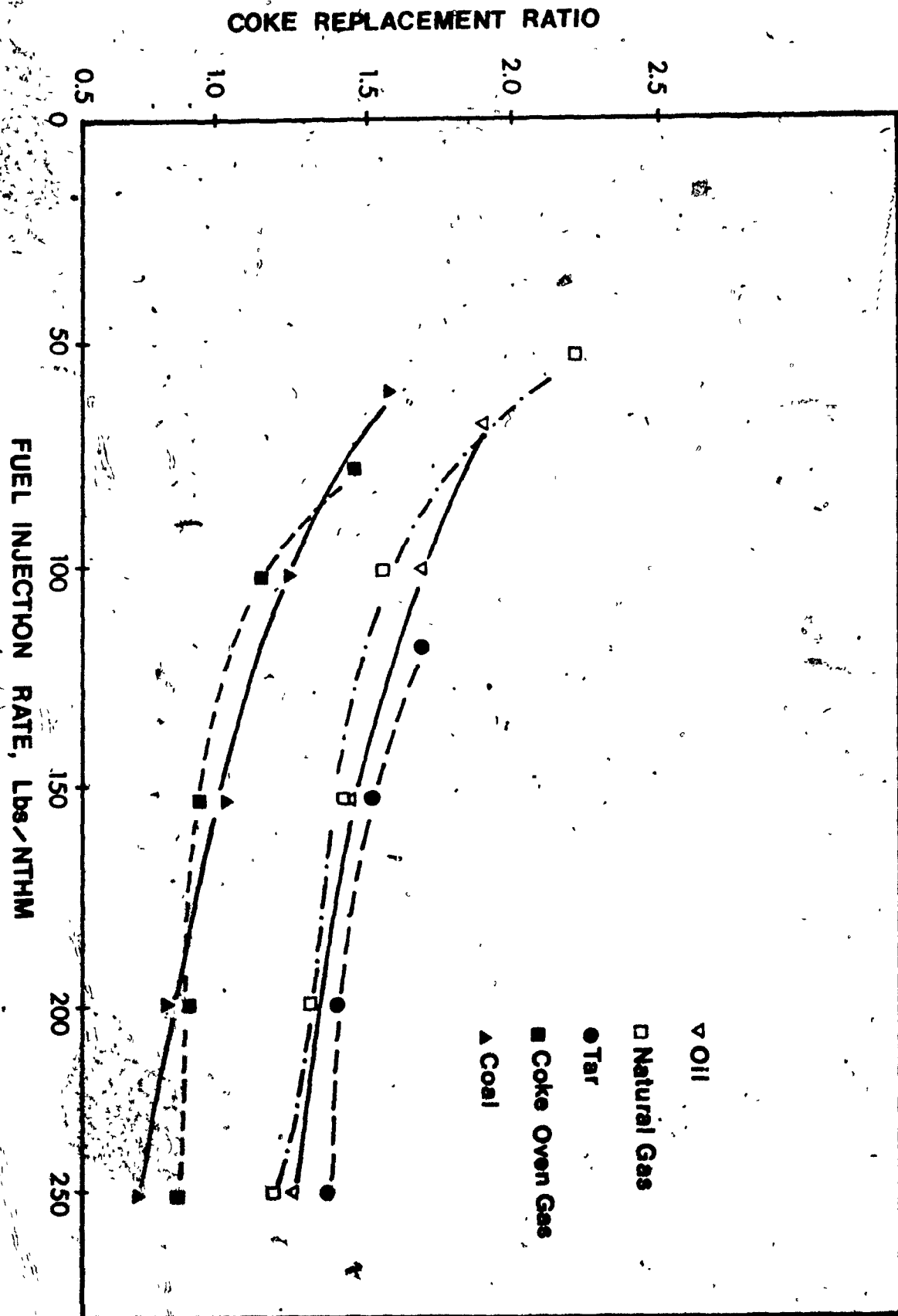


Fig. 10

EFFECT OF OXYGEN ENRICHMENT OF THE BLAST ON
INJECTED FUEL RATE. (28)

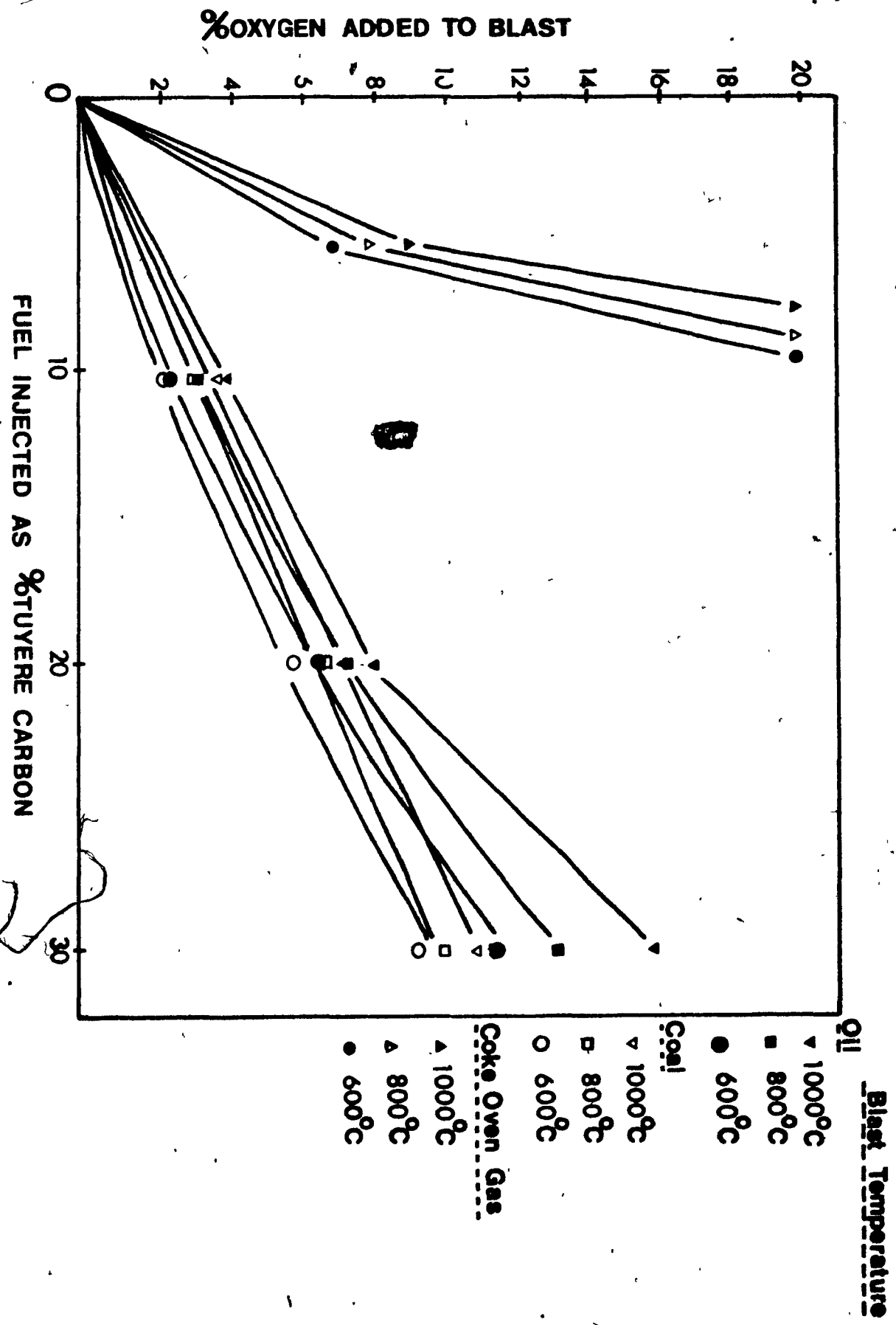


Fig. 11

DIAGRAMMATIC FLOW SHEET OF BLAST FURNACE. (23)

Fig. 12

TUYERE REGION OF BLAST FURNACE.



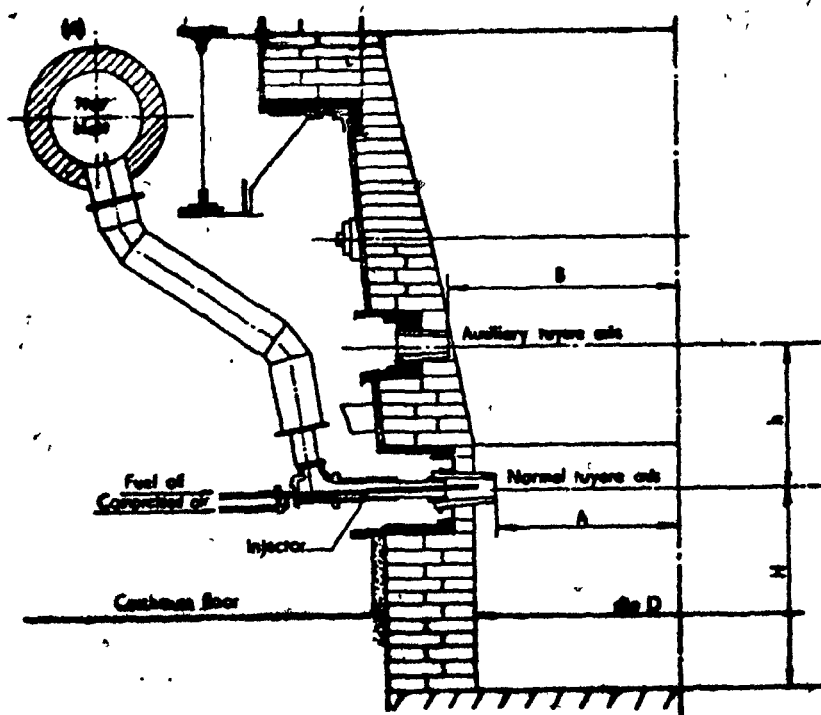
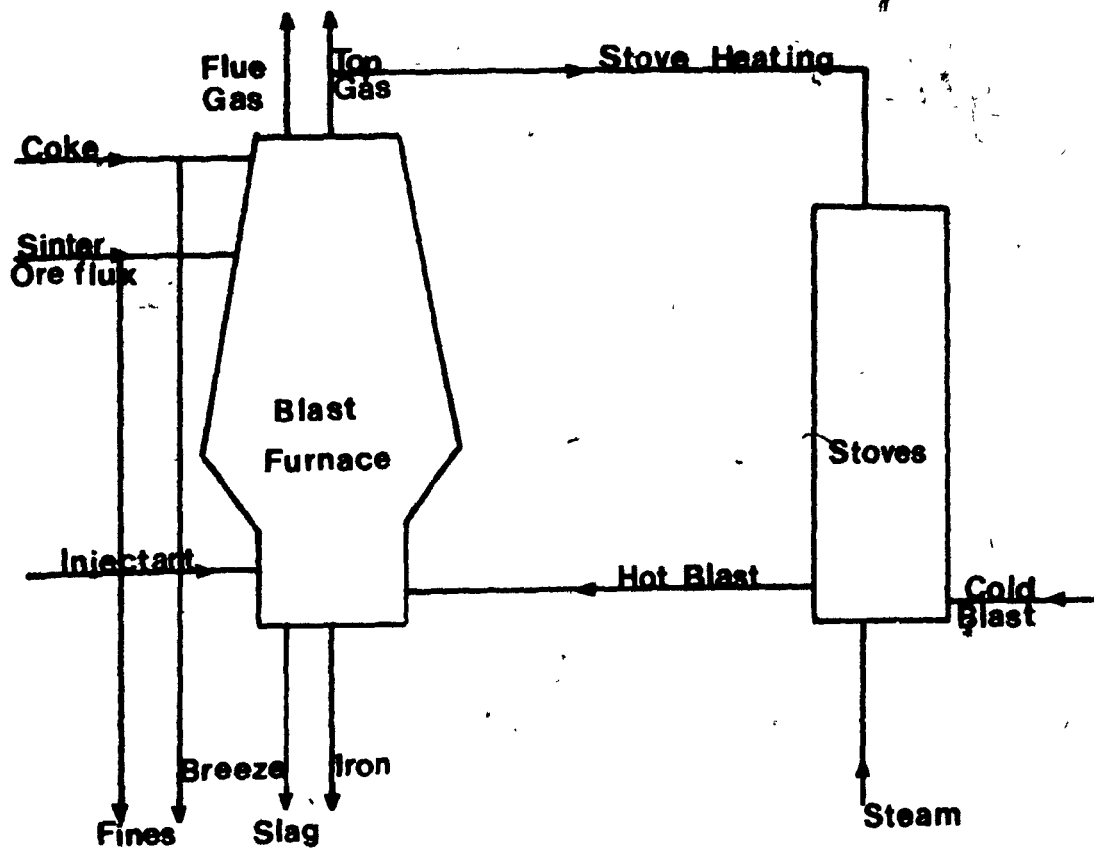
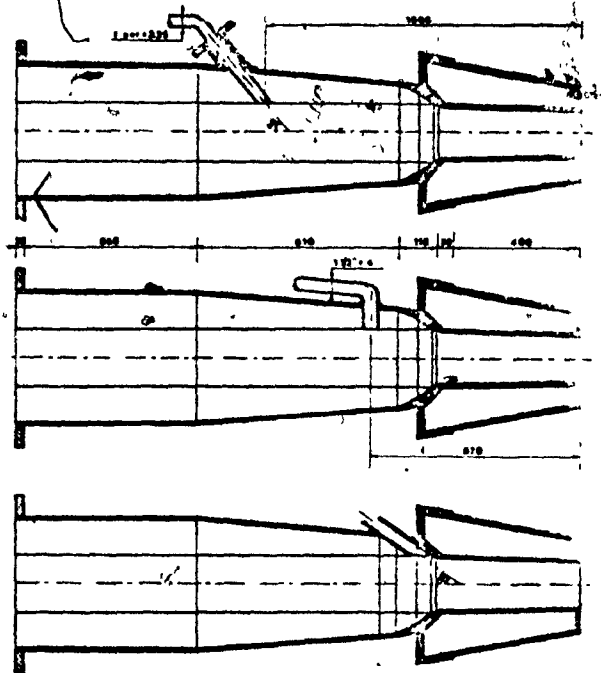
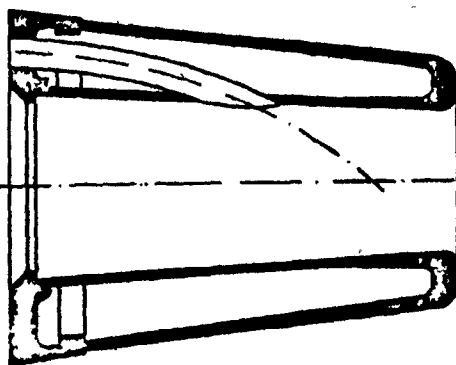


Fig. 13

- (a) SYSTEMS USED EXPERIMENTALLY FOR NATURAL GAS INJECTION.
- (b) CROSS-SECTION OF TUYERE USED FOR NATURAL GAS INJECTION
INDICATING POSITION OF LANCE IN TUYERE WALL.



a.



b.

Fig. 14

VISCOSITY CHART OF BUNKER 'C' OIL. (20)

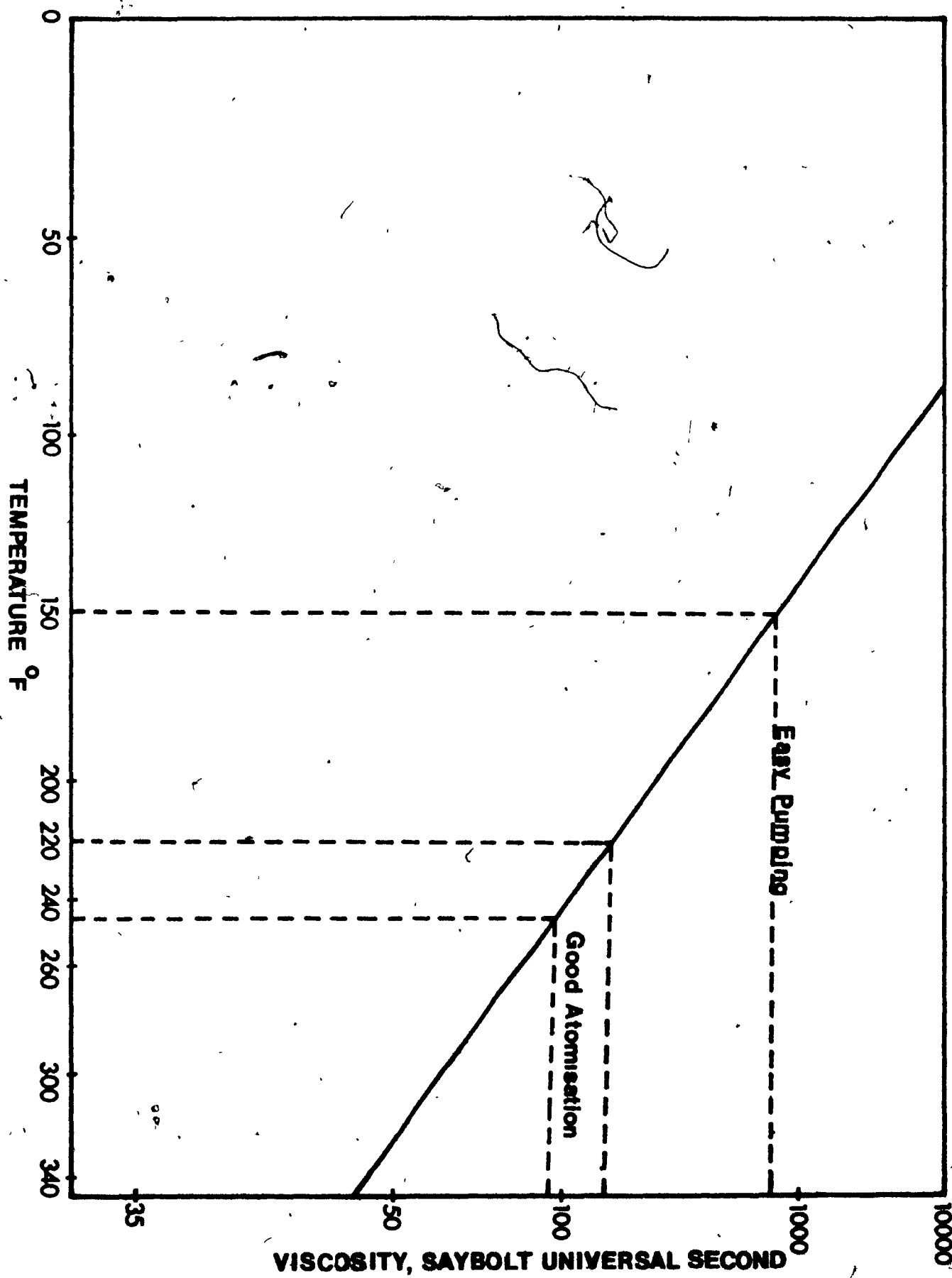


Fig. 15

TYPICAL OIL INJECTION METHODS.

- (a) INJECTION THROUGH PEEP-HOLE INTO BLOW PIPE
- (b) INJECTION THROUGH BLOW PIPE WALL.

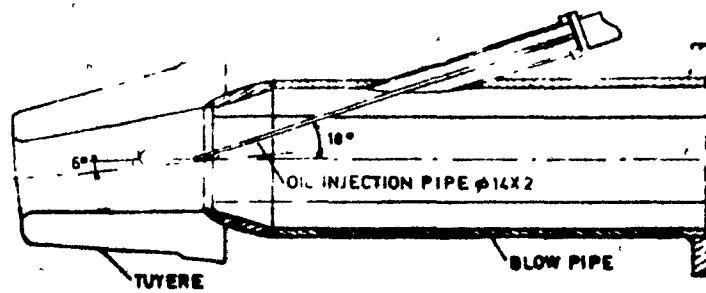
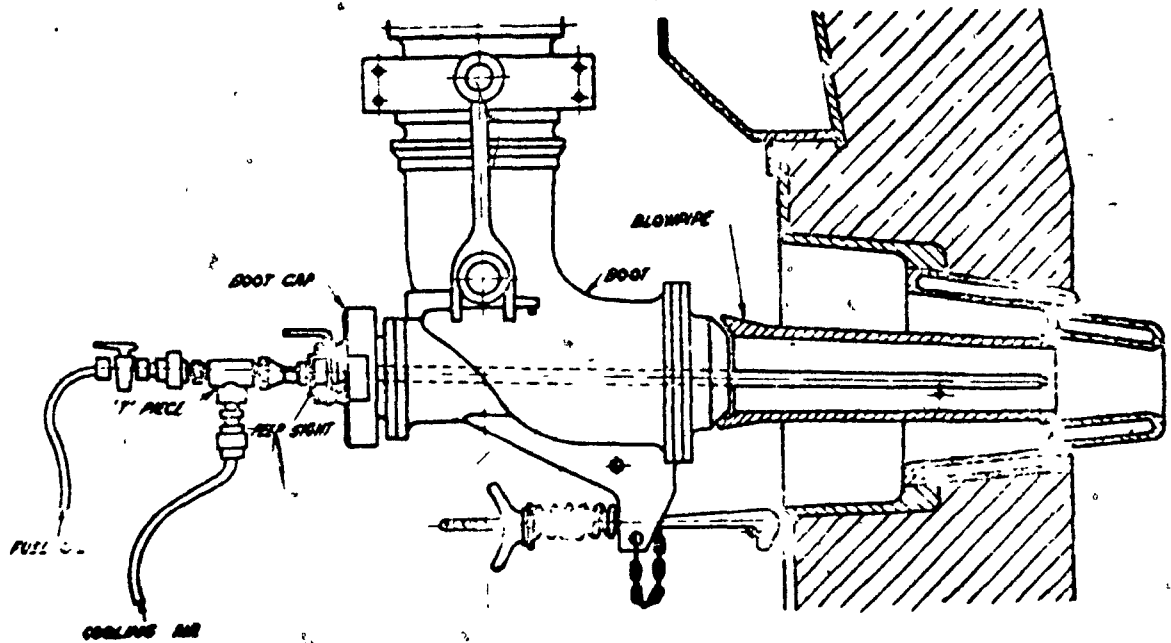


Fig. 16

NOZZLES USED IN OIL INJECTION PRACTICE.

- (a) SIMPLE (STRAIGHT-THROUGH) NOZZLE (PRESSURE)
- (b), (c) COMPLICATED HYDRAULIC NOZZLES (PRESSURE)
- (d), (e) PNEUMATIC (TWIN-FLUID) ATOMISING NOZZLES

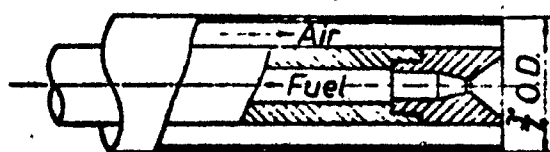
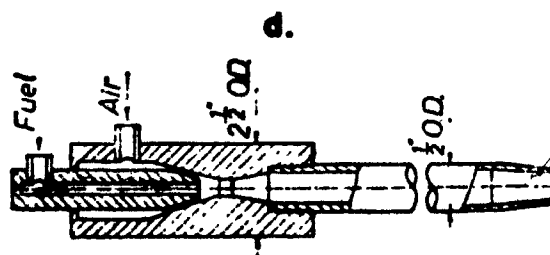
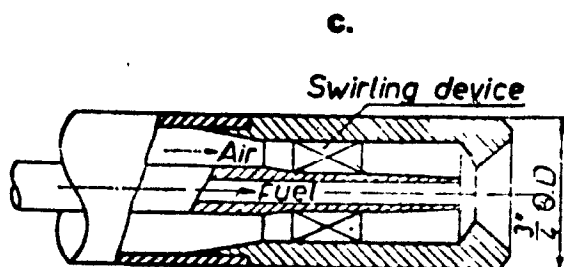
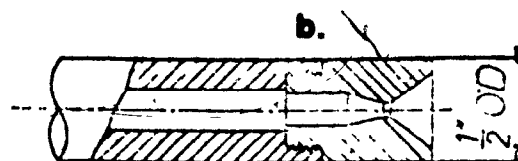
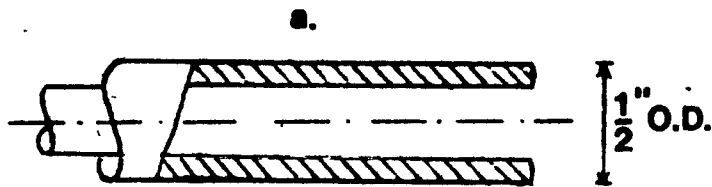


Fig. 17

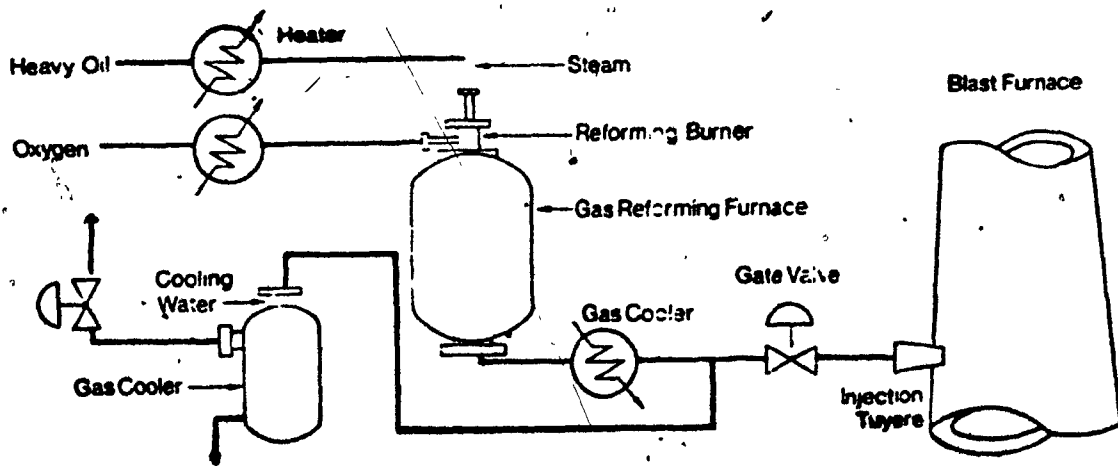
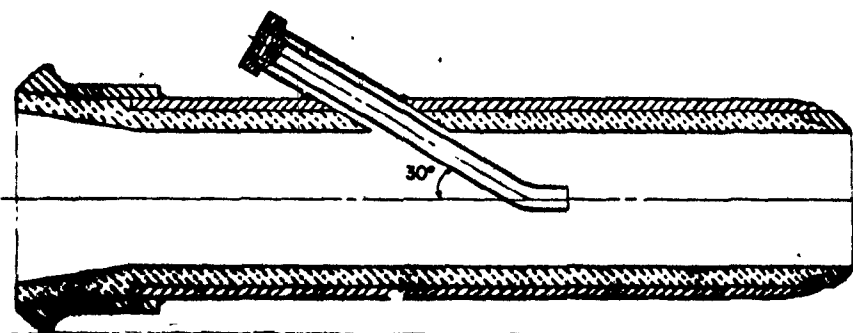
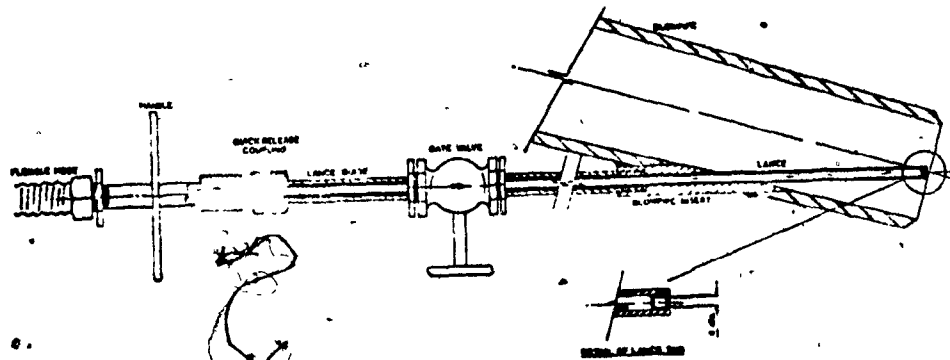
TAR INJECTION SYSTEM

Fig. 18

COAL INJECTION SYSTEM

Fig. 19

FLOW SHEET OF F.T.G. REFORMED GAS PLANT



Chapter 3.

"COMBUSTION".

3.0 INTRODUCTION.

This chapter reviews the mechanisms of fuel ^{combustion,} and, in particular, summarises work on the burning of heavy fuel oils. Finally, the significance of previous studies in indicating criteria for good oil injection practice to blast furnaces is presented.

3.1 MECHANISMS OF COMBUSTION.

According to Masdin and Thring (45), the important steps in the combustion of a fuel spray can be summarised thus;

- (1) Atomisation of the fuel into droplets of suitable size.
- (2) Mixing of the spray with air (and re-circulated hot products of combustion).
- (3) Heat transfer to the droplets by convection from the hot gases and radiation from the walls and flame.
- (4) Evaporation of the liquid.
- (5) Mixing of the inflammable vapour with air (and re-circulated combustion products).
- (6) Ignition of the vapour and subsequent heat transfer to the droplets by conduction from flame front now surrounding them.
- (7) Progressive combustion of the droplets.
- (8) Formation of flame carbon (soot) and, in some cases, carbonaceous residues.
- (9) Combustion of the soot and carbonaceous residues.

The model droplet used in these studies is as shown in Fig. 20.

A similar model was used by Nurrazaman et al (46).

The combustion of heavy residual fuel oil droplets has been

envisaged to be as follows: the volatile material is distilled from the droplet and the customary flame established. Combustion proceeds, swelling and contraction maintaining the droplet diameter at approximately the initial value. The outer droplet shell, becomes more viscous and towards the end of the volatile combustion period, is inflated and finally ruptured by internal gas pressure. Surface tension forces act to decrease the size of the viscous envelope, but almost simultaneously, cracking of the non-volatile residue causes solidification. The resulting carbonaceous material burns heterogeneously by a surface reaction.

3.2 PREVIOUS WORK ON COMBUSTION OF OIL DROPLETS.

Studies (47, 48, 49) have shown that during the combustion of heavy fuel oil droplets, a so-called cenosphere (i.e. a thermally-degraded oil droplet of carbonaceous residue) is formed and that the material consists mainly of residual carbon.

Sakai and Sugiyama (50) have indicated that there are two products of incomplete combustion, as shown in Fig. 21.

- (a) Solid particles in the size range 10-200 microns, resulting from combustion of residual heavy fuel-oil.
- (b) Carbonaceous substances deposited from the gas phase in a diffusion of pre-mixed flame of hydrocarbon fuels i.e. thermal cracking of the volatile content.

Thomas (51) referred to the latter particles as 'soot'. He also stated that carbon particles and soot particles differ in chemical composition. Soot, he suggests, is not carbon, but simply

has a large poly-benzenoid hydrocarbon structure, formed by cracking of the volatile content of the oil.

Clarke and Hudson (52) agree with the idea of soot formation by cracking of the volatile content of the oil, but intimated that in the case of a Bunker oil, a more likely cause of soot is the enhanced tendency of the oil to crack on account of the high carbon/hydrogen ratio (7:1).

It is evident that the combustion phenomena of atomised heavy fuel-oil droplets are complicated. During the combustion of heavy fuel oil, soot particles and carbon particles are produced simultaneously. However, the soot particles may be completely burnt away in the time and space available, because of their smaller diameter (generally less than 0.1 micron), whereas the much larger carbon particles remain.

Kito et al (53) believe that the time required for combustion of droplets is largely occupied by that of combustion of residual carbon particles. Many studies have been undertaken (54, 55, 56, 57) on the combustion of these particles, and Von Bogdandy (22) illustrates the combustion of coal particles. Fig. 22 indicates the burning time of a carbon particle and an oil droplet. As can be seen, the carbon particles require a longer burning time for complete combustion, and in the combustion zone of the furnace, this time is not available. Heynert (21), working from a knowledge of blast velocity and the length of the combustion zone, states a residence time of only 2-5 microseconds is available for complete gasification.

Sakai and Sugiyama have calculated the critical coke generating

diameter of the fuel-oil droplets, by considering the combustion history of a single oil droplet. They postulate the relationship:

$$D_{\text{perit}} = K (k_s O_s)^{\frac{1}{2}} \quad 3.1$$

where

D_{perit} = coke generating diameter.

K = constant = $(k_1 / k_s + k_1)^{\frac{1}{2}}$

k_s = gasification constant (solid).

k_1 = gasification constant (liquid).

O_s = residence time of particle in combustion zone.

Coke particles will be generated from fuel oil droplets greater in diameter than D_{perit} , while with diameters smaller than D_{perit} , the particles are able to burn out completely before emission from the combustion zone, which is considered to be of the order of 2-3 feet.

More studies of the size and structure of the coke particles were reported by Masdin and Thring (46) and Masdin and Foster (58). They correlated the diameter of carbon particles formed during the combustion of pitch-cresote droplets in air at 700°C with the square of the initial droplet diameter.

$$D_o = 0.66 D_o^2 \quad 3.2$$

where

D_o = cenosphere diameter.

D_o = initial droplet diameter

From this relationship, and also from Eq. 1.1, namely

$$D_o^2 - D^2 = K (t - t_o)$$

it can be clearly seen that for efficient combustion, the initial particle size, D_o , is of great importance, and atomisation of the

liquid fuel stream is required for this condition to be met.

3.3 COMBUSTION WITH PRESSURE ATOMISATION.

Joyce (59) considered the effects on combustion of a spray resulting from pressure atomisation. At low pressures (e.g. up to 100 psi.), the spray structure was more uniform in terms of droplet sizes, giving a relatively narrower size range distribution than at high pressures (e.g. over 500 psi.), although at high pressures, the average drop size produced was smaller. Because a considerable proportion of the droplet size range is in the small size range, the initial ignition of the spray is facilitated and the stable continuity of burning promoted. Once the flame is established it is almost certain that many of the small size droplets successively emerging from the atomiser provide a stable gaseous flame region as a foundation for the rest of the flame.

3.4 COMBUSTION WITH TWIN-FLUID ATOMISATION.

Archer and Eisenklam (60) have investigated the twin-fluid atomiser with regard to efficient combustion, the purpose of their study being to compare the effects of air and super-heated steam as the atomising fluid. It is known that the drop size is inversely proportional to the relative velocity between the atomising fluid and the fuel, and inversely proportional to their mass ratios. At high velocities, the mass ratio of atomising fluid to fuel is the most important variable.

The use of an atomising gas at a constant mass ratio of atomising fluid to fuel influences, as expected, the initial spray drop size and

hence the burning time of the fuel.

The researchers found that the same mass flow-rate and pressure, the velocity of super-heated steam at 170°C was twice that of air at 40°C when used as the atomising fluid. At a mass ratio of 1, the drop size was reduced by some 15% by using atomising steam instead of air.

Analysis of experiments to show the effect of possible benefits of steam atomisation revealed that for the same comparative velocities of air and steam, the % fuel which formed carbonaceous solids was 2.9% for air and 2.06% for steam. At the same mass ratio of atomising fluid-to-fuel, the reported figures were 2.9% for air and 1.8% for steam.

3.5 COMBUSTION OF FUEL OIL IN BLAST FURNACES.

In all cases of combustion, the number of big droplets that can be tolerated depends upon the relative proportion of large-to-small droplets (the flame-sustaining capacity of the latter enhance their burning rates).

In general, large droplets of liquid fuels are to be avoided as far as possible, unless there is adequate time for their complete combustion.

As indicated by Haynert (21), the particle size necessary for efficient combustion in the oxidation zone of the tuyeres lies in the size range 25-45 microns, as shown in Fig. 22. To achieve such a small droplet size efficient atomisation in the blow-pipe region of the blast furnace is of the greatest importance.

Another parameter affecting combustion is the temperature of the

air blast. Increasing this temperature, besides improving the overall thermal efficiency of the process, gives a higher initial temperature in the combustion zone, and thereby reduces the ignition lag and overall combustion time.

The two products of incomplete combustion, carbon particles and soot, are always formed during the burning of heavy fuel-oil, the amount depending on the degree of atomisation and the residence time in the combustion zone of the furnace. While the presence of soot particles should pose no problems, due to their small size and thus easy combustion, the carbon particles can be drastically reduced by improving atomisation and increasing residence time in the combustion zone of the tuyere region.

BIBLIOGRAPHY.

- (45) Masdin E.G. and Thring M.W. Journal of Inst. Fuels. 251-260 1962.
- (46) Nurrazaman A.S. et al Journal of Inst. Fuels. 301-310 1970.
- (47) Goodridge M. and Horsley M.E. Journal of Inst. Fuels. 599-606 1971.
- (48) Wright F.J. 12th. Int. Combustion Symp. 1968.
- (49) Hottel H.C. 5th. Int. Combustion Symp. 1955.
- (50) Sakai T. and Sugiyama S. Journal of Inst. Fuels. 295-300 1970.
- (51) Thomas A. Combustion and Flame. 6, 1, 46 1962.
- (52) Clarke J.S. and Hudson G.J. Journal of Marine Engrs. 135-172 1959.
- (53) Kito M. et al Combustion and Flame. 17, 391-397 1971.
- (54) Smith D.F. and Gudmundsen A. Ind. Eng. Chem. 23, 277. 1931.
- (55) Yagi S. and Kunii D. 5th. Int. Combustion Symp. 1955.
- (56) Essenhigh R.H. et al Ind. Eng. Chem. 57, 33 1965.
- (57) Tu C.M., Davis H. and Hottel H.C. Ind. Eng. Chem. 26, 749 1934.
- (58) Masdin E.G. and Foster P.J. Fuel. 39, 413 1960.
- (59) Joyce J.R. Journal of Inst. Fuels. 150-156 1949.
- (60) Archer J.S. and Eisenklam P. Journal of Inst. Fuels. 397-404 1970.

Fig. 20

MODEL OIL DROPLET OF MASDIN AND THRING. (46)



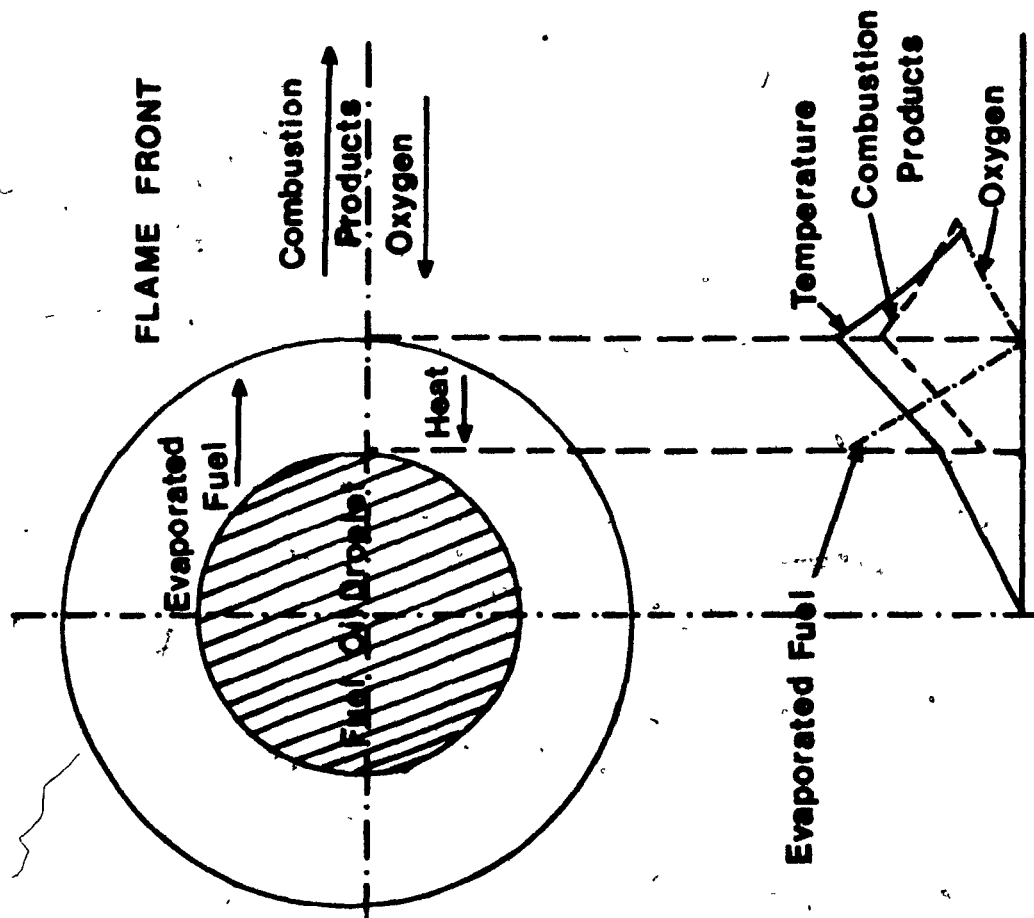
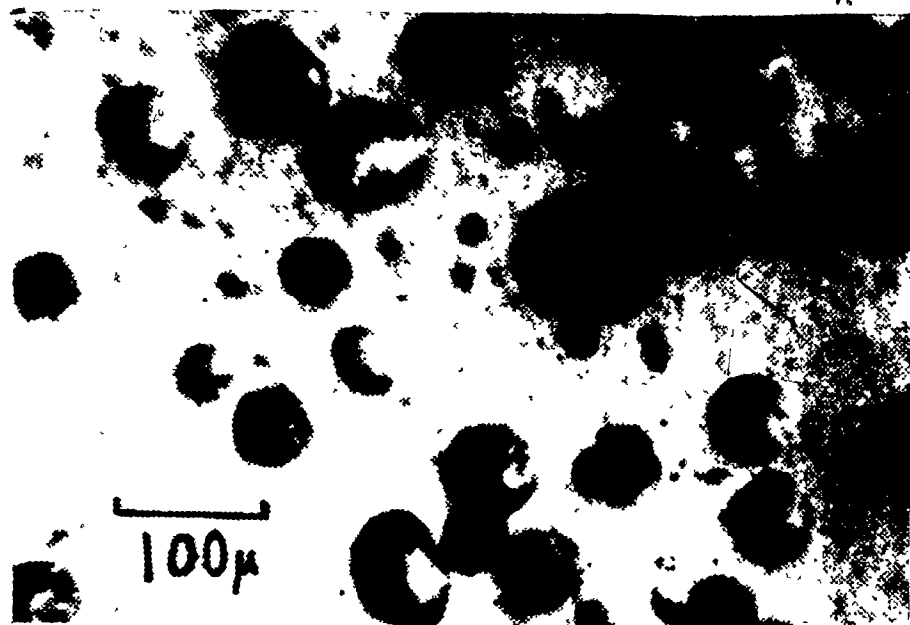


Fig. 21

- (a) PARTICLES OF CARBON BLACK FROM INCOMPLETE COMBUSTION
OF OIL. (50)
- (b) PARTICLES OF SOOT IN GAS-CLEANING PLANT.



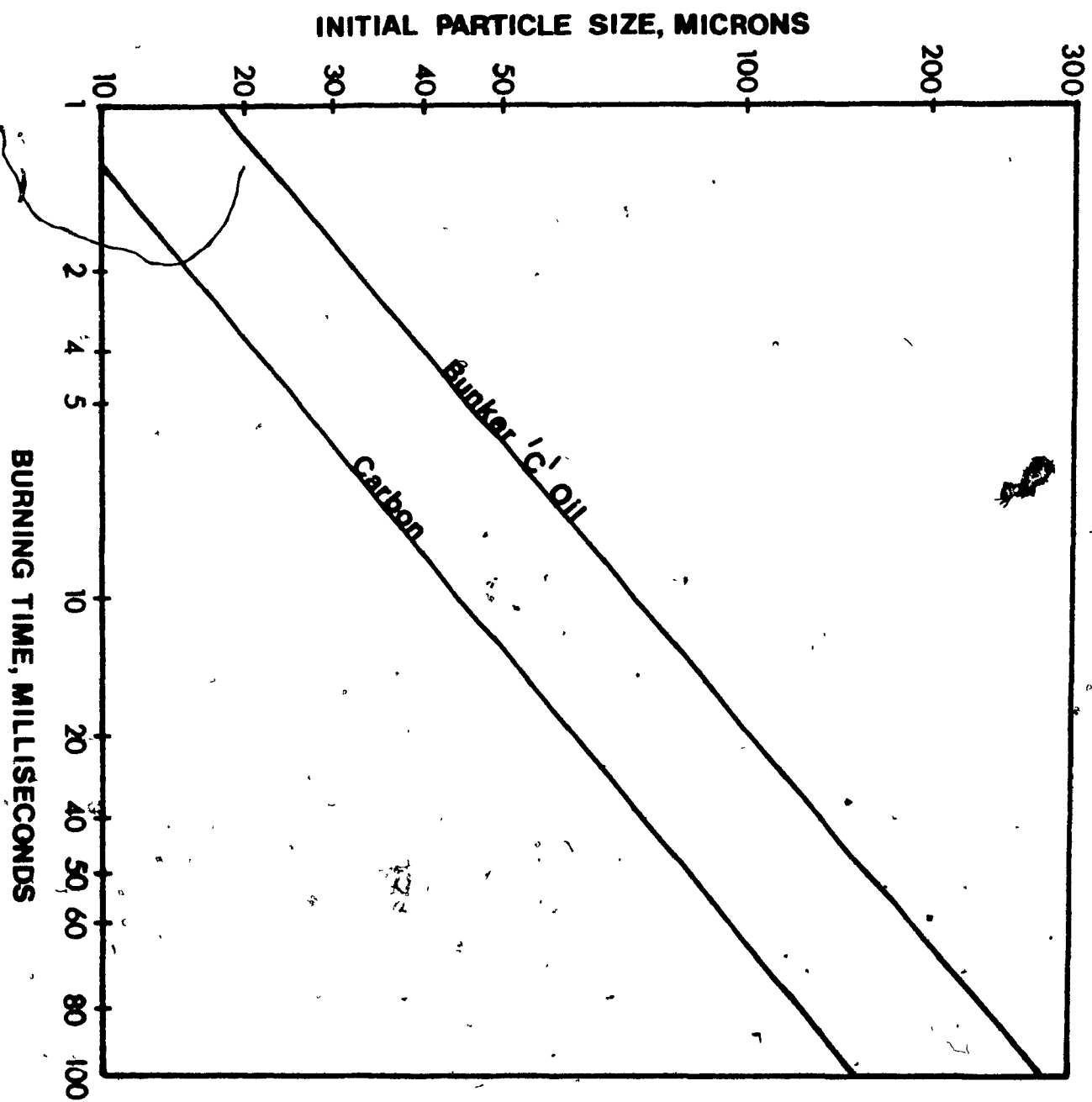
a.

b.



Fig. 22

BURNING TIME OF OIL PARTICLE AND CARBON PARTICLE (52)



Chapter 4

ATOMISATION.

4.0. INTRODUCTION.

The need for atomising fuel oil within the blast furnace blow-pipe has already been underlined in chapter 3. The most common methods of atomising liquid streams are: pressure atomisation, twin-fluid atomisation, rotating-disc atomisation, and much less commonly, atomisation by an electrical charge. However, since only pressure atomisation and twin-fluid atomisation find application in current blast furnace practice, the discussion shall be limited to them.

4.1 PRESSURE ATOMISATION.

The simplest method of causing a stream of liquid to disintegrate is to use pressure energy. By converting it into kinetic energy through acceleration of the liquid, there is a tendency for the liquid to disrupt as it exits from a nozzle. There are two distinct types of pressure nozzle, one which imparts a rotational velocity to the fluid, and one which causes the liquid to exit as a solid stream, or jet, to be disrupted at some distance away from the nozzle.

The swirl spray atomiser, Fig. 23, is the most commonly used nozzle which falls into the pressure atomisation category. Many theories (61-66') have been proposed to explain the principles of atomisation for this type of atomiser. In its simplest form, the atomiser consists of a chamber into which the liquid flows tangentially, and leaves by a centrally-located orifice, of smaller diameter than the spray chamber. A hollow air core is formed concentric with the nozzle axis. The resultant exiting conical sheet, which is very thin, attenuates rapidly, becomes unstable, and disintegrates into droplets.

At low flow rates, the hollow cone may not form properly, the resulting 'drowned spray' giving much coarser droplets.

All simple pressure atomisers suffer from low flexibility, (or turn down ratio) because the discharge rate varies approximately as the (injection pressure)^{1/2}. For certain applications, this can be corrected by using a 'spill-type' nozzle, Fig. 24, where part of the fluid is returned from the swirl chamber to the supply side.

In summary, the pressure nozzle is usually simple and cheap, but it has several disadvantages. It cannot be used to atomise slurries, (because of the possibility of clogging if orifice is small) or very viscous liquids (because of excessive liquid pressure drop or of poor resulting atomisation).

4.2 PNEUMATIC ATOMISERS (OR TWIN-FLUID ATOMISERS).

The twin-fluid atomiser has few of the limitations of the pressure atomiser. It is more adaptable with slurries and viscous liquids, since there are no small orifices to clog. Very fine average drop sizes can be obtained, although the drop-size distribution range is large. Efficient atomisation can be obtained over a wider range of liquid flow rates with twin-fluid atomisers, while high liquid injection pressures are not required.

Unlike pressure atomisation, where all the energy for bringing about liquid disintegration must be contained within the liquid itself, the twin-fluid system also uses the pressure energy of the gas.

Since this energy is independent of liquid flow rate, smaller droplet sizes as well as wider spray angles can be achieved at low liquid

rates, compared to pressure atomisers.

The simplest twin-fluid atomisers are converging nozzles. In these atomisers, a core of liquid is impacted co-axially by a high-velocity gas stream. At low liquid flow rates, the jet is violently disturbed by the impinging gas stream. The liquid stream becomes distorted and is readily blown apart. However, when the liquid throughput is high and the stream diameter large, the energy efficiency of the applied stream is lessened.

As a means of overcoming this limitation, atomisers are constructed with means of spreading the liquid into a thin sheet before being contacted with the gas stream. This is usually accomplished by passing it through a kind of 'swirl-spray' nozzle. This process is called 'pre-filming' and excellent atomisation can be achieved at high liquid flow-rates.

Clare and Radcliffe (67) have designed an air blast atomiser, Fig. 25 for use with viscous fuels. An essential feature of this atomiser is that the fuel is introduced radially inwards into a swirling air stream just before it exits from the atomiser into the combustion chamber. They found that the droplet size depended mainly upon the air/fuel ratio and that the air pressure and fuel gap only affected the droplet size by altering the fuel/air ratio. When the fuel injection pressure was high, it was noticed that the droplets were smaller than for low fuel pressure at the same air/fuel ratio.

4.3 THEORY OF ATOMISATION.

There have been a number of excellent reviews on the principles

of atomisation (68-72). The first contribution to the phenomena of jet disintegration was that by Rayleigh (73), who noted that when a stream of inviscid liquid issues from a pipe at a relatively low velocity, into still air, the probable length before break-up is about 4.5 times the diameter of the liquid jet. This follows from a concept of minimisation of surface energy which shows that under the conditions mentioned, the disrupted stream can form droplets, whose cumulative surface area is less than that of the 'parent' stream. In practice, the size of these droplets depends upon the physical properties of the fuel and gaseous medium into which it is injected (e.g. viscosity, surface tension), as well as the nature and intensity of fluid disturbances created within a given atomiser (74).

Analysis by Schweitzer (75) concluded that jet disintegration could be effected without air action if a high turbulence level was obtained on exiting from the nozzle. However, ordinarily, both turbulence and air friction combine to break up the jet. Hinze (76) also suggested that turbulence caused initial surface disturbances in the jet, but that these were amplified by air friction to form ligaments which tore off from the jet stream.

Where a large tangential velocity is imparted to the liquid, as is the case with the swirl atomiser, the liquid spreads out into a thin conical sheet. Such a sheet is less stable than a jet and is particularly susceptible to disruption by air resistance. It has been shown (77,78) that these thin films tend to develop waves, which build up, whip back and forth (and may eventually curl back completely) to form unstable hollow tubes which break into drops.

Conditions in the blow-pipe of a blast furnace are such, however, that the issuing stream of fluid, whether it be a jet or a thin sheet, is subjected to a high velocity air blast.

4.4 ATOMISATION IN AN AIR STREAM.

A number of studies (79,80,81) have been made with regard to the phenomena of break-up of liquid jets in high-velocity air blasts. These have generally been conducted on single drops, to analyse disintegration mechanisms. However, some investigations (82,83) were of a more practical nature, such as the study of fuel injection into ramjets etc..

The first theory of jet disintegration to gain acceptance was that of Castleman (84) who proposed that disturbances (or ripples) were induced on the surface of the jet by an air blast. Such disturbances were drawn out into 'ligaments', with one end remaining anchored to the bulk liquid. These ligaments were cut off from the bulk to collapse into drops. The important parameter, governing jet disintegration, as postulated by Castleman, was the effect of the relative velocity between the air and fluid streams. This theory was supported by the photographic work of Lee and Spencer (85), Littaye (86), and Sustrunk (87). However, the latter workers disagreed with Castleman's conclusion that a minimum drop size of about 7 microns for oil resulted because increasing the relative velocity caused the ligaments to detach as quickly as they were formed.

Similar theories have been proposed by Mayer (88) and Adelberg

(89). Both considered the shredding of ligaments, and subsequently, of liquid drops, from waves on the liquid surface. The waves were assumed to be initiated by some disturbances, such as internal turbulence, foreign gas bubbles, pressure fluctuations, etc.. The model proposed by Adelberg is as shown in Fig. 26.

These theories are intended for use with a simple pressure nozzle, where there is no atomisation prior to injection into the gas stream. The effect of injecting fluid in such a manner into a supersonic air stream was clearly demonstrated by the photographic work of Szpiro (90). The effect would be the same if subsonic velocities were used, although drop size and spray distribution would undoubtedly be different.

When the liquid is atomised prior to introduction into the air blast the issuing thin sheet is immediately disrupted, ligaments being 'torn-out' and droplets produced. The phenomena of secondary atomisation now proceeds.

This phenomena was initially observed by Hochschweinder (91), but dramatically illustrated by the photographic studies of Lane (92) on the break-up of single drops in an air-stream, Fig. 27. It was observed that as the drop came under the influence of the air stream, it became increasingly flattened, and, at a critical air velocity, it was blown out into the form of a hollow bag attached to a circular rim. Subsequent bursting of this bag produced a shower of fine droplets, and the rim, which contained at least 70% of the mass of the original drop, broke up later into much larger drops.

Similar results have been reported by Simons and Goffe (93),

Nukiyama and Tanasawa (94), and Andersen and Wolfe (95).

The break-up of drops in fast air streams has been observed to be strikingly different from that in a steady stream of air. In this case, the drop is deformed in the opposite direction and presents a convex surface to the air flow. The edges of the saucer shape are drawn into a thin sheet and then into fine filaments which in turn break up into droplets.

Whether or not the droplet is blown into the shape observed depends on surface tension, initial drop size, air velocity, and the nature of the exposure of the drop to air.

Balze and Larson (96) concluded that the maximum stable drop size was proportional to;

$$\frac{\gamma_L}{\rho_A (V_r)^2}$$

where

γ_L = surface tension of the liquid.

ρ_A = density of air.

V_r = relative velocity between air- and fluid- streams.

Ranger and Nichols (97) noted that the impact by a strong shock-wave was an insignificant element in producing the shattering of a liquid drop. The factor causing disintegration was the high-speed convective flow, produced by the shock wave. A drop, originally spherical, would be deformed into an ellipsoid with its major axis perpendicular to the direction of flow. The shearing action exerted by the high-speed gas flow caused a boundary layer to be formed in the surface of the liquid and the stripping away of this layer accounted, for the break-up. These studies further support the fact that the

break-up time is proportional to the initial droplet diameter, and the (liquid-to-gas density ratio)^{1/2}, and inversely proportional to the relative velocity.

Beuthen (98) concluded, in a physical study of blast furnace oil injection, that droplet size did not vary significantly when injection of fuel oil into the hot air blast was undertaken, using both a simple nozzle, where no primary atomisation was effected, and a complex hydraulic nozzle, where there was primary atomisation, intimating the accepted fact that secondary atomisation of the fluid stream by the air blast is the main parameter as regards fineness of droplet size.

Weiss (72), in an excellent study of atomisation suitable for ramjets, observed that the droplet size decreased by some 20-30% when primary atomisation was undertaken. However, at high air blast velocities approaching 650-700 feet/second, the difference in drop size between the two atomising techniques became negligible. It should be noted that the nozzles used by Weiss all exhibited low flow rates, from 0.1 to 1.0 gallons/minute, and thus the results obtained can not be directly correlated to blast furnace practice, but may be useful in indicating expected trends.

BIBLIOGRAPHY.

- (61) Doble S.M. Engineer. 21, 61, 103. 1945.
- (62) Radcliffe A. Proc. Inst. Mech. Engrs. 169, (3), 93. 1955.
- (63) Taylor G.I. Quart. J. Mech. Appld. Math. 11, 129. 1950.
- (64) Warson E.A. Proc. Inst. Mech. Engrs. 158, (5), 187. 1948.
- (65) Taylor G.I. 7th. Int. Congress of Appld. Mech. 280. 1948.
- (66) Dombrowski N. and Hasson D. A. I. Chem. E. J. (7), 604. 1969.
- (67) Clare H. and Radcliffe A. Journal of Inst. Fuel. 510. 1954.
- (68) Longwell J.P. D. Sc. Thesis. M.I.T. 1943.
- (69) Orr C.J.Jr. 'Particulate Technology' McMillan, 1966.
- (70) Giffen E. and Muraszew A. 'The Atomisation of Liquid Fuels'.
John Wiley, New York, 1953.
- (71) Graves C. et al N.A.C.A. Report 1300. 1957.
- (72) Weiss M.A. Ph. D. Thesis. Columbia University, 1958.
- (73) Rayleigh Lord, London Math. Soc. Proc. 10, 4. 1878-9.
- (74) Fraser R.P. 6th. Int. Combustion Symp. 687-701. 1956.
- (75) Schweitzer P.H. Penn. State Coll. Bull. No.12. 1930.
- (76) Hirze J.O. 6th. Int. Congress Appld. Mech. Paris, 1946.
- (77) Fogler N. and Kleinschmidt J. Ind. Eng. Chem. 30, 1372. 1935.
- (78) Larcombe H.L.M. Chem. Age. 57, 563, 597, 621. 1947.
- (79) Kauffman C.W. and Nicholls J.A. A.I.A.A.J. 9, (5), 880-85. 1971.
- (80) Kauffman C.W. et al Comb. Sci. and Techn. 3, 165-178. 1971.
- (81) Lewis H.c. et al Ind. Eng. Chem. 43, 67-74. 1948.
- (82) Weiss M.A. and Worsham C.H. A.R.S.J. 29, 252-9. 1959.
- (83) Weiss M.A. and Worsham C.H. Chem. Eng. Sci. 16, 1-6. 1961.
- (84) Castleman R.A.Jr. J. Res. Nat. Bur. Stand. 6, (3), 369-76 1931.

- (85) Lee D. and Spencer R.C. N.A.C.A. Report 454. 1933.
- (86) Littaye G. Compte. Rend. 217, 304. 1943.
- (87) Sustrunk R. Compte. Rend. 215, 404. 1942.
- (88) Mayer E. A.R.S.J. 12, 1783-5. 1961.
- (89) Adelberg M. A.I.A.A.J. 6, (6), 1143-47 1968.
- (90) Szpiro E.J. M.Sc. Thesis. McGill University, 1965.
- (91) Hochschweinder H. Ph.D. Thesis. Heidelberg, 1919.
- (92) Lane W.R. Ind. Eng. Chem. 43, 1312. 1951.
- (93) Simons A. and Goffe G.R. Aero Research Council. R. & M. No.2343.
- (94) Nukiyama S. and Tanasawa Y. Trans. Soc. Mech. Engr's. (Japan).
5, 1-4, (1939) and 6, s7-s8 (1940).
- (95) Andersen W.H. and Wolfe H.E. 5th. Int. Symp. Shock Tubes.
(Pt. 1 & 2). 1965.
- (96) Balze O. and Larson L.V. A.A.F. Air Material Command.
Rpt. No. MCREXE - 664 - 531B 1949.
- (97) Ranger A.A. and Nicholls J.A. A.I.A.A.J. 7, (2), 285-90 1969.
- (98) Beuthen W. Erdoel und Kohle, Erdgas, Petrochemie.
18, (4), 83-8 1965.

Fig. 23

SWIRL SPRAY ATOMISERS.

Fig. 24

"SPILL-TYPE" SWIRL ATOMISER

Fig. 25

PNEUMATIC ATOMISER OF CLARE AND RADCLIFFE (67)

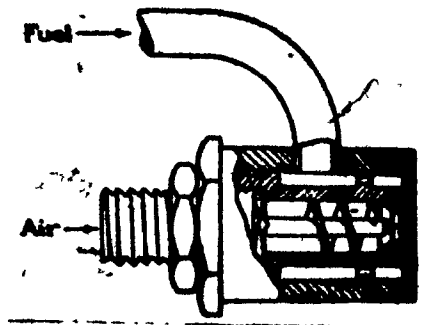
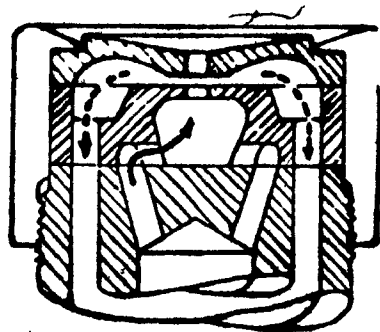
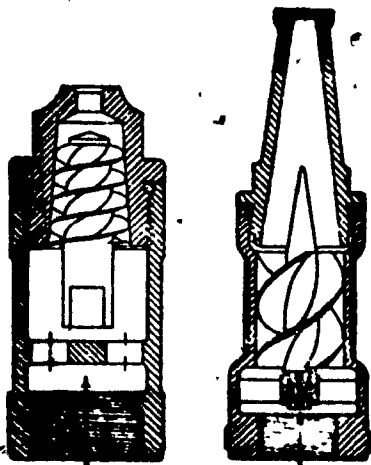


Fig. 26

MODEL FOR JET DISRUPTION.

After Adelberg (89)

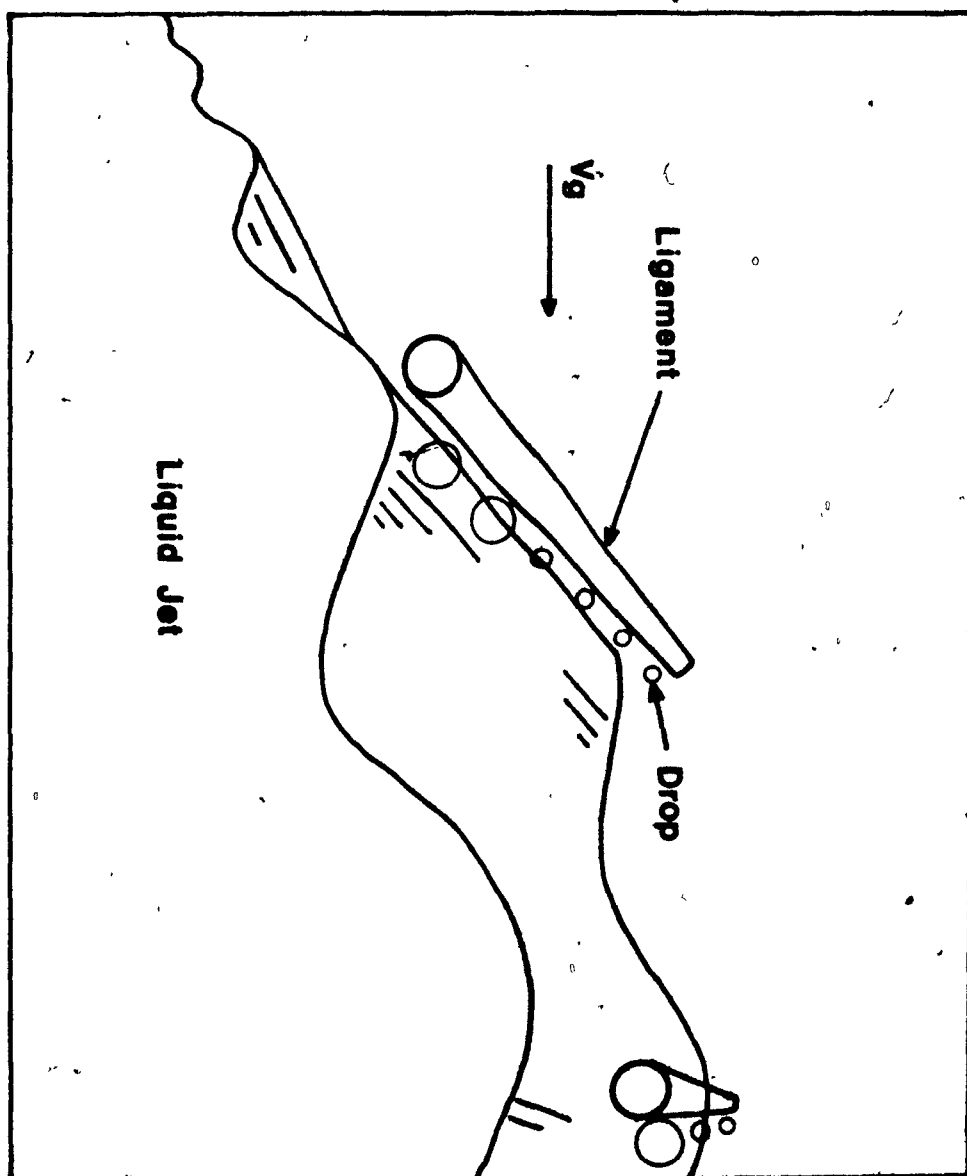
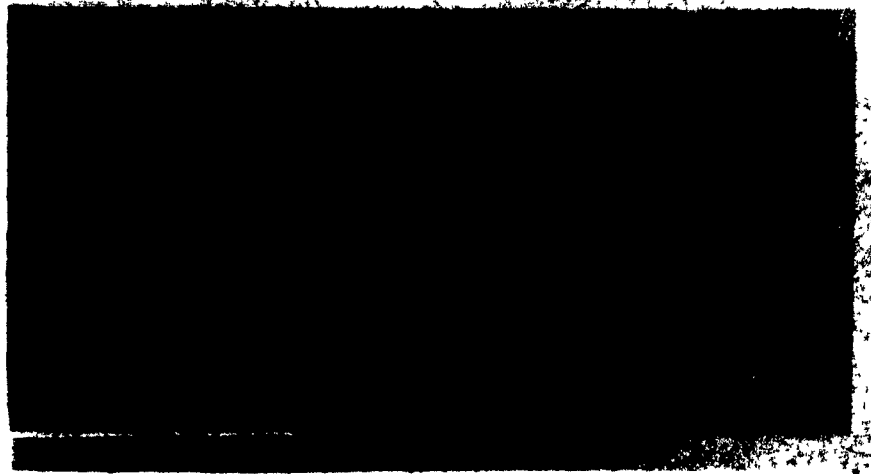


Fig. 27

BREAK-UP OF WATER DROPS IN AN AIR STREAM.

After Lane (92).



Chapter 5.

INJECTION OF WAX INTO STILL AIR.

5.0 INTRODUCTION.

This chapter concerns nozzle design and the performance characteristics of the present corkscrew nozzle operating in still air.

5.1 THEORY OF NOZZLE DESIGN:

As indicated previously, the corkscrew-insert nozzle was designed specifically for trials on No. 3 blast furnace at Dofasco. Thus, the design had to be such that the nozzle made optimum use of pumping pressure. Since the oil pump operating No. 3 oil delivery operated at a maximum allowable exit pressure of 180 psig, and line pressure losses were about 50 psig, down to the oil lances, a two-revolution (or spiral) corkscrew was found to be best suited for obtaining the required oil rates of 2.4 gallons per minute per lance (2000 gallons per hour overall). Guthrie, in his initial design study (20), indicated that, with a blast furnace pressure of about 30 psig, the available pressure differential for atomisation was about 120 psig. As can be seen from Fig. 28, three-spiral corkscrew inserts could not deliver the required flow rates, due to the increased pressure drop across the lances.

The pitch of the insert had to be such that the spray was discharged at an angle, such that, in the high velocity blast, the particles approached the walls of the tuyere, thereby facilitating subsequent mixing prior to evaporation and combustion.

While deciding upon the optimum pitch of insert (the pitch is the number of spirals to the inch), it was found that the only pitch of corkscrew commercially available was one with 4 spirals to the inch,

where each spiral had an angle of 60° . Since this approached the requisite design pitch, and large quantities could be readily obtained, their use was adopted.

In the initial studies, it was thought that there was little chance of the spray being 'thrown out' to the walls of the tuyere, due to the high velocity air blast, and thus the insert was moved $\frac{1}{4}$ " from the lance opening so as to minimise rotational energy losses due to the shearing action of the spinning oil on the walls of the lance. This was considered to be a reasonable compromise between the uniformity of the exiting spray and rotational energy losses.

5.2 INVESTIGATION OF INITIAL NOZZLE DESIGN.

One of the many nozzles that had been used in the plant trials was returned to the laboratory. It was found that in spraying water at a pressure of 80 psig (which was the maximum mains supply pressure), a true hollow cone did not form. The water was sprayed vertically downwards, and collected in a series of containers placed in a circle, at a distance of 18", as shown in Fig. 29. The collected water was then measured to determine the volume in each container, and from this data, an indication of spray uniformity could be obtained.

5.3 CURRENT NOZZLE DESIGN.

The spray lances used in the present investigation were geometrically similar to those used in the plant scale study (i.e. $\frac{1}{2}$ " O.D., $\frac{1}{4}$ " I.D.), but made from acrylic tubing rather than mild steel.

The nozzles were made by screwing the inserts, which measured $\frac{1}{4}$ "

diameter, into the acrylic lance. The insert was then broken off from the original corkscrew, so that two revolutions remained in the tube. The distance from the end of the insert to the exit orifice was varied until a hollow cone spray, with maximum cone angle, was formed. Fig. 30 shows the completed nozzle, with the insert set at the optimum distance of $3/4$ " from the end of the exit orifice.

5.4 MODELLING - EXPERIMENTAL APPARATUS FOR STILL AIR ATOMISATION STUDIES.

Since tests involving heated oil was not possible, with the laboratory facilities available, water was first used as a substitute. As seen in Table 5-1, water has a viscosity of 1 cp (5 SUS), a density of 1 gm. cm.^{-3} and a surface tension of $73 \text{ dynes cm.}^{-2}$, at 70°F , compared with 24 cp (120 SUS), $0.98 \text{ gm. cm.}^{-3}$, and 22 dynes/cm.^2 respectively for Bunker 'C' oil at 220°F .

Although the figures do not correlate precisely, it was decided that the results on spray trials using water would provide a useful indication of optimum injection practice for good spray uniformity.

The apparatus used for these preliminary studies is shown in Fig. 31. Two cylinders, one containing compressed air, the other water, were connected, and a constant high gas pressure maintained in the water cylinder by suitable adjustment of the pressure regulator. When needle valve D was opened, the water was displaced from the cylinder, and into the lance. A pressure gauge on the exit side of the cylinder monitored the exit water pressure, since no significant variations in either air pressure or water pressure occurred during the course of a

run, no needle valve adjustments were necessary to provide constant water flowrates into the lance.

A series of photographs were then taken to study the effect of injection pressure on the cone angle of the issuing spray. This was done using Kodak Tri-X film, with a shutter speed of 1/500 th. second. The injection pressures used in the study were 20, 40, 60, 80, and 100 psig.

5.5 DROPLET SIZE ANALYSIS OF WATER INJECTION.

In view of the importance of particle size and particle size distribution in combustion phenomena, an efficient method of droplet size analysis was essential. However, perhaps as a consequence of the high flow rates involved, from 1.8 gallons per minute (at 20 psig) to 3.2 gallons per minute (at 100 psig), collection of the water spray droplets proved impossible. Dilute solutions of gelatin in water, glycerine, oil with additives, and other techniques failed owing to the tendency of the water to 'spread' across the surface of the collecting medium. In those cases where the water penetrated the surface of the collecting agent, droplet coalescence occurred. Similar difficulties were encountered with collection of the water drops on glass slides covered with MgO or soot.

5.6 INJECTION OF MOLTEN WAX INTO STILL AIR.

Due to the difficulties involved in obtaining particle sizes with water, an alternative system was adopted to provide data on droplet size distribution ⁱⁿ view of its importance in terms of combustion efficiencies. A paraffin wax was finally chosen as being closest to

ideal because of (a) its similarities with Bunker 'C' oil in terms of viscosity, density and surface tension (see Table 5-1), (b) its low vapour pressure (which means no evaporation during testing and thus a reliable final drop size) and (c) the ease of subsequent droplet size analysis by allowing the wax droplets to freeze in flight.

An equivalent system to that previously described for water spray studies was used, as shown in Fig. 32. In the wax cylinder, melting and temperature control were accomplished using a 500 watt heating element, connected in series with a variable resistance. The cylinder was lagged with a $\frac{1}{4}$ " thick refractory cement to prevent excessive heat loss to the surroundings.

The wax chosen as a substitute for oil was Mobilwax 2305, a high melting point paraffin wax. The viscosity chart of this wax is as shown in Fig. 33, where it will be seen that the viscosity of the wax over the temperature range 195-210°F is practically equivalent to that of Bunker 'C' oil injected into blast furnaces between 170-200°F.

Other relevant physical properties are given in Table 5-1, which also close match those of Bunker 'C' oil.

A lower melting point paraffin wax was also used in the initial work. The viscosity of this latter wax was lower than that of Mobilwax 2305, while the surface tension was similar at 13 dynes cm.⁻² (at temperatures from 190-210°F). This allowed the effect of viscosity on droplet size to be ascertained.

Initial experiments involved spraying wax at various injection pressures and determining resultant wax flow rates by spraying it into a large container for a known period of time, and weighing the

amount collected.

An injection temperature of 200°F was chosen so as to give an exiting wax viscosity of about 20 cp (100 SUS), and thereby match the viscosity range of oil injection. It was found that by controlling the temperature of the molten wax, in the cylinder, an exiting wax temperature of 200°F was achieved from the lance when spraying into still air at 70°F.

The height of the nozzle from the ground was set at five feet at a slight upward angle, so that the sprayed wax droplets froze before being collected on a polythene sheet set ten feet from the nozzle, Fig. 34. Using these procedures, the collected wax froze in flight and remained undeformed on impact.

5.7 ANALYSIS OF WAX SPRAY.

Various methods of analysing the droplet size distribution of the sprayed wax were tried. The simplest considered was that of mechanical sieving, whereby the solid wax could be sized according to the mesh sizes of different screens. This method proved unsatisfactory, due to softening of the wax, and subsequent clogging of the mesh.

The method finally adopted was to riffle the collected wax down to a weight of 50 grams, this being deemed to be representative of the whole of the wax sprayed (typically, 1000 grams). Portions of the riffled sample were placed on glass slides and random areas photographed on a Vickers Projection microscope, using a macrographic lens, at a magnification of X40. The photographs were taken using Polaroid Type 42 film, which provided the necessary resolution and

depth of field. It was decided to take photographs at two different focus settings, in order that both the large droplets and small droplets could be sized whilst in focus.

The droplets were then sized using an accurate scale, directly from the photographs, although some sizing was done directly from the microscreen. Sizing of the droplets was undertaken by measuring the diameter of the particle. Some 500-600 particles were sized in the initial spray test in order to find the necessary number of particles to be counted for a representative and reproducible value.

Similar work was done using the low viscosity wax at the same temperature as used previously, and under the same conditions.

5.8 DROPLET SIZE ANALYSIS.

The droplet size was determined as the volume-area diameter, or the Sauter Mean Diameter. This had been found in previous studies to be appropriate for combustion work, and the like, since it takes into account the diameters of the large particles, which determine the efficiency of evaporation and subsequent combustion. The Sauter Mean Diameter, or D_{32} , is defined mathematically as $\sum D^3 N / \sum D^2 N$, and was determined by taking a size range, say, 0-50 microns, 51-100 microns, etc., and counting the number of particles whose diameter fell in that range. This analysis was done for all the particles over the entire size range.

5.9 EXPERIMENTAL RESULTS AND DISCUSSION OF RESULTS.

5.9.1 NOZZLE SPRAY CHARACTERISTICS.

From a study of one of the original injection lances used in the

plant trials, the data collected from the water studies was correlated, and Fig 35a), which is a diagrammatic presentation of the spray distribution, obtained. As can be seen, the appearance of the spray was that of a 'drowned cone', i.e. an incomplete hollow cone where one part of the cone was similar to a fan spray. This effect would reduce the uniformity of the spray in the blast furnace blow-pipe, and could be a contributing factor to the results obtained in plant trials.

A similar study of the spray sheet resulting from a nozzle of current design produced; Fig. 35b) reveals that the spray was more uniform, being a near-perfect hollow cone, with little or no deformation at any part of the spray sheet. Consequently, the nozzle design, whereby the corkscrew insert was set $3/4"$ from the lance exit orifice, was deemed satisfactory for further work.

5.9.2 DETERMINATION OF FLOW RATES AND CONE ANGLE AS A FUNCTION OF INJECTION PRESSURE.

Fig. 36 is a study of the formation of cone angle and spray pattern as a function of injection pressure. The pressure used were from 20 psig to 100 psig. From analysis of the photographs of the spray, it was seen that at low pressures, the spray was irregular, due to the cone not being completely uniform, i.e. surface disturbances could be seen. Increase in injection pressure, (and thus flow rate), caused the spray to become more uniform, and at 60 psig, the observed spray exhibited all the characteristics of a good hollow cone.

However, the spray remained as a 'sheet' for some distance from the

nozzle, before break-up of the sheet into drops occurred, by the phenomena of surface disturbances discussed previously in chapter 4. Subsequent increases in injection pressure caused the sheet to be disrupted closer to the nozzle, and at 100 psig, the spray sheet was disrupted immediately on exiting, the resulting spray being composed of myriads of droplets of varying sizes, with a 'blanket' of fine particles on the outside of the cone, surrounding the main 'cone' of coarser particles.

Again from the photographs of Fig. 36, a plot of cone angle versus flow rate was obtained. The cone angles were evaluated from the photographs by drawing a tangent from the nozzle exit orifice to the spray. The results were then plotted as a function of the wax flow rate, as shown in Fig. 37. It was seen that at low flow rates of 1.8 gallons per minute, the cone angle was 75° , due to the incomplete formation of the spray cone. Increase in the flow rate caused the cone angle to increase, and a maximum cone angle of 86° was exhibited at maximum flow rate of 3.2 gallons per minute.

Fig. 38 represents a plot of injection pressure as a function of flow rate. As can be seen, the flow rate of fluid exiting from the nozzle increased from 1.8 gallons per minute (108 gallons per hour) at an injection pressure of 20 psig up to 3.2 gallons per minute (192 gallons per hour) at an injection pressure of 100 psig. These values contain the range of flow rates of oil to the tuyeres as presently practiced in many blast furnaces (99).

The injection pressures used in the investigation depended upon the capability of the pressure regulator governing the constant

pressure head to the fluid being atomised. This regulator had a maximum capacity of 112 psig, but it was decided to use an upper limit of 100 psig for injection.

In order to maintain a stable spray cone, which is essential for consistent drop size analysis, as well as producing a uniform spray distribution, the nozzle should exhibit an approximately linear relationship between the flow rate and the square root of the injection pressure

$$\text{i.e. } K = Q/P^{1/2}$$

where

Q = Flow rate, Imperial gallons per minute.

P = Injection Pressure, psig.

The constant K is a characteristic of any particular nozzle. From a plot of Q vs. $P^{1/2}$, Fig. 39, it can be seen that the relationship was linear and that K is of the order 20. Consequently, it was felt that subsequent drop size studies would be reproducible due to spray cone stability.

5.9.3 DROP SIZE ANALYSIS OF WAX PARTICLES.

Due to the method chosen for wax injection, i.e. no lagging of the lance, it was thought that some problems may be forthcoming due to freezing of the wax in the lance. However, this did not prove to be so, and wax injection proceeded smoothly.

The spray wax was collected on the polythene sheet. The wax particles were noted to form in flight, i.e. sheet disruption was observed, the resulting sheet appearing as a 'mist' of droplets. The

wax droplets were solid on impact, indicating that the spraying distance of ten feet was adequate to allow freezing of the wax in flight. Due to the nature of the waxes, i.e. both exhibited softening tendencies in the conditions prevailing in the laboratory (high humidity and a high room temperature), collection, and subsequent handling, was done with care. The collected wax was then placed in a freezer, prior to examination, to facilitate handling.

When the particles of wax sprayed into still air had been collected and frozen, they were photographed and a photographic study is presented in Fig. 40. The injection pressures were 40 psig, Fig. 40a), 60 psig, Fig. 40b), and 80 psig, Fig. 40c), with an exiting wax temperature of 200°F. From the observations on the Vickers microscope, it was seen that the collected wax particles were, in general, perfectly spherical. There was no indication that any distortion of the particles had resulted on impact with the collecting sheet. Particles of many different sizes were noted, although it appeared that large particles of 300 microns diameter and greater were in the majority. Subsequent analysis proved this to be the case.

No evidence of particle coalescence was noted, although Joyce (100) has reported that small drops can unite in flight to form a larger drop.

A magnification of X40 was found to be adequate for the optical examination and subsequent sizing.

In order to establish the necessary number of particles to be counted, so that any result would be representative and consistent, a number of particles were sized from the photographs, and the Sauter Mean Diameter found, then more particles were sized, and the new

Sauter Mean Diameter found. This technique was continued until the Sauter Mean Diameter was reasonably constant. In all, some 700 particles were sized, with trials being done at two different injection pressures. The results of this analysis can be seen in Fig. 41, where a consistent droplet size was obtained when more than 500 particles were sized. It was seen that fewer than this number resulted in a variable Sauter Mean Diameter, the variation in some cases being 20%.

During the course of this particular study, it was noticed that the Sauter Mean Diameter appeared to be strongly biased towards the diameter of the larger particles, due to the method of calculation. Consequently, the appearance of a particle of greater diameter than the majority would cause the Sauter Mean Diameter to be increased, while a calculation of the Linear Mean Diameter ($\sum ND / \sum N$), would be relatively unaffected.

5.9.4 DROP SIZE AS A FUNCTION OF FLOW RATE.

From a plot of the Sauter Mean Diameter versus the flow rate, Fig. 42, it can be seen that both waxes exhibit similar behaviour, namely that the drop size decreases with increase in flow rate, up to 2.8 gallons per minute, and then increases with further increase of flow rate. This can be explained by noting that at low flow rates, the spray is irregular and not fully formed, and thus breakdown of the spray sheet into 'ligaments' resulted in the formation of coarse drops. Increase of flow rate caused the spray sheet to become more regular, and at 2.8 gallons per minute, the spray was almost at its maximum cone angle, thus subsequent disruption of the sheet resulted in a

proportionate increase in smaller drops. Increase of flow rate beyond this point then caused the particle size range to increase (i.e. an increase in the proportion of both small and large drops was noted), which caused an increase in the Sauter Mean Diameter, due to the increased volume of wax to be atomised, although the spray sheet was disintegrated immediately upon exiting. This phenomena of increase of mean drop size with increase in flow rate, at a stable cone angle, has been reported in many other studies (101, 102, 103), and is a feature of atomisation.

5.9.5 DROP SIZE AS A FUNCTION OF VISCOSITY.

In the atomisation of fluids, it is known that the variables which affect droplet size are (a) properties of the fluid (i.e. surface tension, viscosity, density) and (b) properties of the gaseous medium (density). It is generally agreed that the surface tension and density of the fluid (oil or wax) will not change more than marginally during the process of atomisation. Thus, by maintaining conditions in the laboratory, so that the density of the air did not change, the only variable which could affect the particle size was the viscosity of the wax.

It can be seen from Fig. 42 that at the low viscosity (40 SUS, 2 cp), the Sauter Mean Diameter was significantly lower than that obtained under identical conditions with the high viscosity wax (110 SUS, 5 cp). This is due to the fact that droplet size is directly proportional to the viscosity of the fluid, and hence any decrease in viscosity will result in a decrease in droplet size.

This is significant in blast furnace fuel oil injection in that an increase in the pre-heat temperature of the oil decreases the viscosity, and hence the droplet size, thus affording more efficient combustion.

5.9.6 DROP SIZE DISTRIBUTION OF THE SPRAY.

From an analysis of particle diameters, a size distribution of the collected particles was obtained. There are many possible ways of presenting this data, such as the Rosin-Rammler Distribution and the Nukiyama-Tanasawa Distribution. However, it was decided to make use of a normal distribution, i.e. a simple plot of % particles in the spray whose diameters fall within a certain size range, since this gave an immediate indication of the results.

Such a distribution is presented in Fig. 43, where the flow rates investigated were 1.8 gallons per minute, 2.8 gallons per minute and 3.2 gallons per minute.

It can be seen that at low flow rates, the drop size range was large, from particles of diameter 25 microns up to particles of 1 mm. diameter. However, the majority of particles were in the region of the Sauter Mean Diameter (550-600 microns), and few particles had diameters of less than 100 microns.

With increase in flow rate, the spray sheet became more uniform, and at 2.8 gallons per minute, reached optimum uniformity. This was reflected in the distribution of the particles, since the particle distribution range was narrower, with an increased proportion of droplets having diameters less than 100 microns. Further increase of flow rate caused the distribution range to increase slightly,

with some particles exhibiting diameters of up to 700 microns.

5.9.7 REPRODUCIBILITY OF RESULTS.

In the droplet size analysis, the figures reported are the mean value of results obtained at each variable increment, whether it was injection pressure or flow rate. At least three trials were done at each increment of pressure/flow rate. It was noted that in most cases, the reproducibility was good, being of the order 5-7%. However, particularly at the high flow rates, where an increased size range was noted, the errors were somewhat higher, being 10-15%, due to the appearance of a large particle, which would cause the Sauter Mean Diameter to increase. Nevertheless, the trend of drop size as a function of the variables already mentioned does follow previously reported ones.

It is difficult for any investigator to be completely unbiased in the selection of areas for counting and sizing, and hence in some trials, photographs were taken of areas where no visual observation had been undertaken prior to photography. Drop size analysis did not reveal any major differences in the Sauter Mean Diameter between the two methods of photography.

5.10 EFFECTIVENESS OF WAX FOR INJECTION STUDIES

The purpose of this initial study of wax injection into still air was to test the performance of the modified nozzle under operating conditions, and also to justify the use of Mobilwax 2305 as a 'replacement fluid' for Bunker 'C' oil. Because the viscosity and

surface tension of both fluids is similar at the appropriate temperatures, the results obtained with wax indicate a similar trend for atomisation of oil. Satisfactory operating conditions were experienced with the wax, with few problems of premature solidification in the lance or wax vessel.

Once the nozzle had been proven in still air, the next aim of the investigation was to inject molten wax into a high velocity air stream, and study the effects produced.

BIBLIOGRAPHY.

- (99) A.I.S.E. Blast Furnace Quarterly Listings. 1973.
- (100) Joyce J.R. Shell Report ICT/7. 1945.
- (101) Dombrowski N. and Wolfsohn D.L. Trans. I. Chem. Eng. 50, 259 1972.
- (102) Kim K.Y. and Saunders E. American I. Chem. Eng. (Ann. Meetings)
1968.
- (103) Hasson D. and Mizrahi J. Trans. I. Chem. Engrs. 39, 915. 1961.

Table 5-1

COMPARITIVE PHYSICAL PROPERTIES OF BUNKER 'C' OIL,
MOBILWAX 2305, PARAWAX AND WATER.

	<u>BUNKER °C° OIL.</u>	<u>MOBILWAX 230°.</u>	<u>PARAWAX.</u>	<u>WATER.</u>
Carbon %	85.8	-	-	-
Hydrogen %	12.2	-	-	-
Sulphur %	1.4	-	-	-
Specific Gravity	0.945 (at 15°C)	0.982	0.904	1.0
Flash Point (°C)	125	235	192	-
Pour Point (°C)	20	80	53	-
Viscosity (SUS)				
at 100°C	110	80	38	5
at 75°C	500	150	45	5
Surface Tension	22.0	18.0	13.0	73.0
dynes/cm ²				

Fig. 28

EFFECT OF FLOW RATE ON PRESSURE DROP ACROSS CORKSCREW LANCE ASSEMBLY.

After Guthrie (20).

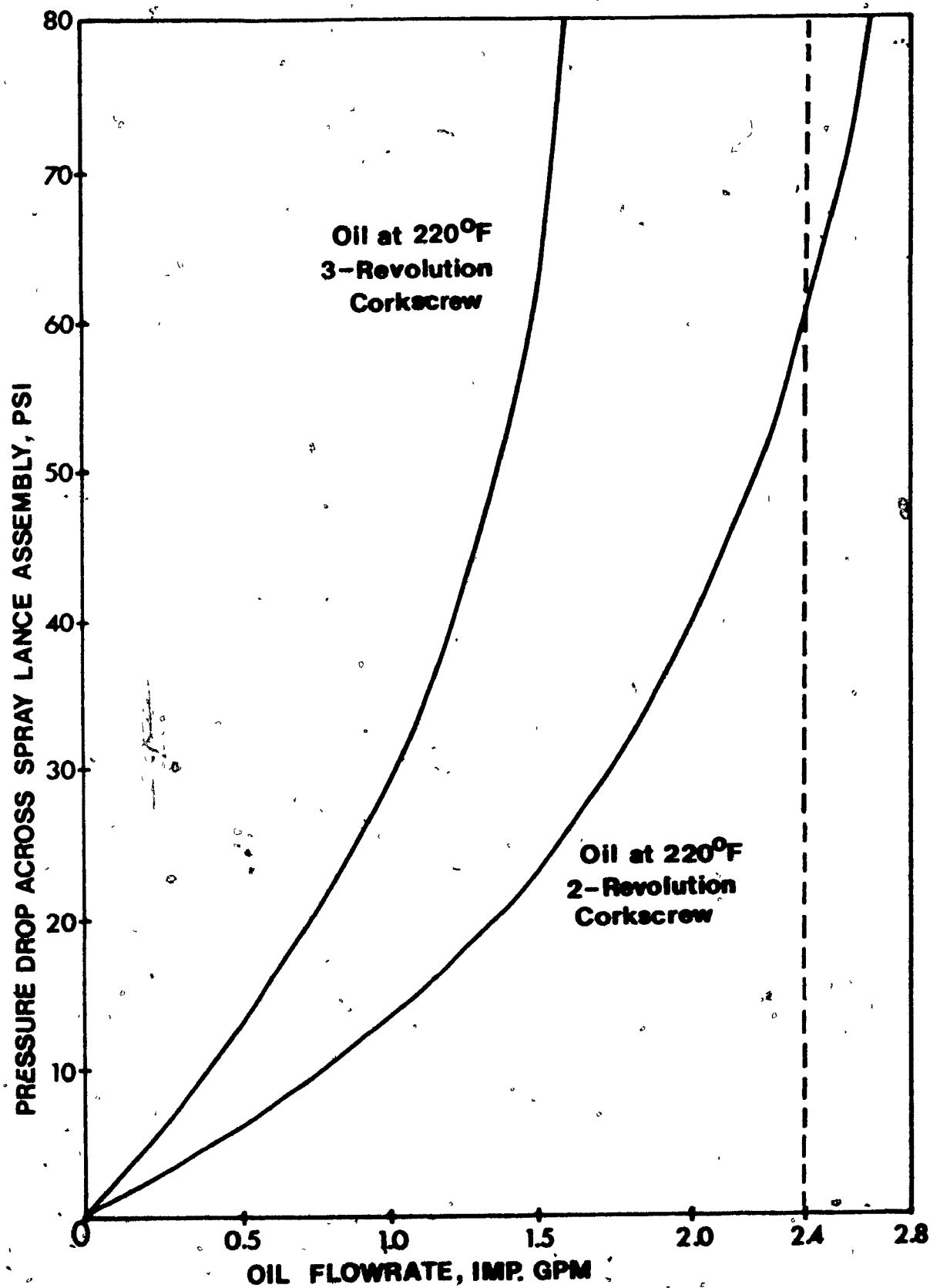


Fig. 29

METHOD OF CONE SYMMETRY ANALYSIS

Fig. 30

COMPLETED NOZZLE

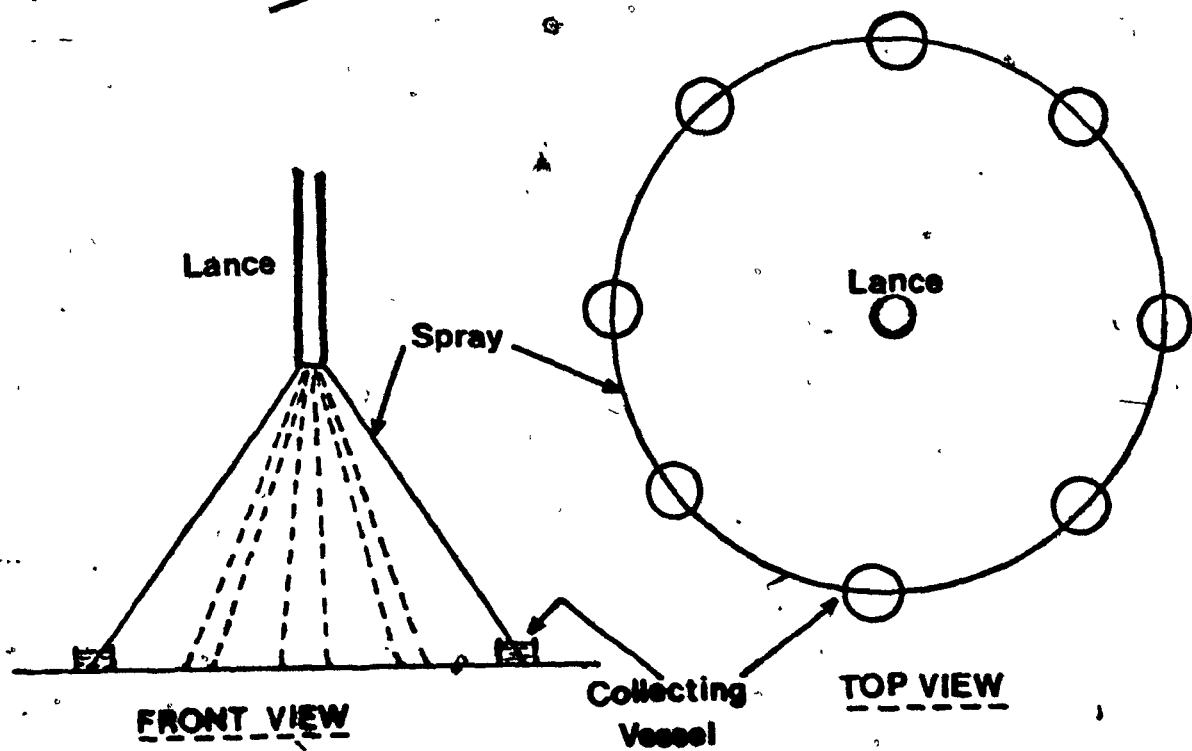
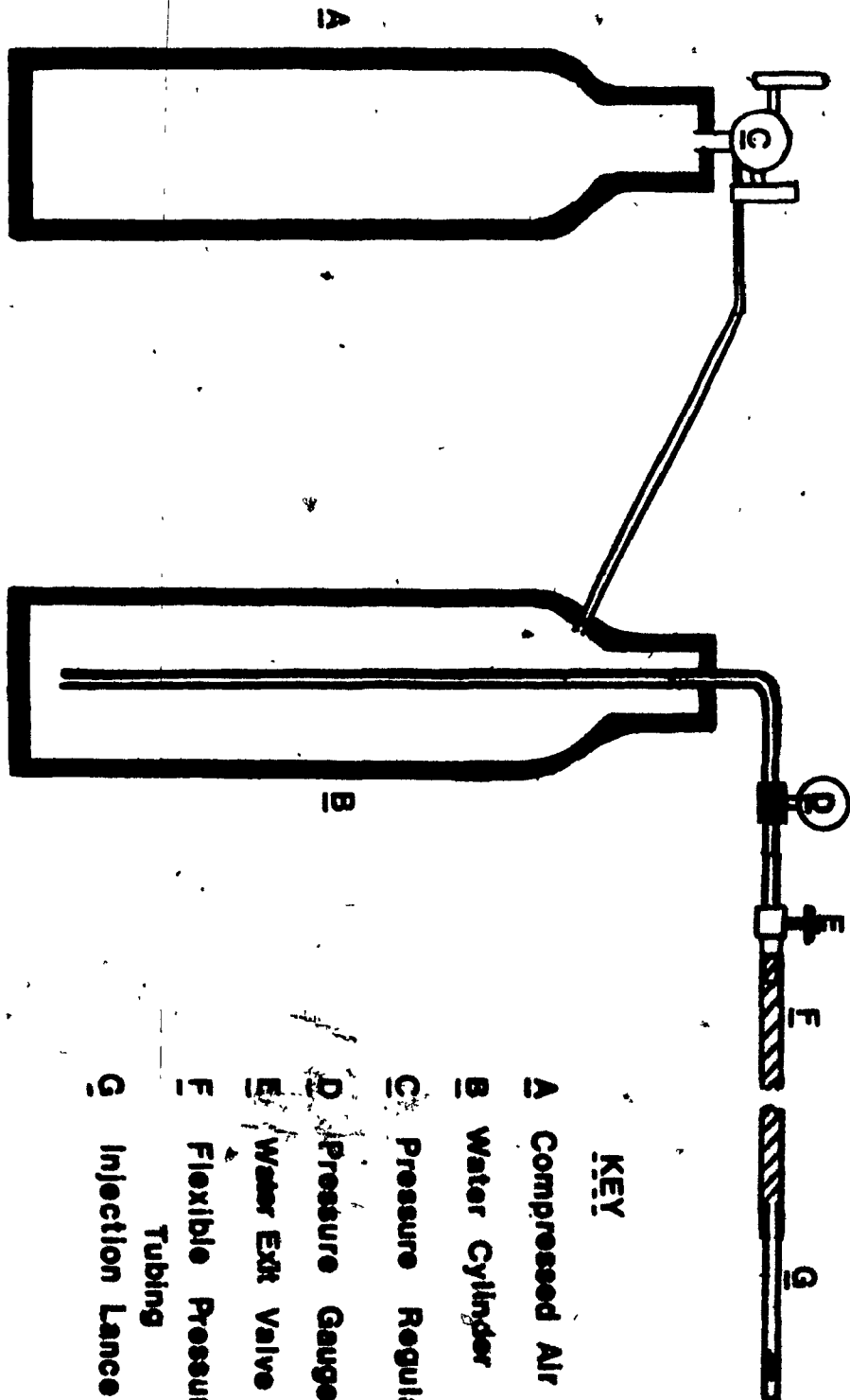


Fig. 31

EQUIPMENT USED FOR INJECTION OF WATER.

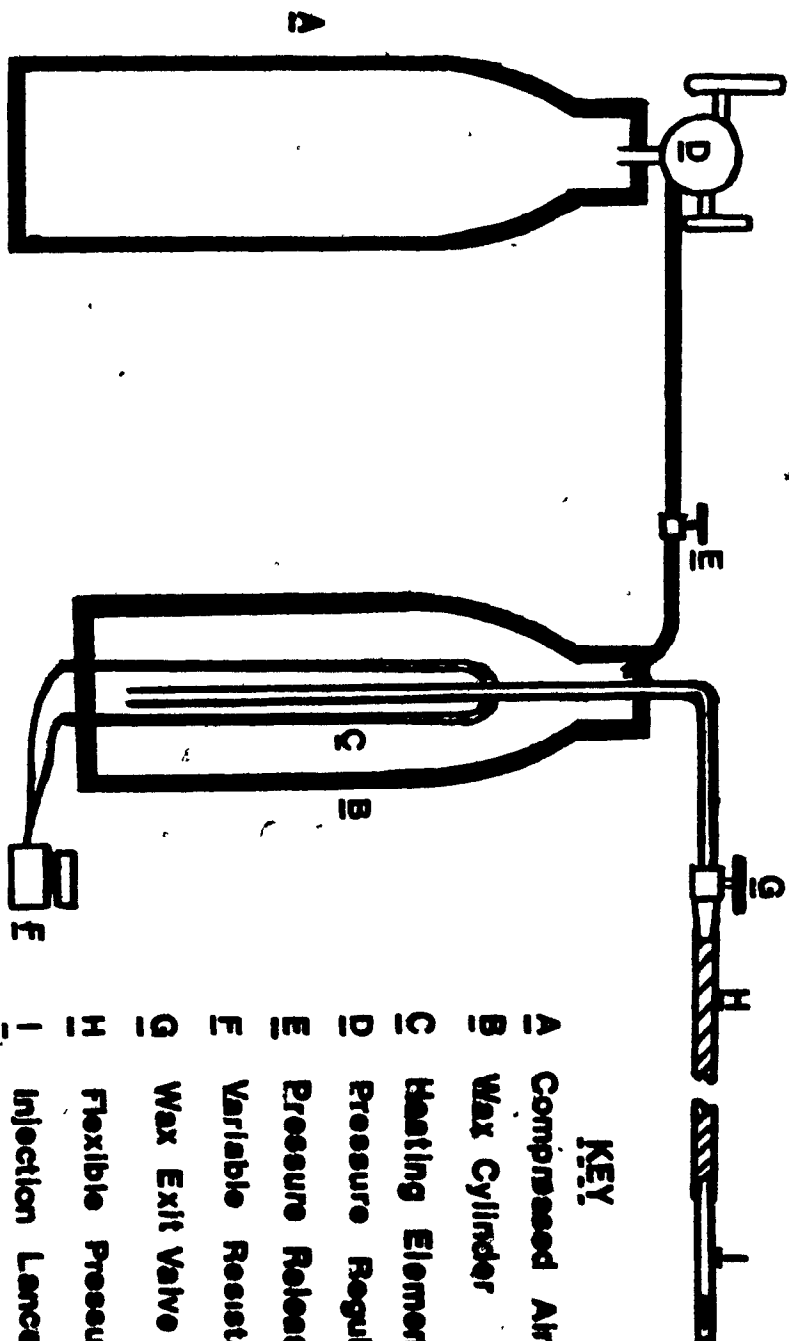


KEY

- A** Compressed Air Cylinder
- B** Water Cylinder
- C** Pressure Regulator
- D** Pressure Gauge
- E** Water Exit Valve
- F** Flexible Pressure Tubing
- G** Injection Lance

Fig. 32

EQUIPMENT USED FOR INJECTION OF MOLTEN WAX.



KEY

- A Compressed Air Cylinder
- B Wax Cylinder
- C Heating Element
- D Pressure Regulator
- E Pressure Release Valve
- F Variable Resistance
- G Wax Exit Valve
- H Flexible Pressure Tubing
- I Injection Lance

Fig. 33

VISCOSITY CHART FOR MOBILWAX 2305

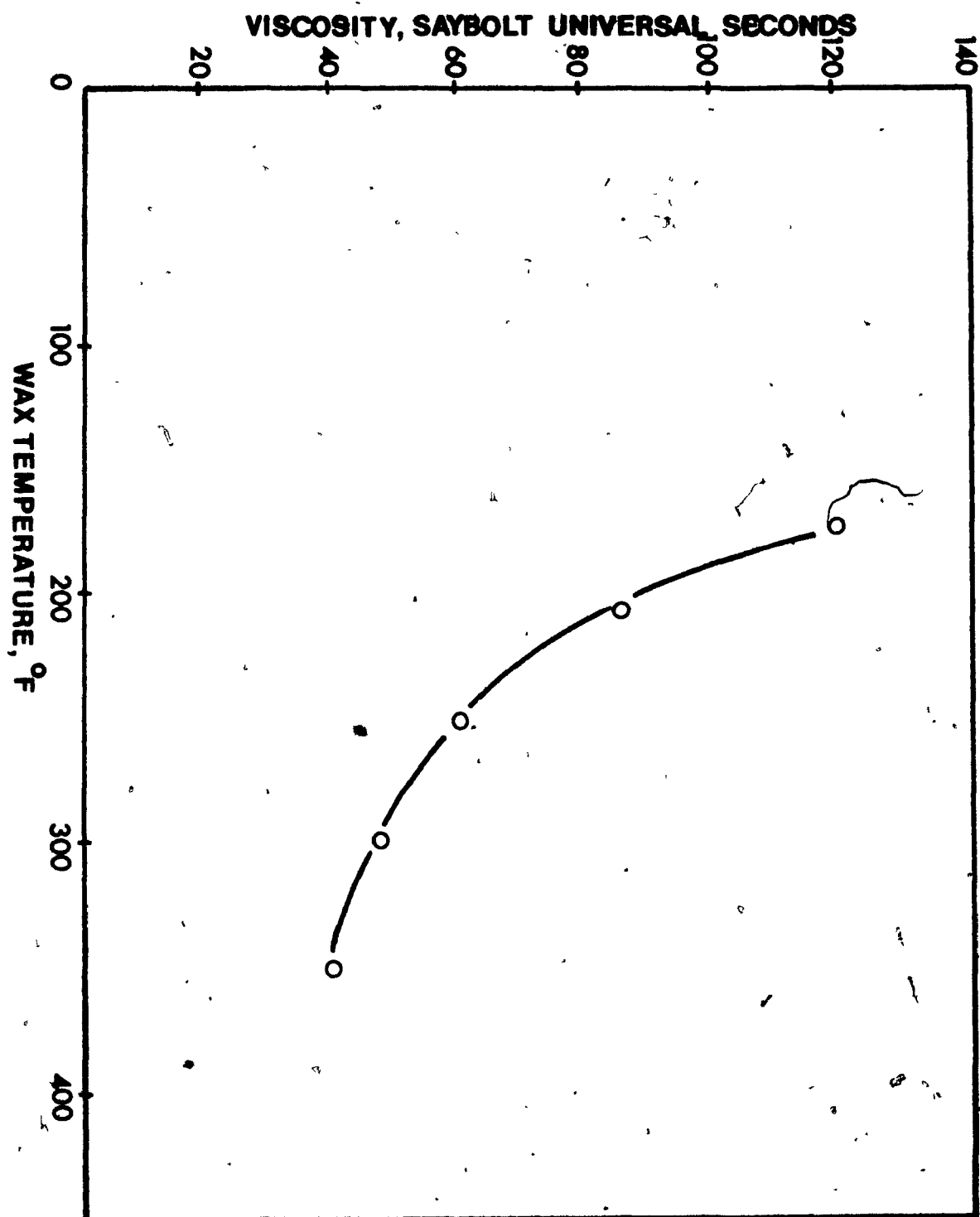


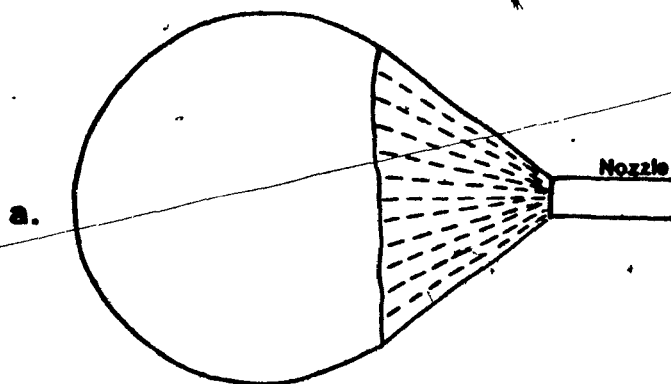
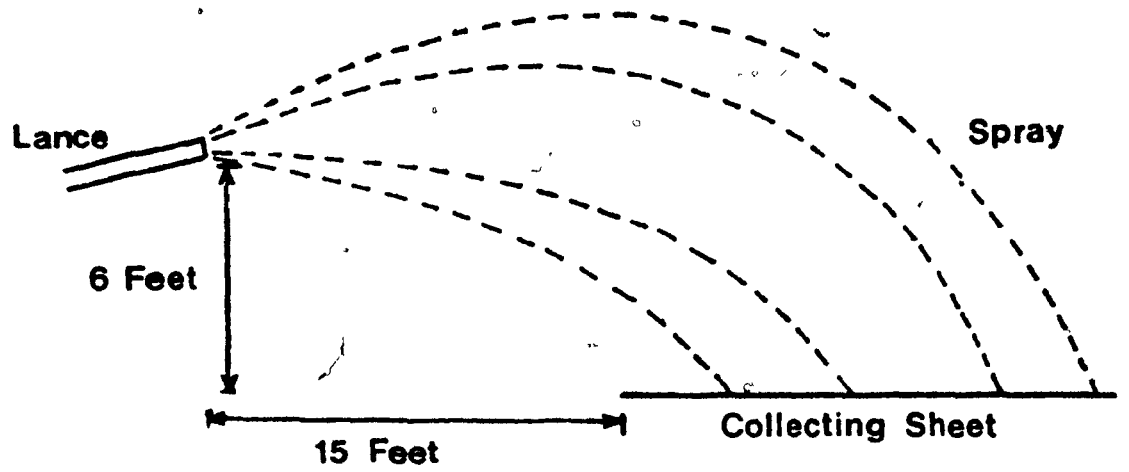
Fig. 34

TECHNIQUE FOR WAX INJECTION IN STILL AIR

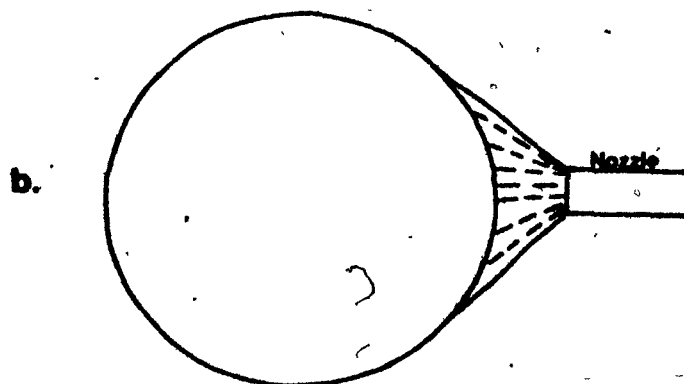
Fig. 35

DIAGRAMMATIC REPRESENTATION OF SPRAY PATTERN FROM CORKSCREW LANCE

- (a) DROWNED CONE FROM ORIGINAL LANCE
- (b) HOLLOW CONE FROM MODIFIED LANCE



DROWNED CONE SPRAY



HOLLOW CONE SPRAY

Fig. 36

PHOTOGRAPHS OF CONE ANGLE DEVELOPMENT AND SPRAY PATTERN

(a) INJECTION PRESSURE, 20 psi, (FLOW RATE, 1.8 gallons/minute)

(b) INJECTION PRESSURE, 40 psi, (FLOW RATE, 2.4 gallons/minute)



a

b

b



Fig. 36

- (c) INJECTION PRESSURE, 60 psi, (FLOW RATE, 2.8 gallons/min.)
- (d) INJECTION PRESSURE, 80 psi, (FLOW RATE, 3.0 gallons/min.)
- (e) INJECTION PRESSURE, 100 psi, (FLOW RATE, 3.2 gallons/min.)



c



d



25

Fig. 37

CONE ANGLE AS A FUNCTION OF WAX FLOW RATE

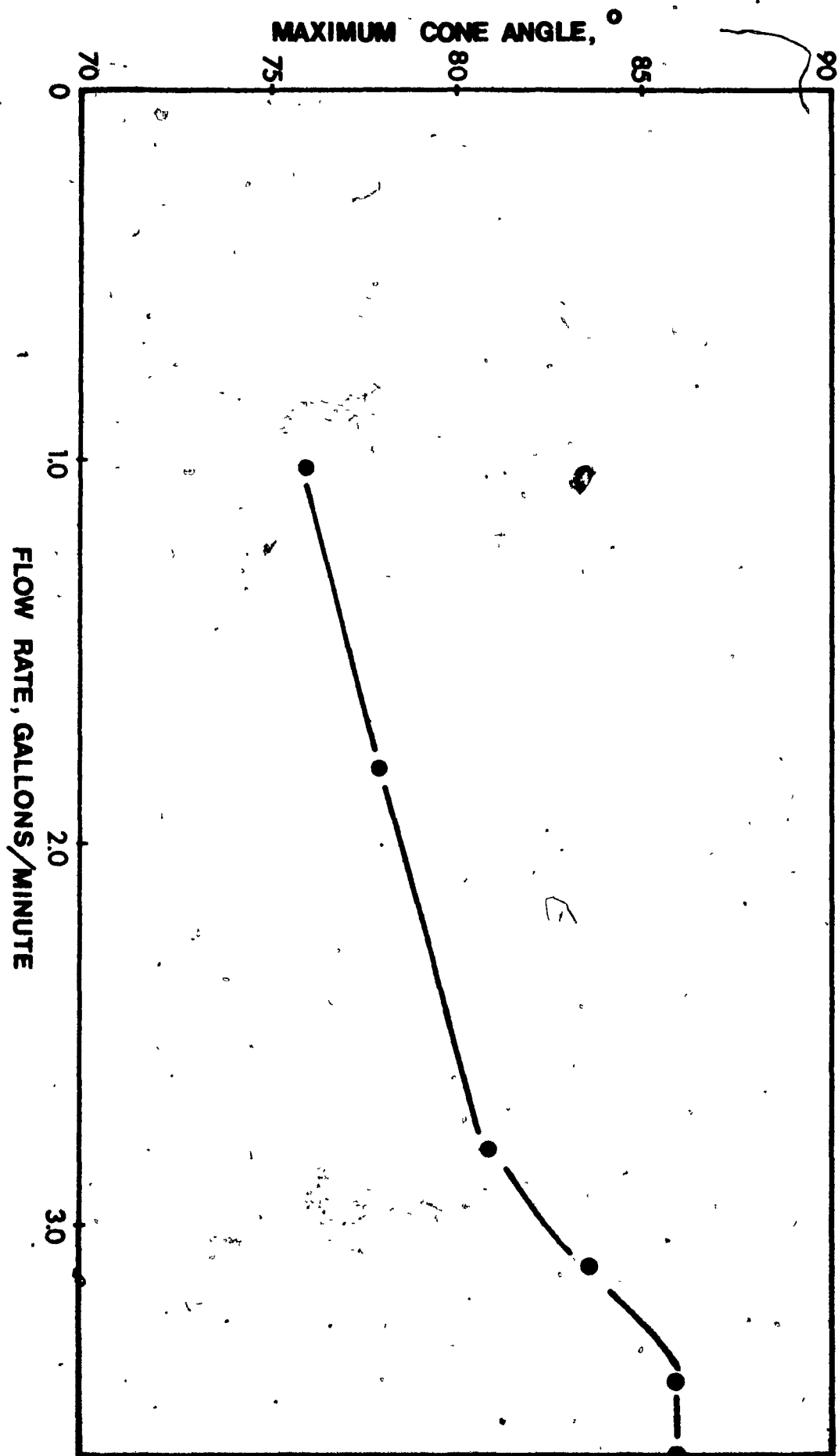
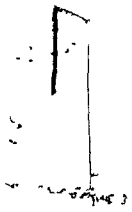


Fig. 38

FLOW RATE AS A FUNCTION OF INJECTION PRESSURE



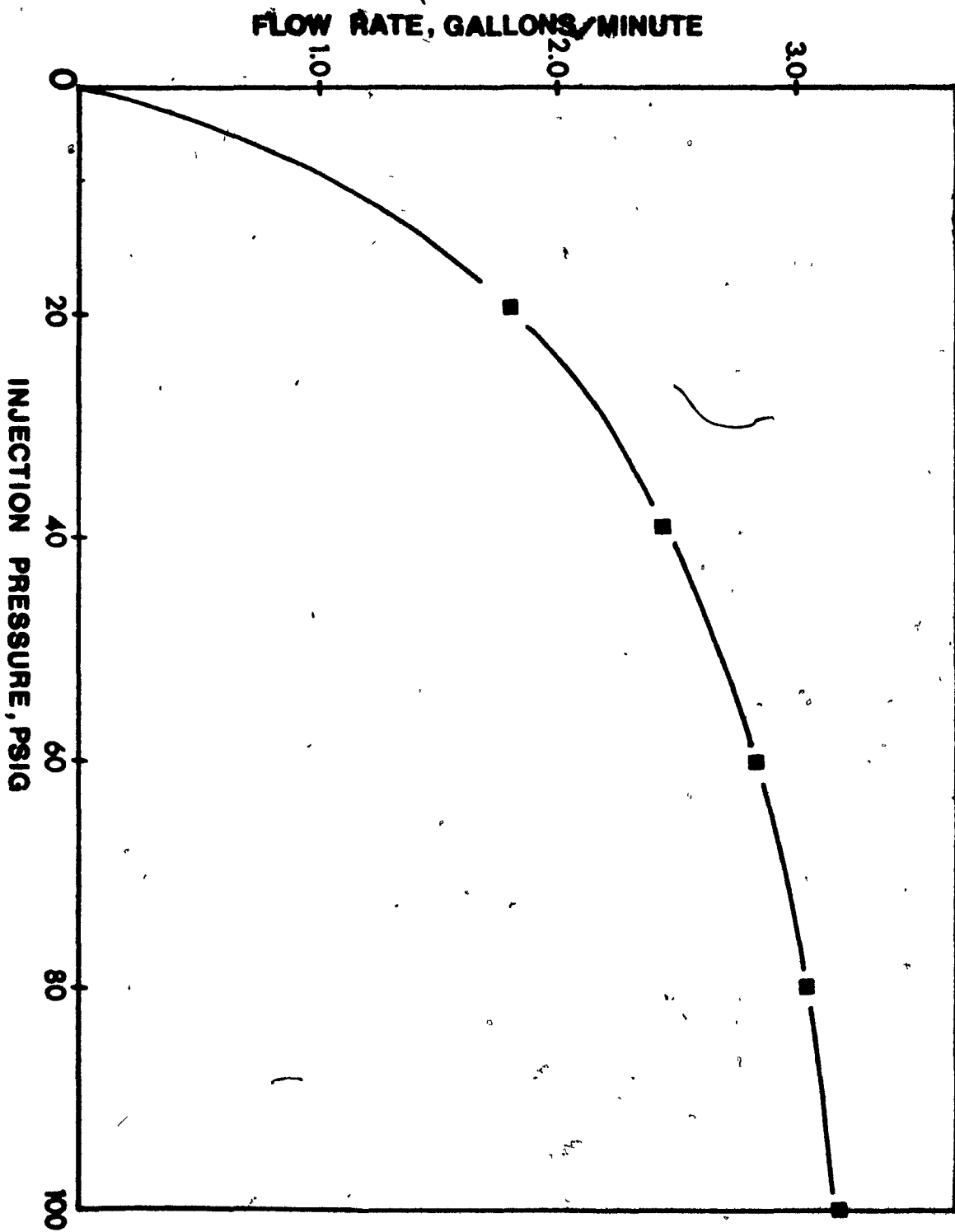


Fig. 39

FLOW RATE AS A FUNCTION OF (INJECTION PRESSURE)^{1/2}

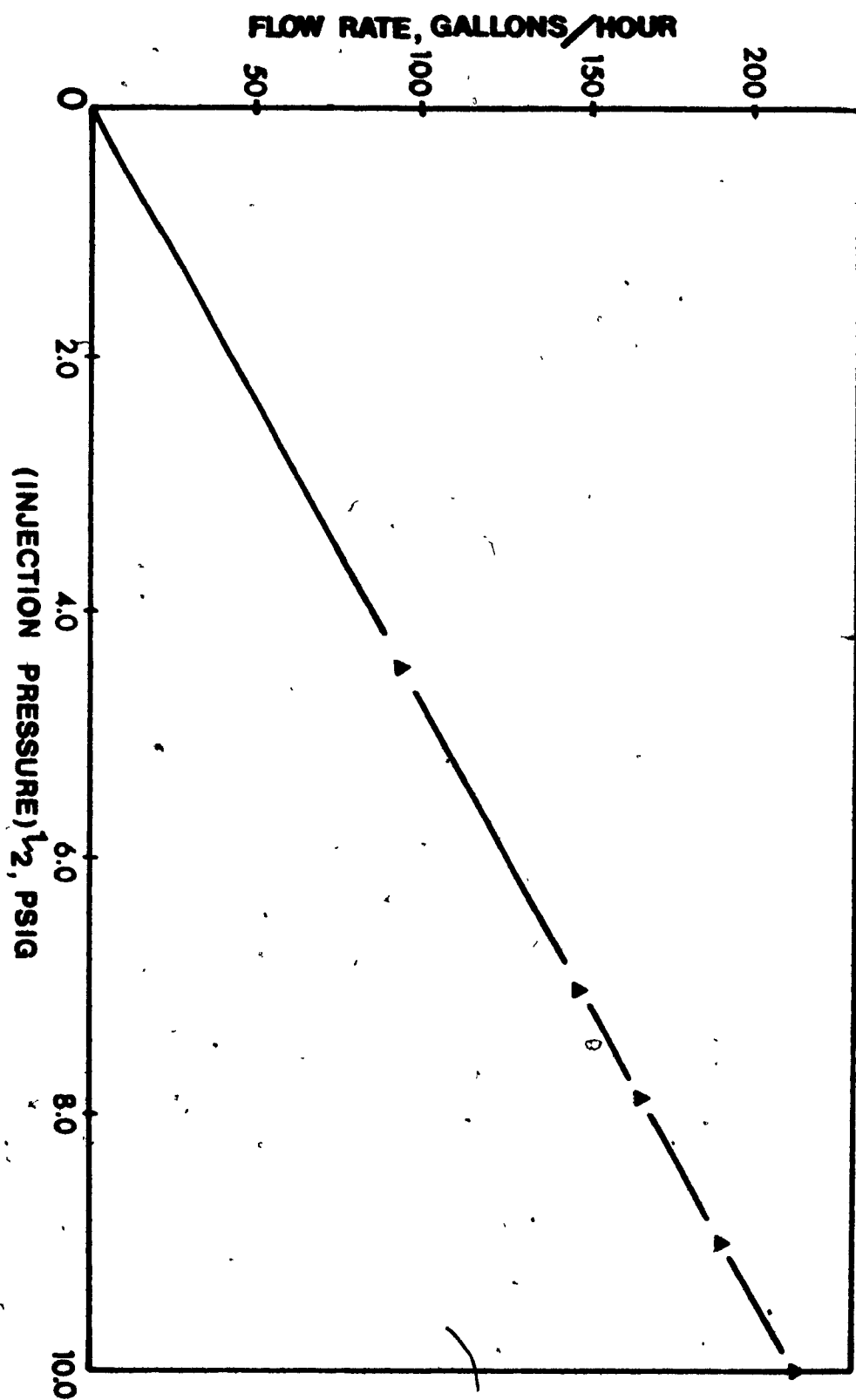


Fig. 40

PHOTOGRAPHS OF COLLECTED WAX PARTICLES, X40.

(a) FLOW RATE, 2.4 gallons/minute.

(b) FLOW RATE, 2.8 gallons/minute.

(c) FLOW RATE, 3.0 gallons/minute.



a.



b.



c.

Fig. 41

SAUTER MEAN DIAMETER OF SPRAY AS A FUNCTION OF NUMBER OF
PARTICLES COUNTED.

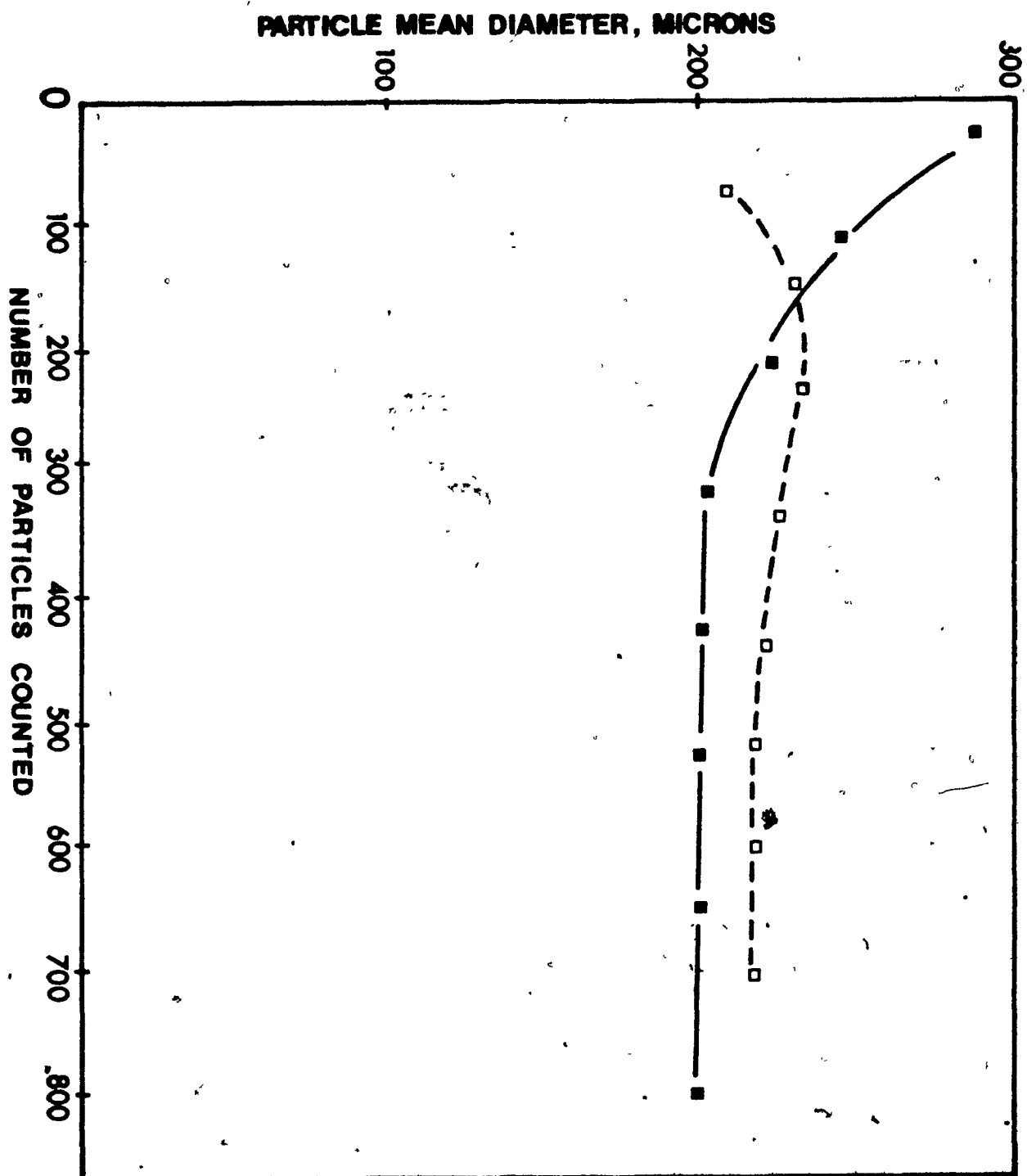


Fig. 42

SAUTER MEAN DIAMETER OF SPRAY AS A FUNCTION OF WAX FLOW RATE

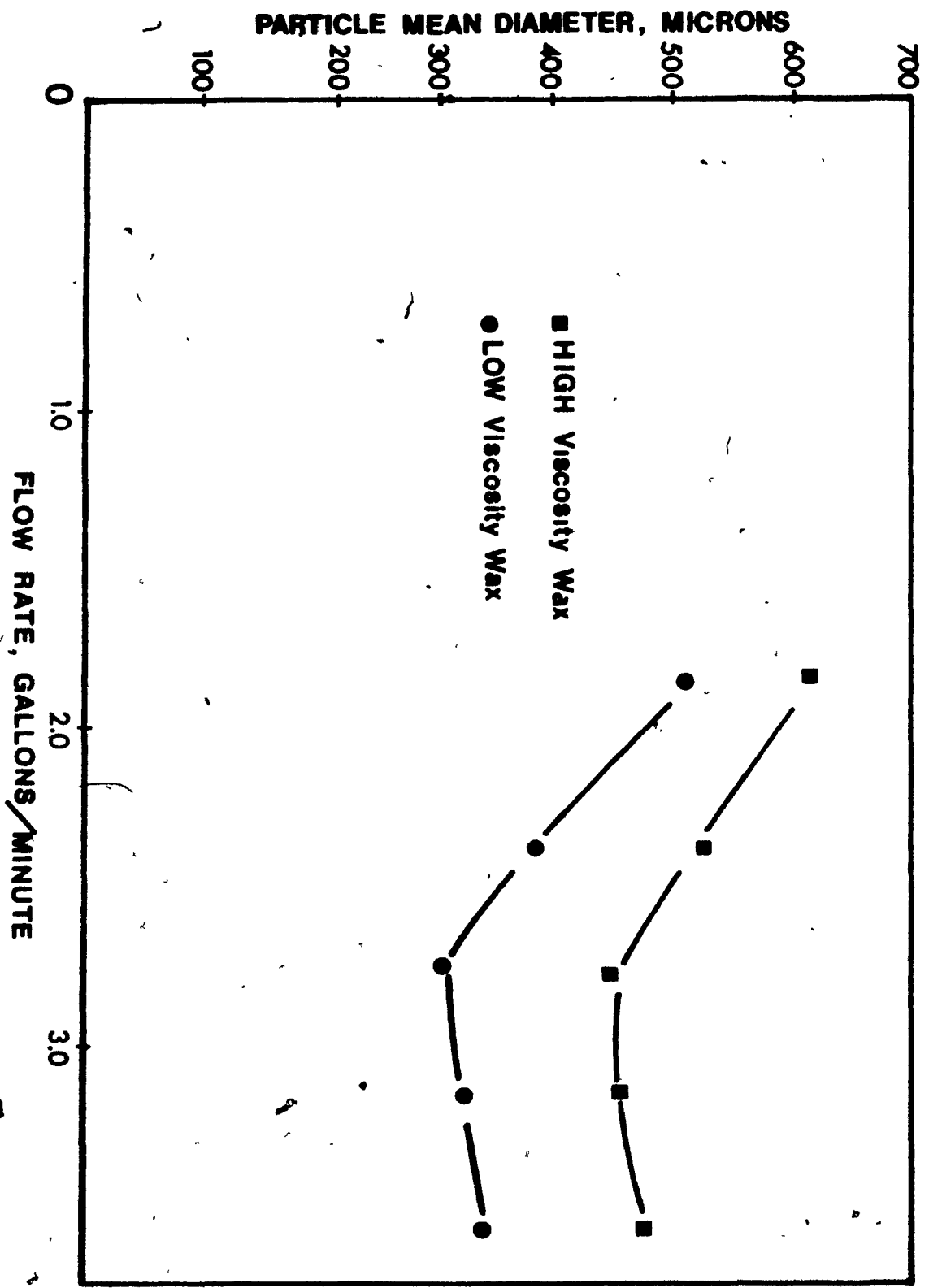
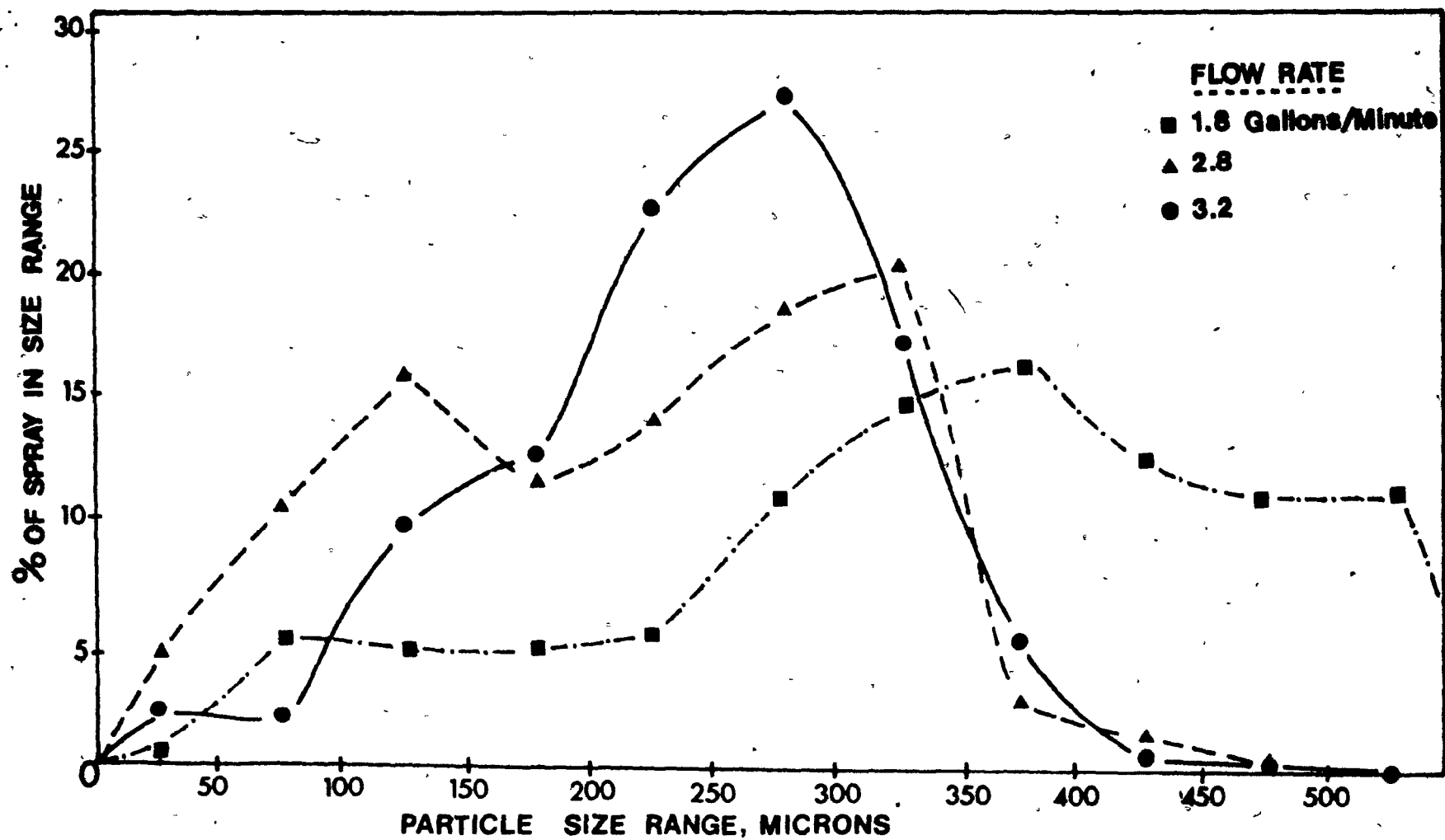


Fig. 43

NORMAL DISTRIBUTION OF COLLECTED WAX PARTICLE DIAMETERS.



Chapter 6.

INJECTION OF MOLTEN WAX INTO HIGH VELOCITY AIR STREAMS.

6.0 INTRODUCTION.

In this chapter, the effects of wax injection into high velocity air streams will be discussed. These studies were made in order that a full-scale model of oil injection could be obtained, with a view to optimising the process of oil injection into blast furnaces.

6.1 EXPERIMENTAL MODELLING OF BLAST FURNACE BLOW PIPE.

In the tuyere region of the blast furnace, Fig. 12, the blow pipe is a steel pipe, some 6-7 feet long and 6-7 inches internal diameter, lined with refractory material to a thickness of about one inch, and connected to the bustle-pipe by a 'goose-neck'.

The simulated blow pipe was a 5 foot length of plexiglas tube, with an internal diameter of 6 inches and a wall thickness of $\frac{1}{4}$ inch. Plexiglas was chosen so that the spray characteristics of the simple (straight through) nozzle and corkscrew nozzle could be readily observed.

It was decided to treat the blow pipe and the tuyere as one unit, although it is appreciated that in practice, this is not the case, the tuyere being located at the end of the blow pipe, and having a taper down to its nose, thereby reducing the internal diameter from 6-7 inches to about $5\frac{1}{2}$ inches. However, it was felt justifiable to use this simplified treatment since neither the resultant spray characteristics nor the final drop size produced would change if the blow pipe were tapered.

In order to study the effects of injection angle on the resultant spray, holes were located in the plexiglas tube at angles of 15° , 30° ,

60°, and 90°. These angles were chosen in order that a complete study of effect of injection angle could be obtained. In addition, these injection ports were located in such a way that injection could be done at distances of 18 inches and 27 inches from the end (or nose) of the blow pipe. This is illustrated in Fig. 44.

The equipment used to produce the high velocity air streams consisted of two large tanks, each measuring 5 feet in diameter and 8 feet long, with a combined volume of 314 cubic feet. They were pressurised to 125 psig by a compressor, and were thus capable of delivering the required velocities. The tanks were emptied through a 6 inch internal diameter globe valve, located in a 6 inch internal diameter pipe, whose end was fitted with an 11 inch flange.

An 11 inch diameter plexiglas flange was made and fixed to the blow pipe. The whole assembly was then bolted to the pressure tanks, as indicated in Fig. 45. Finally, the plexiglas blow pipe was held rigid by two heavy metal supports.

6.2 EXPERIMENTAL TECHNIQUE FOR INJECTION INTO HIGH VELOCITY AIR STREAMS.

6.2.1 MEASUREMENT OF AIR VELOCITY.

In order that the velocity of the air stream be known at the point of injection, a pitot tube was constructed, and standardised in the air stream against a previously calibrated pitot tube. Both the pitot tube and a static pressure tube were connected to a mercury manometer, and the resulting stagnation and static pressures found at various air stream velocities. The velocity of the air stream was

then found by application of:

$$V_o = \sqrt{\frac{2g_o K P_o}{(K-1)\rho_o} \left[1 - \left(\frac{P_o}{P_1} \right)^{\frac{K-1}{K}} \right]}$$

where

V_o = velocity of air stream, feet per second.

g_o = gravitational constant = 32.2 ft. lbm./lb.f. sec.

K = ratio of specific heat of air at constant pressure and
constant volume = 1.4.

P_o = static pressure, lbf./ft.²

P_1 = stagnation pressure at pitot tube, lbf./ft.²

ρ_o = fluid density, = 0.0735 lb./ft.³ @ 300°K, and 1 atm.

A pitot tube traverse of the blow pipe was performed in order that any pressure fluctuations be noted. No significant fluctuations on the mercury level in the manometer were noted during this traverse.

When a calibration chart for velocities as a function of the differential pressure had been constructed, it was decided to keep the air velocities below 450 feet per second, because of the problems associated with evacuating a large volume of high velocity air into the confined space of the laboratory. As will be discussed at a later stage in this chapter, the air velocities used in this study are generally lower than those used in general blast furnace practice, yet any trends resulting from injection of wax into these relatively low velocity air streams can be extrapolated to encompass trends at the higher air velocities.

6.2.2 WATER INJECTION INTO HIGH VELOCITY AIR STREAMS.

In order that the potential of the experimental equipment be tested, water was first injected into the air stream, since the injection of water had proven much easier in still air tests, and in the low humidity of the laboratory, the water drops would evaporate, thus negating the need for collection. Water was sprayed into the air stream at different flow rates (1.8 gallons per minute to 3.2 gallons per minute) and injection angles (15° to 90°) and the spraying characteristics noted.

The technique of water injection (and also wax injection) was, referring to Fig. 45, the globe valve was opened until the differential pressure indicated the desired air velocity, and a pitot tube traverse done. The water (wax) was then injected, at the desired flow rate, for a known period of time, usually 10 seconds.

The use of water proved that injection into the blow pipe could be done easily, since the air velocity remained constant during the period of testing, and the plexiglas injection lances remained rigid, even at high air velocities of 450 feet per second.

Photography of the injection of water was undertaken, and to aid the optical resolution of the spray, a small amount ($1\frac{1}{2}$) of nigrosine black dye added.

6.2.3 WAX INJECTION INTO HIGH VELOCITY AIR STREAMS.

Some problems with wax injection were anticipated prior to testing. The first, and perhaps the most urgent one, was the prospect of the wax freezing in the lance during injection, due to the temperature

difference between the wax and the air stream. In previous studies, two solutions had been used (a) heating of the air stream to the same temperature as that of the fluid being injected (68), and (b) the use of heating tape and insulation tape wrapped around the lance (100). Longwell (68) had used an air pre-heat temperature of 300°F, and this had been successful in eliminating the problem of wax freezing in the lance. However, this could not be utilised in this study due to the fact that the existing pressure tanks had no facility for heating the air. Furthermore, the initial drop size immediately after injection was required, and the use of high air temperatures would delay freezing, and hence alter the resultant drop size.

The use of a heating tape was rejected, since this would result in increased bulk of the lance, and would cause the lance to waver in the air stream, due to a looser fit in the injection ports. The result would be an unequal spray distribution, due to the movement of the lance.

Another problem was that of wax temperature measurement. In the air stream, the viscosity of wax decreases with time, and hence, the wax temperature alters rapidly, causing difficulty in recording accurate viscosity measurements. A thermocouple located at the exit orifice of the lance gave some indication of wax temperature. Longwell has indicated that the use of wax for oil atomisation modelling can only give a useful trend, due to the increase in viscosity of the wax, which results in a slightly larger particle size than would be obtained with oil injection under the same conditions.

The wax vessel was heated to 212°F, and stabilised at that

temperature for thirty minutes for temperature equalisation, by the use of the rheostat and continuous stirring of the molten wax.

Injection into the air stream, whose temperature was measured at 80°F, caused a substantial heat loss in the wax, the exiting wax temperature being in the range 185°F-190°F, as measured on the thermocouple.

However, this still gave a wax viscosity of 110-125 SUS (4.5-6 cp), which was deemed to be within the viscosity range of oil injection, and thus satisfactory for further studies. No freezing of wax was noted during the course of injection, but wax did freeze in the lances after the wax flow was turned off, and the lances needed cleaning before another experiment could be done. Cleaning of the lances was done by the use of hot water, which sufficiently softened the wax that it was readily blown out of the lance by passage of a high velocity blast of air.

Wax was injected at flow rates from 1.8 gallons per minute up to 3.2 gallons per minute, into air streams of velocities from 250 feet per second up to 450 feet per second, at injection angles from 15° to 90°, and injection distances from 18 inches to 27 inches from the nose of the blow pipe.

During the course of the injection trials, it was observed that wax droplets were being deposited on the sides of the blow pipe wall. This necessitated cleaning, using Varsol, before each successive run, and hence it was decided to tape a plastic insert into the blow pipe. Polyvinyl chloride was found sufficiently pliable to fit inside the tube, and a piece of 18 inches (or 27 inches, depending on injection distance) long by 19 inches wide by 1/16 inch thick, was so positioned,

and taped securely to the walls. Passage of a high velocity air stream did not disrupt the insert. The insert, after injection was completed, was removed for further examination.

No photography of wax injection could be undertaken because of the impact of some of the wax spray on the walls of the blow pipe.

6.2.4 PARTICLE COLLECTION AFTER INJECTION.

This was effected by positioning a large sheet 15 feet from the end of the blow pipe. The sheet measured 17 feet wide by $13\frac{1}{2}$ feet high, and was supported from the roof and floor by high-tensile cord. Although somewhat crude in design, it proved extremely effective. With the passage of an air stream, the sheet billowed out, much like a sail, and caused the particles to adhere. On the floor, in front of the sheet, a large sheet of polythene was spread in order that the particles falling from the sheet could be collected. Particles adhering to the sheet were removed by shaking the sheet, the frozen droplets dropping onto the polythene. Since the particles were very small, care was observed in handling, the collected particles being placed in the freezer prior to sizing.

6.2.5 PARTICLE SIZING AND CALCULATION OF PARTICLE MEAN DIAMETER.

The same technique was used in this part of the study as outlined previously in chapter 5. However, because the particles were now much smaller than those resulting from the still air experiments, higher magnifications were necessary for accurate measurement of particle diameters. The magnifications used varied from X90 up to X670,

although above X90, resolution of the particles became difficult due to the inherent inability of the optical microscope to focus on spherical objects at high magnifications, i.e. the optical microscope has a low depth of field.

From the photographs taken, the diameters of the particles were noted and the Sauter Mean Diameter, as well as a normal distribution, calculated.

6.3 EXPERIMENTAL RESULTS AND DISCUSSION OF RESULTS.

6.3.1 PHOTOGRAPHIC STUDY OF WATER INJECTION INTO HIGH VELOCITY AIR STREAMS.

A short study of water injection is presented in Fig. 46.

From visual observation, it was seen that the behaviour of the two lances, i.e. the simple nozzle and the corkscrew nozzle, were quite different.

As can be seen from Fig. 46a), at low air velocities, up to 350 feet per second, injection through the simple nozzle did not cause atomisation until some distance from the lance, i.e. the penetration distance of the solid core of water before disruption was of the order of 2 inches. Also, the resulting atomisation did not produce a uniform spray, since the observed 'zone of atomisation' was quite small. Subsequent increase in air velocity caused the penetration distance to decrease, and at 450 feet per second, the water was disrupted immediately on exiting, Fig. 46b).

In contrast, the corkscrew nozzle, operated under the same conditions of flow rate (3.2 gallons per minute) and air velocity, caused atomisation of the water on exiting, Fig. 46c) and d), and this was further disrupted by the effects of the air stream. It was seen, Fig 46c), that at low air velocities, the cone angle of the spray was still high, the air velocity not being high enough to cause substantial 'bending' or 'bowing' of the sheet. Increasing the air velocity to 450 feet per second, caused the cone angle of the issuing spray to diminish greatly, Fig. 46d), due to the increased bending of the spray sheet.

The impingement of the air blast on the water stream was more evident when injection was done at 90° . From Fig. 46e) and f), the 'bowing' of the water stream from the simple nozzle can be seen to be quite considerable, and with an air velocity of 250 feet per second, the penetration distance of the water is greater than that when an air velocity of 450 feet per second is used. Similar studies of the corkscrew nozzle, Fig. 46g) and h), indicated that the 'bow-wave' is less evident, due to the nature of the spray sheet.

The penetration distance of the spray for the simple lance was seen to be most at a 15° injection angle, and least at 90° , which is as expected, since a greater surface is offered to the air stream, when injection is done at right angles to the air blast. Because of the nature of the spray produced by the corkscrew nozzle, i.e. a hollow cone, the effects of injection angle is substantially less as regards secondary atomisation, since the air blast impinges on a thin sheet of liquid, which is easily disrupted.

With the simple nozzle, it was seen that as the air blast velocity increased, so the penetration distance decreased, for all angles of injection, Figs. 46a), e), i), until at an air blast velocity of 450 feet per second, the liquid was atomised immediately on exiting, Fig. 45b), f), j). However, it appeared that a good atomisation pattern did not develop until some distance from the nozzle. This is considered to be due to the time needed for (a) disruption of the stream into ligaments, and (b) formation of drops prior to the process of secondary atomisation. Once secondary atomisation begins, the spray is disrupted into many small droplets, thereby 'filling' the blow pipe.

The effect of increased air velocity on the performance of the corkscrew nozzle was to produce a 'bow-wave' on the issuing sheet, which caused the sheet to 'bow', the extent increasing with increasing of air velocity. In addition, increase of blast velocity caused secondary atomisation to begin sooner, (i.e. nearer the lance exit orifice), since the sheet was disrupted sooner, although the resulting 'zone of atomisation' was more confined than at the lower velocities. The combined effect was thus to produce quicker atomisation, and an initially confined spray pattern, which expanded rapidly, and appeared uniform at a distance of some 6 inches from the injection lance.

During the course of these trials, it was noticed that water was impinging on the walls of the blow pipe, when injection was done through the simple nozzle. This was more noticeable at low air velocities, which was to be expected, since the penetration distance was greater. The observed effect was that when the water impinged, it immediately formed a 'river', which was pushed along by the air

blast, until at the nose of the blow pipe, the 'river' was either re-atomised, or simply ran out onto the floor. This effect depended on the air stream velocity, since at the higher velocities, the tendency was for the river to be re-atomised. This impingement was noticed at air velocities up to 400 feet per second, although the effect decreased with increased air stream velocity.

The same effect was noted with injection through the corkscrew nozzle, but only up to an air stream velocity of 300 feet per second, and even then, the effect was much less than that observed with the simple nozzle, with the result that re-atomisation of the 'river' was obtained at the nose of the blow pipe.

The effect of flow rate on the spray characteristics of water injected through the corkscrew nozzle was such that at low flow rates, the cone had not formed completely, and thus the spray was somewhat similar to that produced by the simple nozzle. However, increase in flow rate caused the cone to become established, and the full benefit of the nozzle was obtained.

6.3.2 SPRAY SHEET VELOCITY.

In order to calculate the initial relative velocity between the air stream and the exiting wax stream, the spray sheet velocity for the corkscrew lances was needed. This was calculated based on a knowledge of flow rate and cone angle, and by assuming the sheet thickness.

From the mathematical determination of these values (see Appendix 1), Fig. 47 was obtained and provides an indication of the sheet

velocity of the wax spray at specific distances from the nozzle exit. It can be seen from Fig. 47 that the velocity increases with increase in flow rate. This can be important in the realm of relative velocity i.e. the velocity difference between the air-and-liquid streams. Since the absolute thickness can not be determined experimentally to obtain sheet velocities, various hypothetical sheet thicknesses were used. A sheet thickness of 0.05 cms. has the greatest velocity, but it is most improbable that the sheet could be this thickness, since a particle of 700 microns is unlikely to be formed from a sheet of 500 microns thickness. It is much more likely that the sheet thickness lies between the values of 0.15 cms. and 0.20 cms., since below these values, the same argument as previously used can be applied, and above these values, the spray velocity becomes equal to that of the core of fluid issuing from the simple nozzle. The spray velocity was calculated based on a cone angle of 43° , which remained constant over a horizontal distance of 10 cms. This approach was entirely justified, since penetration of the sheet in the high velocity air stream, prior to break-up, was very small.

It can be seen from Fig. 46 that the resulting sheet velocities are quite small, being in the range 10-25 feet per second (depending on flow rate). Consequently, the relative velocity will not be too different from the air stream velocity. The relative velocity with a low injectant flow rate is only slightly higher than the corresponding value with a high injectant flow rate, and thus the resultant drop size, produced at any particular injectant flow rate for a given air stream velocity, should not be too different.

6.3.3 INJECTION OF MOLTEN WAX INTO HIGH VELOCITY AIR STREAMS.

(a) Photographic Study of Wax Droplets.

When injection of the molten wax had been completed, the particles were collected and photographed for sizing. Fig. 48 indicates the droplet sizes produced by injecting molten wax at 212°F (exiting wax temperature being 185°F - 190°F), with a flow rate of 3.2 gallons per minute, into air streams of velocities 300 feet per second up to 450 feet per second. Both the simple nozzle and the corkscrew nozzle were used in these studies. A magnification of X40 was used in the photographic study in order that visual comparison between the droplet sizes obtained in air stream studies and those in still air could be obtained.

Under the microscope, it was seen that the particles were indeed smaller than those of the still air studies, and, in most cases, perfectly spherical, indicating that the droplets had frozen in flight.

Fig. 48a) is a photomacrograph of a random sample of the spray produced by injection of molten wax through the simple nozzle at a flow rate of 3.2 gallons per minute into an air stream of 300 feet per second, while Fig. 48b) is the corresponding photograph of droplets produced from injection through the corkscrew nozzle, under the same conditions. It can be seen that in both cases, the size range has decreased considerably from that obtained in the still air studies, with many particles having diameters less than 50 microns, and few having diameters greater than 250 microns. It can also be seen that average sizes of droplets produced by the corkscrew nozzle are smaller than those from the simple nozzle.

Figs. 48c) and d) are an indication of the particles produced from the simple nozzle and corkscrew nozzle respectively in an air stream of velocity 350 feet per second. It can be seen that the majority of the particles exhibit diameters less than 100 microns, and in the case of the droplets produced from the corkscrew nozzle, Fig. 47d), few particles with diameters greater than 150 microns are evident.

Figs. 48e) and f) illustrate the particle sizes produced by injection of wax into an air stream of 450 feet per second, through a simple nozzle and a corkscrew nozzle respectively. As can be seen, the particles produced in both cases are very small, and sizing of these particles could not be done accurately at this magnification, Fig. 48g) is a photomacrograph of an area of Fig. 48f), magnified to X670.

Photography of such fine particles proved extremely difficult, due to the rapid softening of the wax at room temperature. This led to some 'smearing' of wax on the glass slides, which, while it caused less than perfect photographs, did not prevent accurate sizing to be carried out.

(b) Particle Size as a Function of Wax Flow Rate.

In Figs. 49, 50, 51 and 52, the effect of increasing the wax flow rate on the particle size produced is presented.

(1) Injection through the Simple Nozzle.

With injection of wax into an air stream of 250 feet per second velocity, at different flow rates, a small increase in the particle mean diameter, D_{32} , with increase of flow rate was noted, as shown in

Fig. 49. This can be explained by the fact that since the relative velocity is the main parameter governing the final droplet size, increase of flow rate increases the velocity of the spray, and hence decreases the relative velocity. Thus, the tendency for secondary atomisation to shatter the large droplets is lessened, with the result that large drops appear during sizing.

Another reason for the increase can be seen from the observed features of water injection, whereby increase in flow rate at the lower wind velocities caused an increase in the penetration distance of the stream. Although this effect could not be observed in wax injection, due to the impaction of wax particles, it is thought that a comparable effect does take place. Therefore, a longer break-up time of the stream of wax ensues, and the particles freeze before the full benefit of secondary atomisation is obtained.

Beyond 350 feet per second, the air velocity is high enough for the effect of spray velocity to be neglected, and the resulting particle mean diameter of the spray remains fairly constant, as shown in Fig. 50, where the air velocity is 450 feet per second.

(ii) Injection through the Corkscrew Nozzle.

Because the spray exits as a thin sheet, secondary atomisation is able to proceed almost instantaneously. At the flow rates (up to 2.8 gallons per minute), the cone has not properly formed, and hence disruption of the sheet is not as uniform as at the higher flow rates. As can be seen in Fig. 51, the particle mean diameter of the spray impacted with a 350 feet per second air stream decreases from a high

at a flow rate of 1.8 gallons per minute to a low at 2.8 gallons per minute, and then increases slightly with further increase in flow rate. By comparison, in an air stream or 450 feet per second velocity, Fig. 52, the particle mean diameter remains fairly constant with increase in flow rate.

It would appear that with the corkscrew insert, the factor governing the droplet size, as a function of flow rate, is the development of (a) the cone angle and (b) the uniform spray, since the mean diameter of the spray ^{droplets} decreases, until the spray sheet is fully developed. Once this has occurred, the effect of a decrease in relative velocity becomes apparent, leading to a slight increase in the particle mean diameter.

From this part of the experiments, it would appear that with injection through a simple lance, if the obtainable air stream velocity is low (up to 350 feet per second), then a low injectant flow rate should be used. If the system under investigation is the blow pipe of a blast furnace, a low oil rate would cause quicker break-up of the stream, and hence faster combustion, although it is realised that both of these factors would be marginal at best. However, in blast furnace practice, it is unlikely that the wind velocity would be quite so low, and hence a flow rate of 3.2 gallons per minute could be used.

With the corkscrew nozzle, no such limitations occur, and a high flow rate of 3.2 gallons per minute can be used, without any substantial increase in the droplet mean diameter.

As a consequence of results obtained in this section, it was decided that a wax flow rate of 3.2 gallons per minute would be utilised

in future work. A high flow rate is important in blast furnace oil injection practice if large amounts of oil are to be injected, and thus the characteristics of sprays produced by lances injecting 3.2 gallons per minute was deemed sufficiently important to concentrate on this particular flow rate.

(iii) The Effect of Injection Angle on Resultant Spray Characteristics.

In order that the optimum injection angle be found, wax was injected through the injection ports at angles of 15° , 30° , 60° and 90° to the air stream.

At the lower air velocities, the particle mean diameter increased from a low at an injection angle of 90° up to a high at 15° . This is illustrated in Fig. 53, where the air velocity was 250 feet per second and the wax flow rate was 3.2 gallons per minute. As can be seen, both the simple nozzle and corkscrew nozzle exhibit similar behaviour. This was to be expected since when the spray is presented to the air stream at 90° , the relative velocity is higher than at say, 15° . Thus, a greater shattering of the stream ensues, with a smaller resulting droplet size. Also, the penetration distance of the spray decreases at 90° , and secondary atomisation occurs sooner.

At the higher air velocities, the difference in relative velocity is less, and thus a smaller decrease in particle mean diameter, from 15° up to 90° , is noted. This is illustrated in Fig. 54, where the air stream velocity is 400 feet per second and the wax flow rate, 3.2 gallons per minute.

As will be discussed in chapter 6.3.4, injection at 90° caused an

increased proportion of the spray to impact on the walls of the blow pipe. This phenomena of impaction decreased with decrease of injection angle, and also with increase in wind rate.

At an angle of 90° , the distance from the end of the lance to the wall of the blow pipe was only 3 inches. With a wax flow rate of 3.2 gallons per minute, it would seem practically impossible for the air stream of up to 350 feet per second velocity to sufficiently disrupt the spray, without causing considerable impaction, whereas, at decreasing injection angles, the distance to the wall increases (almost 12 inches at 15°), and hence affords a greater distance for stream disruption before impaction.

At higher air stream velocities, the spray was disrupted more readily, and the effect of injection angle diminished, although a 15° injection angle still appeared to be the most satisfactory.

Thus, from a study of effect of injection angle, it appears that although a slightly smaller particle size results with an injection angle of 90° , the most satisfactory injection angle for practical use is 15° , due to the decrease in the impaction of wax on the walls of the blow pipe.

As indicated by Rombough (16), impaction of oil onto the walls of the water-cooled tuyere would result in the formation of soot. Thus, an injection angle is needed whereby little or no impaction is recorded.

(iv) Particle Size as a Function of Relative Velocity.

Wax was injected into air streams, whose velocities ranged from 250 feet per second to 450 feet per second, at a flow rate of 3.2 gallons

per minute, and at an injection angle of 15° . The resulting particles were sized, and with a knowledge of the spray velocity, the relative velocity calculated, and Fig. 55 plotted.

As can be seen from Fig. 55, as the relative velocity increased (i.e. the air stream velocity was increased, the spray velocity being constant), so the particle mean diameter of the wax spray decreased, from a high of 182 microns, at a relative velocity of 235 feet per second, to 45 microns, at 435 feet per second relative velocity, with injection through the simple nozzle, and from 168 microns to 39 microns at the corresponding relative velocities with the corkscrew insert. This is to be expected if conditions within the blow pipe are maintained, i.e. if the viscosity of the wax does not alter, and the density of the air stream is constant, since it has been postulated that the effect of relative velocity is the main parameter governing droplet size.

Thus, the corkscrew insert does appear to produce a consistently smaller droplet size at the relative velocities in the study, being some 10-15% smaller than that produced by the simple nozzle. However, at the high velocities, the trend does seem to indicate that increasing the air stream velocity beyond 500 feet per second will cause an equally-sized droplet, independent of the type of lance.

Even so, at the high air stream velocity of 450 feet per second (435 feet per second relative velocity), it can be seen that the particle mean diameter does fall into the range specified by Heynert (21) of 25-45 microns. Although Heynert does not specify it to be so, it is assumed that his particle mean diameter is the Sauter Mean Diameter, as is used in this report. If the Linear Mean Diameter

($\sum ND / \sum N$) of the spray were used, the particles would have much lower mean diameters, being 25 microns and 20 microns for the simple nozzle and the corkscrew nozzle respectively, at an air stream velocity of 450 feet per second.

The trend of results recorded here is consistent with those of other workers. Weiss (72) indicated a 25-30% difference in droplet size, with the hydraulic nozzle being the more efficient. Beuthen (98), some of whose results are indicated in Fig 55, reported no difference in droplet size produced by oil injection through a simple and complicated hydraulic lance, but it is interesting to note that the droplet sizes obtained in his study compare very favourably with those presented here.

If, as has been stated by Longwell, a slightly larger particle size will be produced by wax injection into a high velocity air stream than by oil injection under the same conditions of viscosity, air density and relative velocity, then the results obtained are even more encouraging,

In blast furnace practice, blast velocities are commonly of the order of 550 feet per second (21), and thus it can be seen that the droplet size produced by the injection of oil into an air stream of such a velocity would be conducive with good combustion, regardless of what system of injection were used.

(v) Effect of Injection Distance.

From a short study on the effect of injection distance, it was observed that no decrease in particle size resulted when injection of

wax was done into the air stream at a distance of 27 inches from the nose of the blow pipe, as compared to that done at 18 inches from the nose. The reason for this is quite logical, since the wax spray will solidify over the same distance, no matter how far away from the nose of the blow pipe injection takes place, the resulting spray distribution being similar.

With injection of oil into the furnace, the injection distance is generally no more than 18-20 inches from the nose of the tuyere. Increasing this distance would increase the time available for combustion, allowing any soot particles to burn away, but would cause detrimental damage to the tuyeres, due to excessive heat produced by the increased length of the flame front.

(vi) Effect of Lance Centring.

Another short study was undertaken, using the simple nozzle, to determine whether centring of the lance was important. Since it was known that the droplet size was unchanged with increase in injection distance, the logical study was that of spray pattern. From observation of the inserts, it was seen that up to 400 feet per second, centring of the lance was in fact decreasing the uniformity of the spray, since with an injection angle of 15° , a lance set one inch off centre, i.e. one inch nearer the injection port, caused less impaction than did a lance perfectly centred. Obviously, a lance set closer to the opposite wall caused increased impaction.

At air stream velocities of 450 feet per second, the effect was minimised due to the fact that at both lance positions, a good

uniform spray was produced.

If Heynert's blast velocities are considered as being representative, then there is no need for the strict observance of lance centring that some plants stipulate, if (a) the lance is not too near the opposite wall, and (b) decrease in lance length does not appreciably increase the spraying distance.

6.3.4 SPRAY DISTRIBUTION AND SPRAY PATTERN.

Observation of the inserts taped inside the blow pipe gave an indication as to the distribution and pattern of the spray. Injection of wax through the 90° injection port caused considerable impaction of wax, at all air velocities with the simple nozzle (centred), Fig. 56a), and up to 400 feet per second with the corkscrew nozzle (centred), Fig. 56b). As can be seen, there was no definite pattern to the impacted wax, merely the molten wax had hit the wall, collected as a 'river', had been blown along by the air stream, and eventually the wax had frozen. The effect of the air stream was seen by the appearance of 'ripples' in the pattern, where the wax, being blown along, had frozen. At the lower air velocities, (250-350 feet per second), the stream tended to exit from the blow pipe without too much re-atomisation at the nose of the blow pipe, Fig. 56c), the majority of the stream flowing onto the floor. Increasing the air velocity caused total re-atomisation of the 'river', in some cases well away from the nose of the blow pipe, Fig. 56a).

Some evidence of the process of secondary atomisation can be found in the impaction of wax droplets on either side of the 'river'. These

droplets were observed to be of various sizes, and are thought to be representative of the particle mean diameter of the spray.

Decreasing the injection angle decreased the amount of wax collected on the plastic inserts, and also changed the pattern of impaction. That produced at an injection angle of 60° , and an air stream velocity of 350 feet per second, was perhaps the most interesting, because, as can be seen in Fig. 56d), the spray from the simple nozzle on impaction formed a definite 'cone'. This 'cone' had two different components, (a) a thin ($\frac{1}{4}$ ") outer shell of solid wax, beginning at the point of impact of the spray and ending at the nose of the blow pipe, and (b) 'ripples' of wax within the solid wax shell. These ripples were due to the action of the air stream pushing the wax along until it froze, but the reason for the appearance of the solid 'shell' of wax is not understood.

In this instance, the wax droplets caused by secondary atomisation were seen to have a definite pattern also. Impaction of larger droplets was seen to have occurred near the 'cone', and that of smaller drops at increasing distances away from it. This is due to the phenomena of secondary atomisation, since the break-up of the large droplet results in the production of many smaller ones, of different sizes, and the smallest ones will be thrown out further than will the larger ones.

Further decrease in the angle of injection produced patterns similar to those of 60° , although the 'cone' of solidified wax was narrower and shorter, since a greater distance exists between the exit orifice of the nozzle and the wall of the blow pipe. At 15° , the 'cone' of wax measured only 4 inches in length and $2\frac{1}{2}$ inches in width,

compared to 15 inches and 7 inches respectively, with an injection angle of 60° . The solidified wax pattern at 15° injection angle and an air velocity of 350 feet per second is shown in Fig. 56e).

At 350 feet per second air stream velocity, and an injection angle of 15° , the corkscrew insert was seen to produce a uniform spray distribution, as shown in Fig. 56f), whereby all the solidified wax on the plastic insert was in the form of droplets. These droplets covered the entire surface of the insert, and appeared to be uniformly distributed. Subsequent microscopic analysis of this insert revealed that the particles had deformed on impact, and the majority had lost their original spherical shape. From observation of those spherical particles remaining, it was noticed that the droplets impacted on the wall varied from 10 microns to 120 microns, i.e. a fair cross-section of the droplet sizes produced by atomisation.

At the same relative velocity, but with injection through the simple nozzle, it was seen that the wax was still impacting as a cone, mentioned previously, and it was not until an air stream velocity of 450 feet per second, that a uniform spray resulted from this nozzle, Fig. 56g).

The effect of lance centring, as discussed in section 6.3.3 (vi), can be seen in Fig. 56h), where a narrower 'cone' of solidified wax is obtained with a lance one inch off centre (towards the injection port).

Fig. 57 indicates the weight of a cross-section of the wax pattern shown in Fig. 56d). As can be seen, the weight of wax at the nose of the blow pipe is greater than that at the point of wax impaction, due

to the effect of the air stream blowing the molten wax along the blow pipe until it froze.

Injection of wax at 15° into the air stream revealed, that at a constant flow rate of 3.2 gallons per minute, the amount of wax which solidified on the walls of the blow pipe decreased with increase in the air blast velocity, as shown in Fig. 58. The amount deposited decreased from nearly 20% of the total wax sprayed at 250 feet per second, down to 6.4% at 450 feet per second, with injection through the simple nozzle, and from 15.8% at 250 feet per second down to 5% at 450 feet per second with the corkscrew insert. At the lower air stream velocities, up to 350 feet per second, the 'cone' of solidified wax accounted for most of the weight of impaction, and at higher velocities, most of the weight was due to the impact of the wax droplets.

The value of this study is that the corkscrew insert proved more successful in generating a uniform spray pattern at a lower air stream velocity than did the simple nozzle.

At the higher air blast velocities of 450 feet per second, both nozzles proved to be successful in that the injected wax in contact with the air stream was completely and efficiently atomised.

6.3.5 DISTRIBUTION OF PARTICLE SIZES.

As done previously, the normal distribution was plotted for particle sizes produced by injection of molten wax at 3.2 gallons per minute into high velocity air streams, and Fig. 59 is a representation of the results obtained. As can be seen, at the low air velocity of 250 feet per second, the spray size range was somewhat large, with the largest

particle being 300 microns. The majority of the spray was concentrated in the size range 20-120 microns. This effect is the same, essentially, for both nozzles. D

Increasing the air stream velocity to 350 feet per second caused the size distribution to narrow, and the majority of particles were now concentrated in the size range 0-40 microns.

Further increase in the air velocity to a maximum of 450 feet per second caused the size distribution to narrow considerably, the largest particle noted being 140 microns for injection through the simple nozzle, and 120 microns for injection through the corkscrew nozzle. The majority of the particles were seen to be in the size range 0-20 microns, which is the reason for the low particle mean diameters by both nozzles at 450 feet per second air velocity.

6.3.6 PARTICLE TRAJECTORIES.

The computation of the trajectories of various sized particles underlined that no mathematical concept of secondary atomisation can be derived. The trajectories presented in Fig. 60a) were computed on the basis of an angle of injection of 15° , an initial cone angle of 43° , and an air stream velocity of 450 feet per second. For the purpose of this study, the particles must be assumed to be solid, and no secondary atomisation takes place. At no time in the blow pipe did any particle impact take place on the wall. A particle of 5 cms. (5000 microns) approached nearest to the wall, but this is of no practical consequence because the largest particles are known to be 130 microns. Consequently, the 'zone of atomisation' is small, since the particles of 0.01 cms.

(100 microns) and less quickly lose their injection momentum, and assume the velocity of the air stream. Consequently, if the process of secondary atomisation did not play an integral part in the process of fuel oil injection, the spray pattern would be extremely narrow, and oxygen starvation within the 'zone of atomisation' would result, likely causing soot formation.

Fig. 60b) is an illustration of the computed trajectories for injection at an angle of 30° , and with the other parameters as before. Again, it can be seen that the 'zone of atomisation' is narrow, in fact, slightly narrower than that at 15° injection.

Fig. 60c) is a similar illustration to those of a) and b). The injection angle in this case is 90° . The effect of the 'bow-wave' can be seen, yet again, the 'zone of atomisation', between the trajectories of the 100 micron particles on either side of the axis of the blow pipe, is narrow.

Fig. 60d) is an indication of the effect of the increase of air velocity on the computed trajectories. As can be seen, the effect is as expected, since increase of air velocity causes a greater 'bowing' of the sheet, and the trajectories of the small particles at the high air stream velocities of 550 feet per second and 650 feet per second are hardly in evidence.

Fig. 60e) was computed for hypothetical spray sheet velocities of 30 feet per second, 50 feet per second and 70 feet per second. As can be seen, by increasing the spray sheet velocity, a wider 'zone of atomisation' results, which would help the process of combustion by affording a greater surface area for oxidation. However, it can not

be envisaged as to how such a spray sheet velocity can be achieved practically, since a velocity of 30 feet per second represents a flow rate of 3.2 gallons per minute, and a spray sheet thickness of 0.15 cms.

Thus, from all five figures, it can clearly be seen that in the blow pipe of a blast furnace, injection of oil would be wasteful, if not for the process of secondary atomisation, which spreads the spray uniformly inside the blow pipe and tuyere, so that oxygen starvation can be avoided, and combustion effected in a reasonably efficient manner.

6.4 OPTIMUM CONDITIONS FOR BLAST FURNACE OIL INJECTION.

From a study of results obtained in the injection of molten wax into high velocity air streams, a number of operating parameters become obvious. Since oil is a viscous fuel, a high pre-heat temperature is necessary in order that the viscosity be low enough to permit small droplet size production. Although no variance in viscosity was attempted with wax injection into air streams, observation of wax injection into still air indicated that lowering the viscosity caused a decrease in the particle mean diameter of the spray. Thus, the oil should be injected with as high a pre-heat temperature as possible, without approaching the flash-point too closely, in order that the viscosity be about 120 SUS (5-6 cp).

In most blast furnace plants, conditions within the blow pipe are such that the high velocity air stream is available. Thus, use of either a simple nozzle or a complicated nozzle would result in droplets of the desired size for efficient combustion. At these velocities, the

resultant spray would be uniform in particle size distribution, although that produced by the corkscrew insert would form slightly sooner, due to the initial particle size offered for secondary atomisation. In either case, the distribution of the spray within the tuyere should be such as to afford good mixing for evaporation and subsequent combustion.

The angle of injection which proved most successful in the wax injection studies was one of 15° , since this afforded a greater distance between the wall and the exit orifice of the nozzle, and thus greater space for spray distribution. Such an angle appears to have found widespread use in blast furnace practice, and the findings of this study merely confirm this view. It should be noted that Weiss found a smaller mean particle size resulted from injection contra-stream (i.e. into the air stream in the opposite direction to its flow) than co-stream. However, such practice in blast furnaces would prove difficult due to the foreseen problems of accretions on the nozzle orifice.

The relative velocity between the air stream and the injected fuel has been found to be of importance, and a velocity of greater than 450 feet per second should prove sufficient to produce droplets of suitable size for efficient combustion. In plants where a high air stream velocity is as yet unavailable, such as at Voest- Linz (19), where the air velocity is 400 feet per second, the drop size will be out of the range specified by Heynert. In such a case, two alternatives offer themselves, (a) having a slightly narrower blow pipe, whereby passage of the same quantity of air will cause an increase in its velocity, and (b) the inclusion within the blow pipe of a venturi-insert which causes the air at that point to go supersonic. This has

been postulated by Duthion et al (104), and is currently under investigation in France.

In consequence, the economic survival of the blast furnace will depend to a large extent on the ability of greater quantities of coke being saved by the increased injection rates of oil. This study has underlined the parameters which were found to give the optimum results with injection of molten wax, although this does not necessarily mean that application of these parameters would immediately solve the problems currently associated with oil injection. Conditions within any part of the blast furnace cannot be reproduceable exactly on a laboratory scale, yet it is felt that this study does indicate trends which may improve the practice of oil injection.

BIBLIOGRAPHY.

(104) Duthion E.L. et al U.S. Patent 3,596,894.

Fig. 44

PLEXIGLAS BLOW PIPE ASSEMBLY.

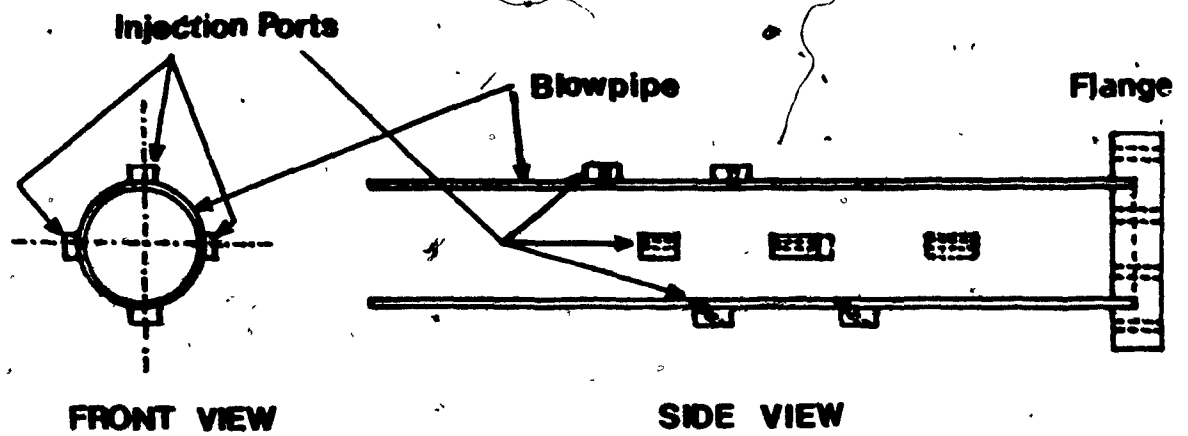




Fig. 45

ASSEMBLY FOR THE INJECTION OF WAX INTO AIR STREAM.



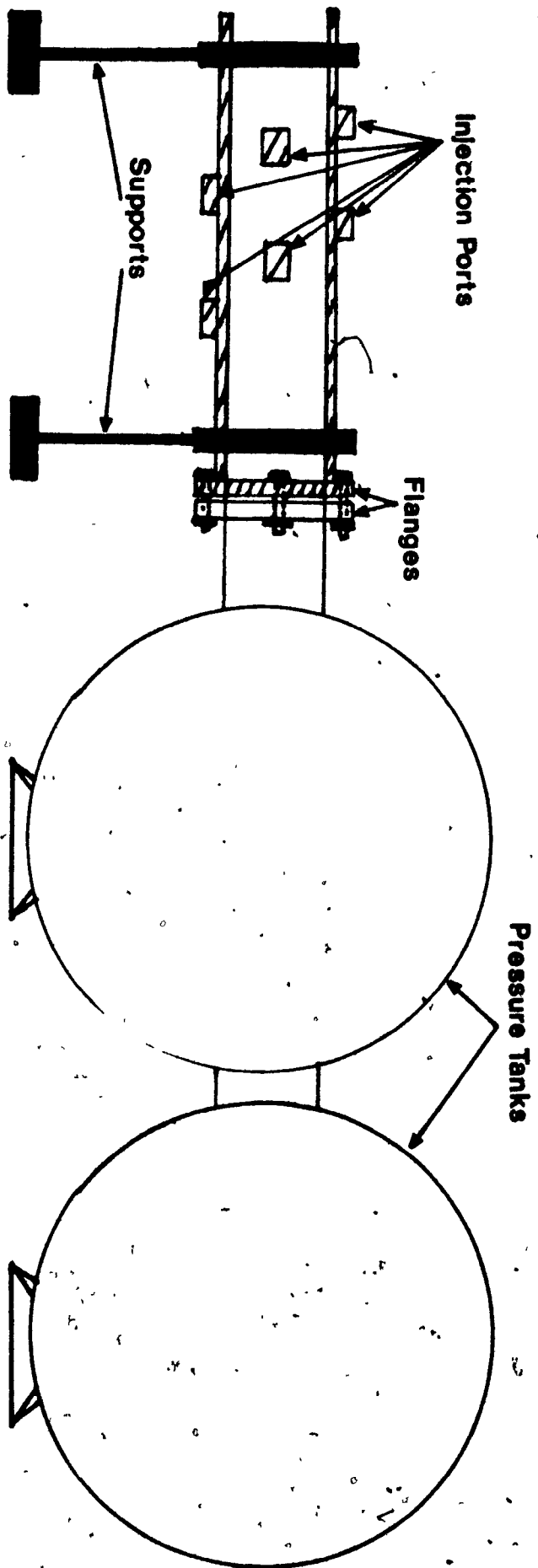
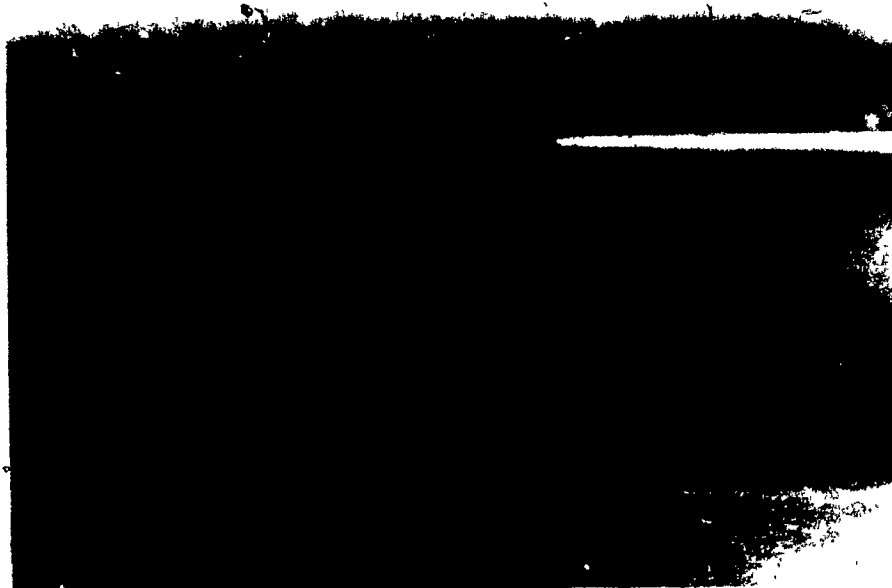


Fig. 46

WATER INJECTION INTO AIR STREAMS.

- (a) Simple Nozzle, 250 feet/second air velocity, 15° injection angle.
- (b) Simple Nozzle, 450 feet/second air velocity, 15° injection angle.



a.

b.

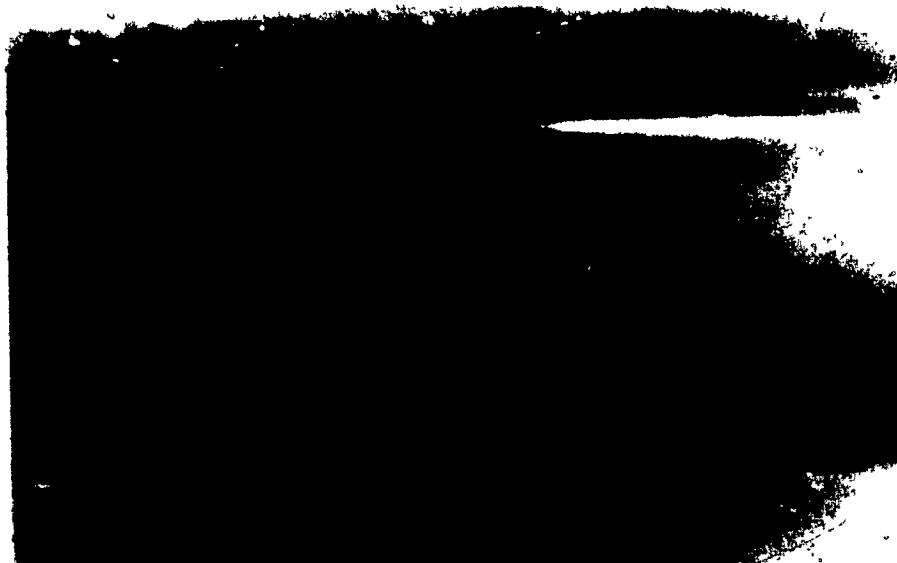
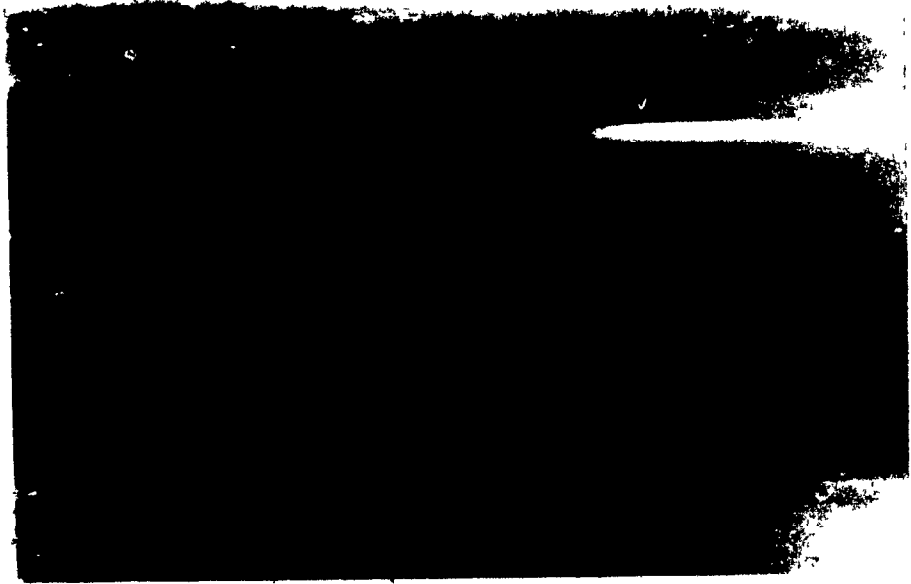


Fig. 46

(c) Corkscrew Nozzle, 250 feet/second air velocity, 15° injection angle.

(d) Corkscrew Nozzle, 450 feet/second air velocity, 15° injection angle.



c.

d.



Fig. 46

- (e) Simple Nozzle, 250 feet/second air velocity, 90° injection angle
- (f) Simple Nozzle, 450 feet/second air velocity, 90° injection angle



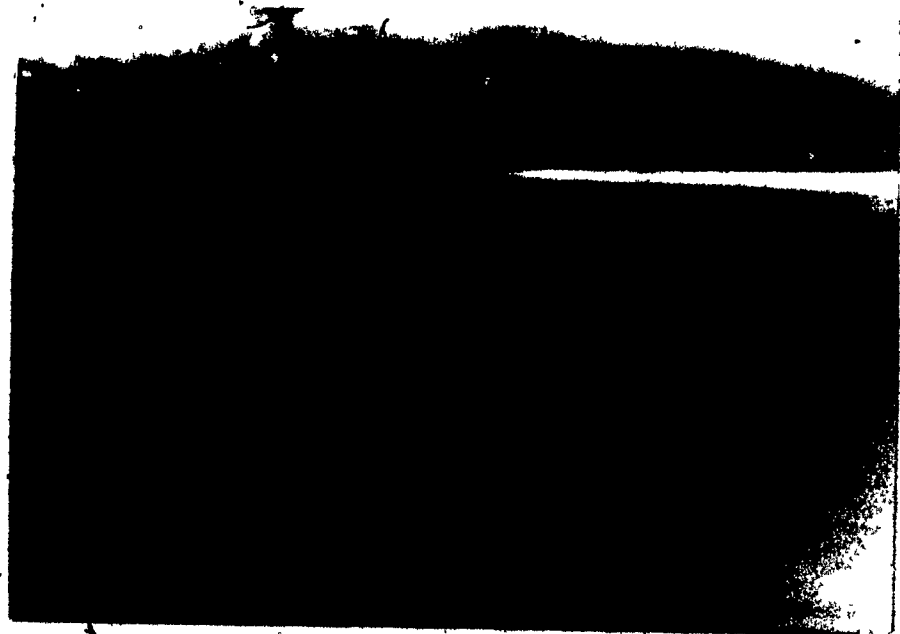
Fig. 46

(g) Corkscrew Nozzle, 250 feet/second air velocity, 90° injection angle

(h) Corkscrew Nozzle, 450 feet/second air velocity, 90° injection angle



g.



h.

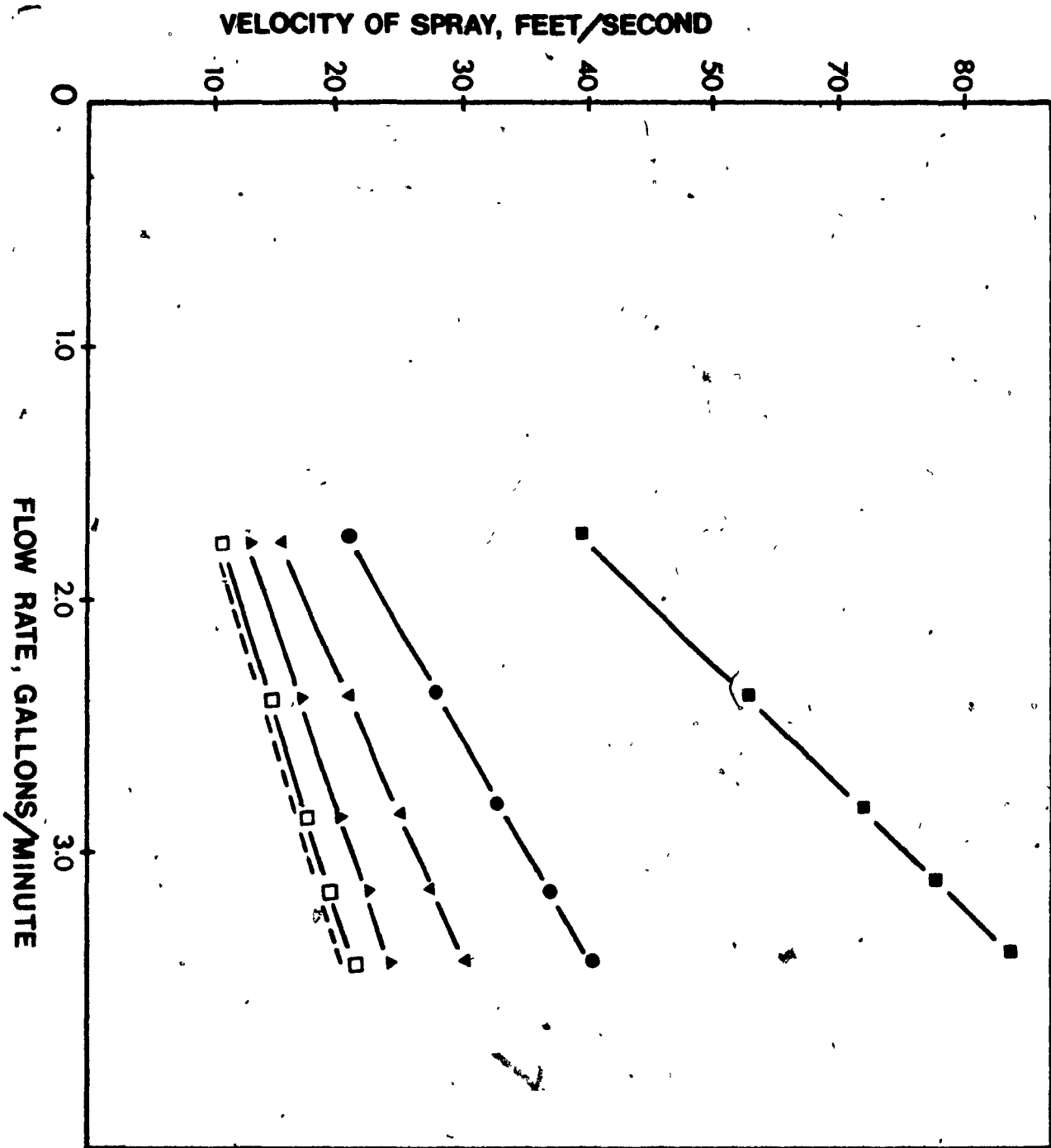
Fig. 46

- (i) Simple Nozzle, 250 feet/second air velocity, 60° injection angle
- (j) Simple Nozzle, 450 feet/second air velocity, 60° injection angle



Fig. 47

COMPUTED VELOCITIES OF SPRAY SHEET FROM CORKSCREW NOZZLE



— Corkcrew
 - - - Insert
 - - - Simple Nozzle
 Sheet Thickness
 ■ 0.05 cm
 ● 0.10
 ▼ 0.15
 ▲ 0.20
 □ 0.25

Fig. 48

PHOTOGRAPHS OF WAX PARTICLES PRODUCED BY INJECTION INTO AIRSTREAMS

- (a) Simple Nozzle, 300 feet/second air velocity, 3.2 gallons/minute
wax flow rate, 15° injection angle. X40
- (b) Corkscrew Nozzle, 300 feet/second air velocity, 3.2 gallons/minute
wax flow rate, 15° injection angle. X40



a.



b.

Fig. 48

(c) Simple Nozzle, 350 feet/second air velocity, 3.2 gallons/minute
wax flow rate, 15° injection angle. X40

(d) Gorkscrew Nozzle, 350 feet/second air velocity, 3.2 gallons/minute
wax flow rate, 15° injection angle. X40



c.

d.

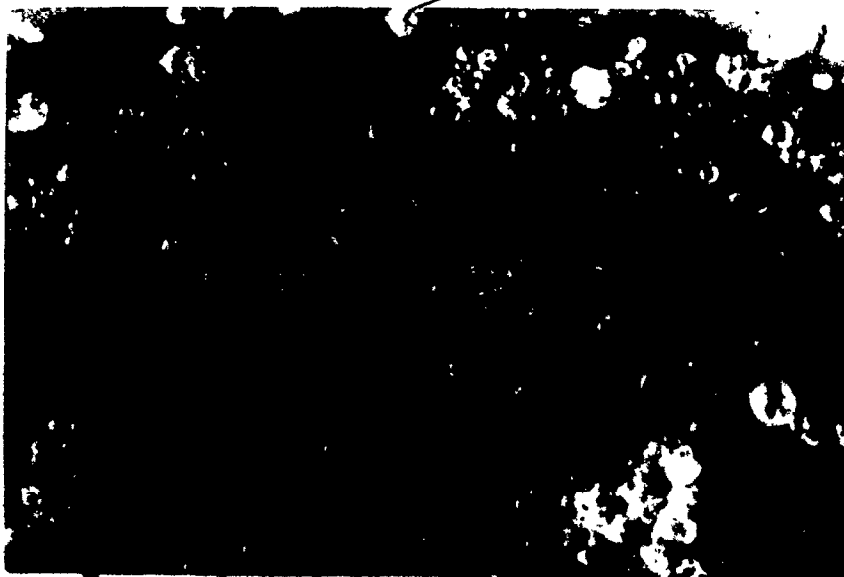


Fig. 48

- (e) Simple Nozzle, 450 feet/second air velocity, 3.2 gallons/minute
wax flow rate, 15° injection angle. X40
- (f) Corkscrew Nozzle, 450 feet/second air velocity, 3.2 gallons/minute
wax flow rate, 15° injection angle. X40
- (g) Corkscrew Nozzle, 450 feet/second air velocity, 3.2 gallons/minute
wax flow rate, 15° injection angle. X670



e.



f.



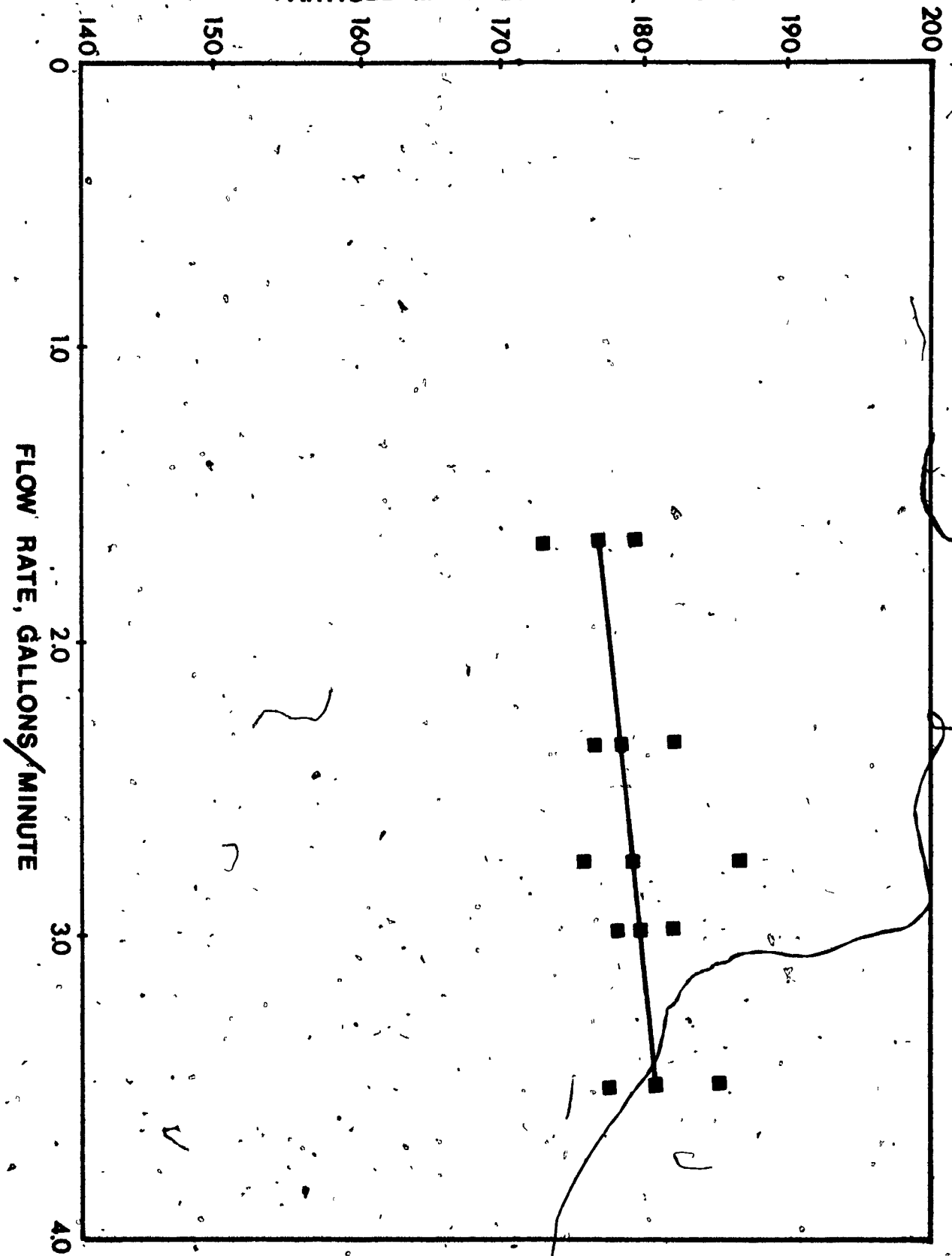
g.

Fig. 49

PARTICLE MEAN DIAMETER AS A FUNCTION OF WAX FLOW RATE

Simple Nozzle, 250 feet/second air velocity.

PARTICLE MEAN DIAMETER, MICRONS



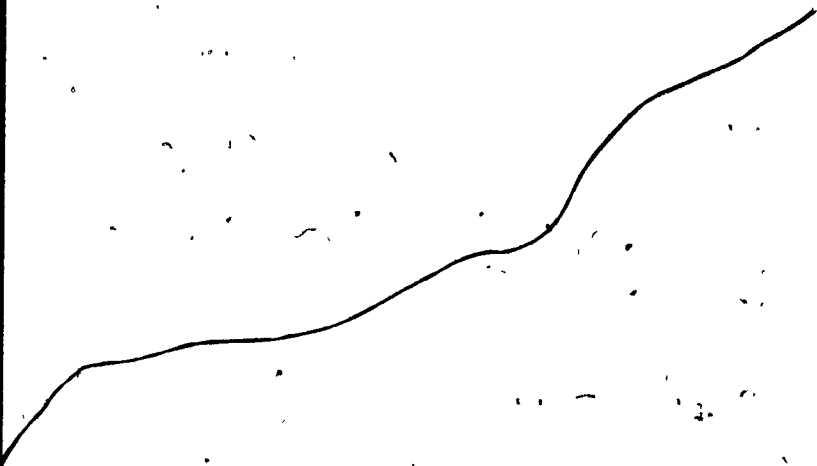


Fig. 50

PARTICLE MEAN DIAMETER AS A FUNCTION OF WAX FLOW RATE.

Single Nozzle, 450 feet/second air velocity.

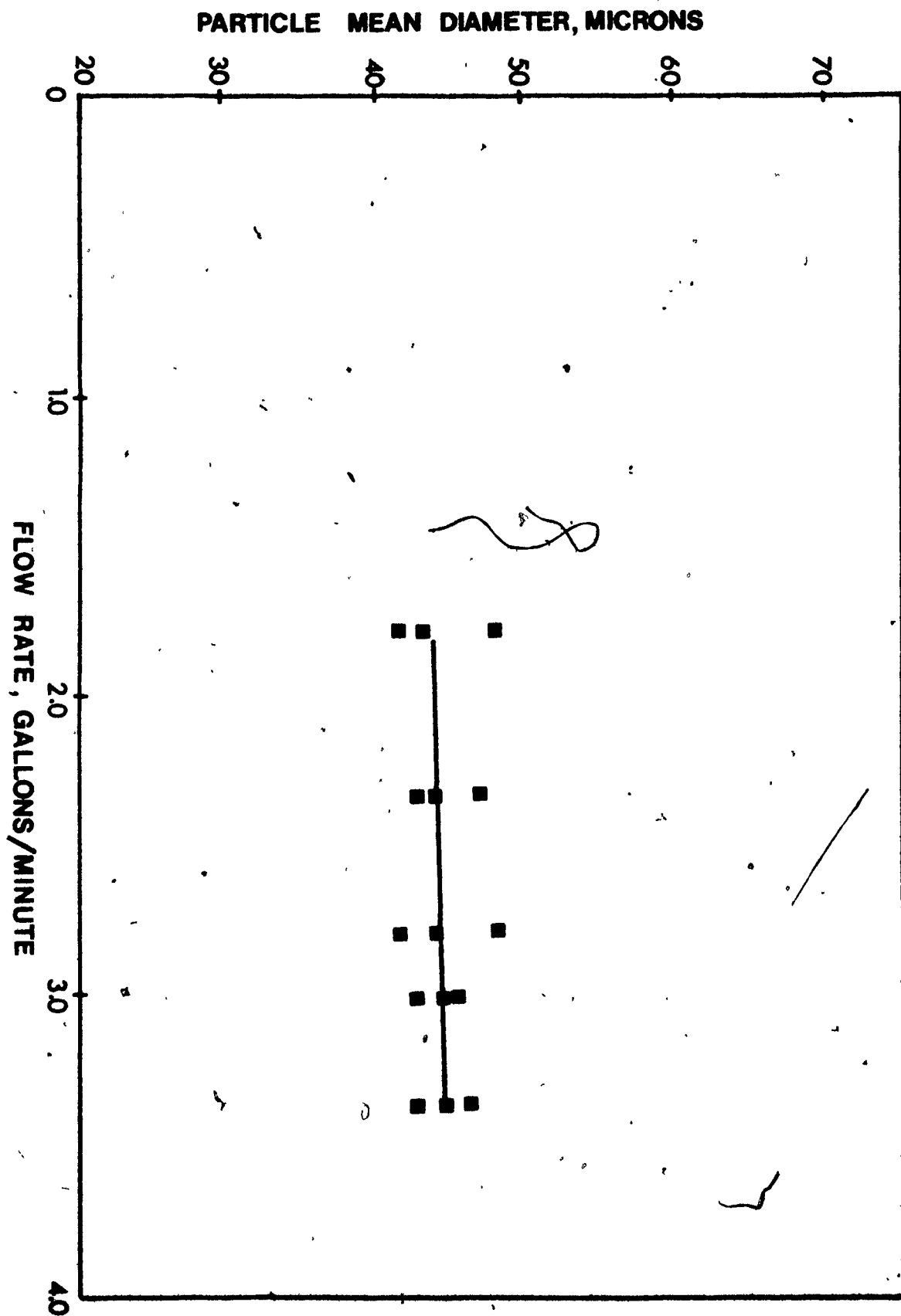


Fig. 51

PARTICLE MEAN DIAMETER AS A FUNCTION OF WAX FLOW RATE

Corkscrew Nozzle, 350 feet/second air velocity.

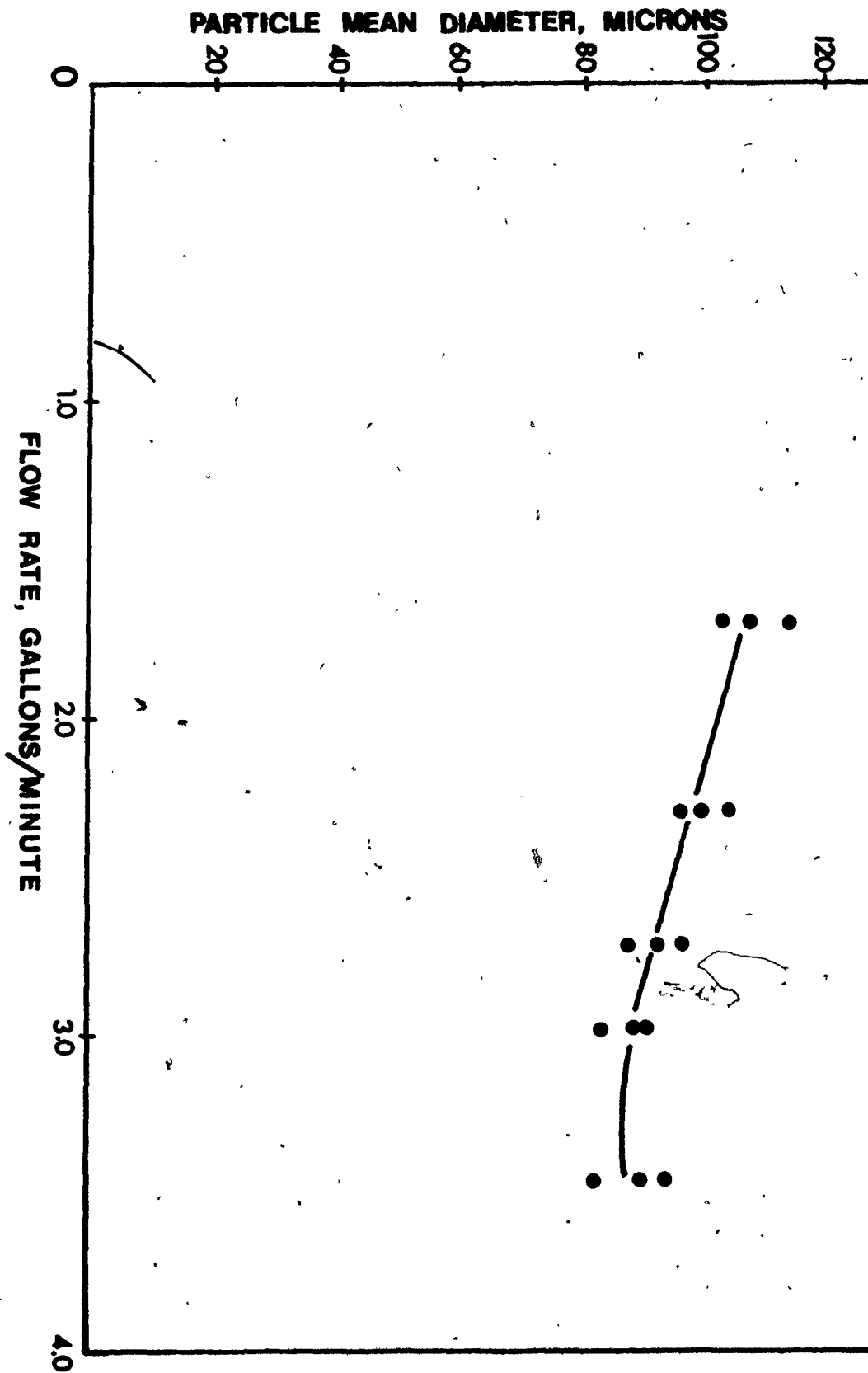


Fig. 52

PARTICLE MEAN DIAMETER AS A FUNCTION OF WAX FLOW RATE

Corkscrew Nozzle, 450 feet/second air velocity.

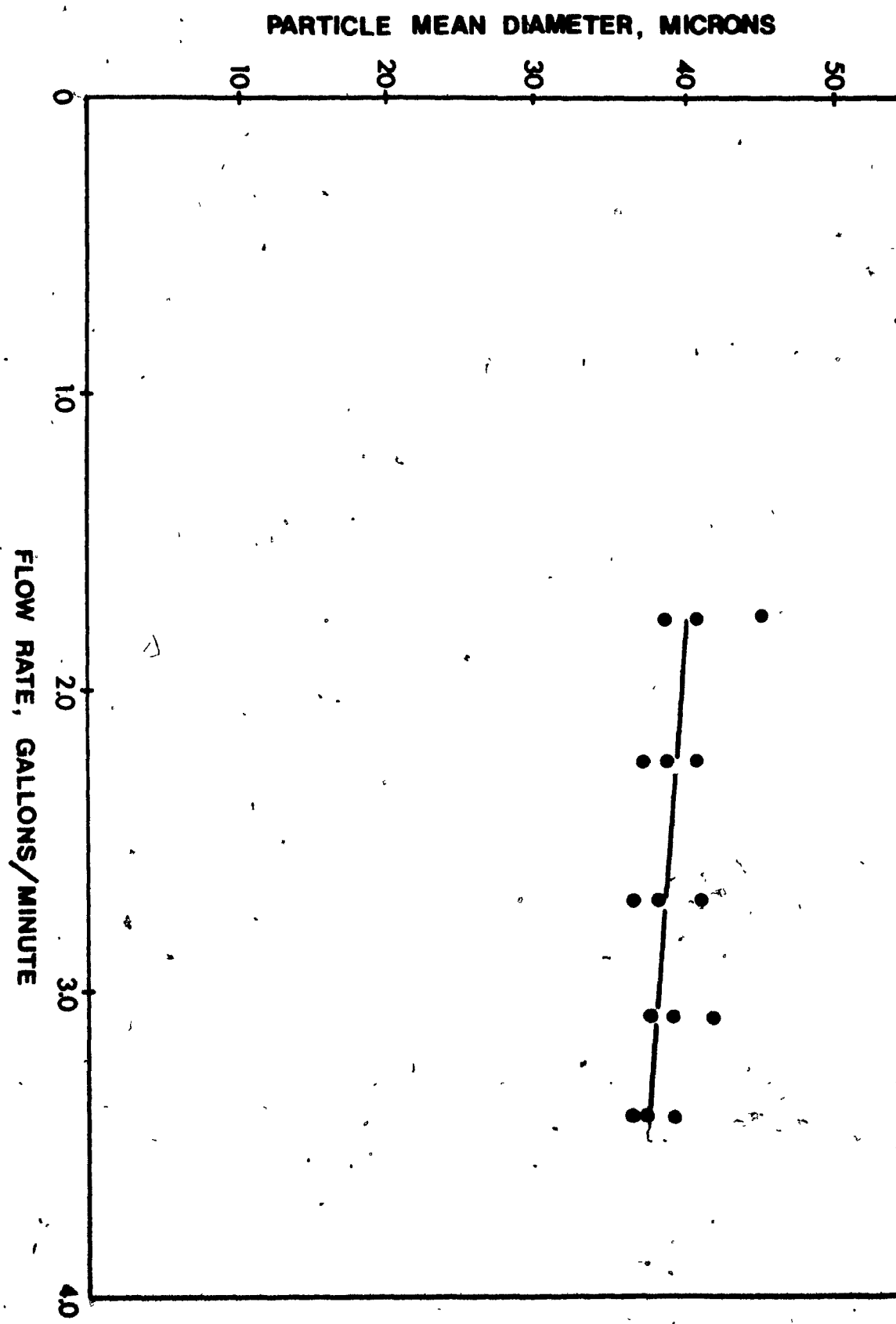


Fig. 53

PARTICLE MEAN DIAMETER AS A FUNCTION OF INJECTION ANGLE.

250 feet/second air velocity, 3.2 gallons/minute

wax flow rate.

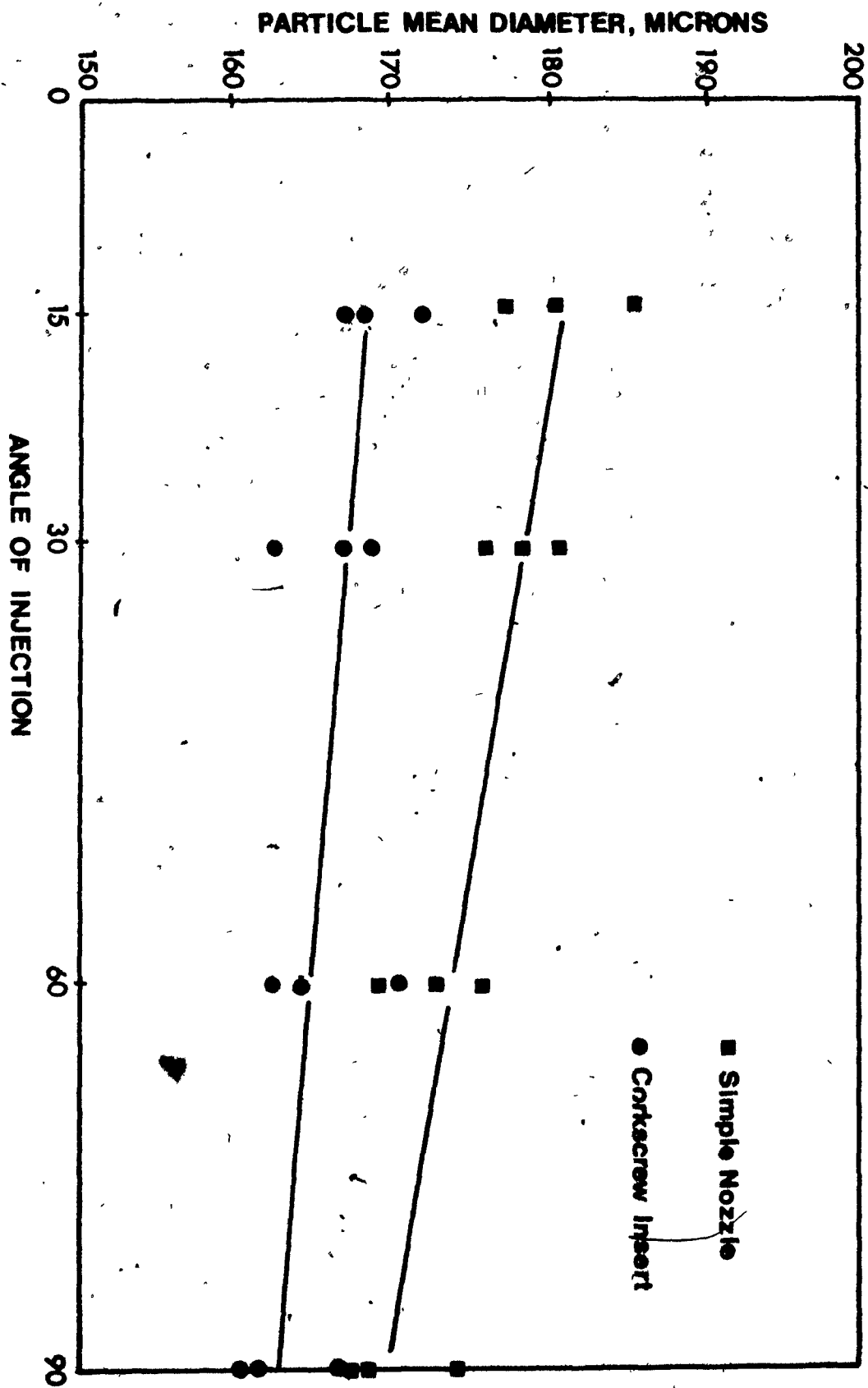


Fig. 54

PARTICLE MEAN DIAMETER AS A FUNCTION OF INJECTION ANGLE

400 feet/second air velocity, 3.2 gallons/minute

wax flow rate.

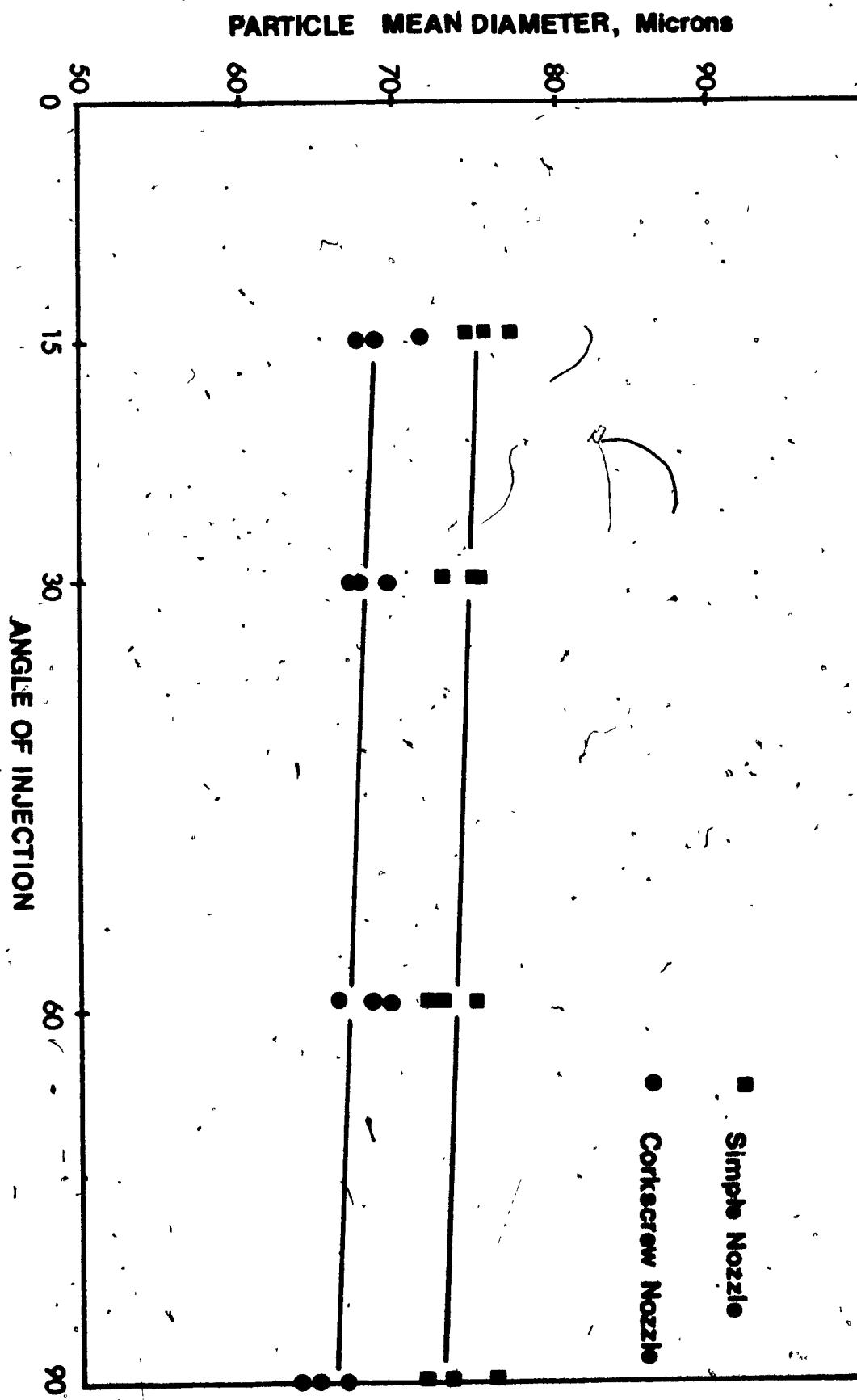


Fig. 55

PARTICLE MEAN DIAMETER AS A FUNCTION OF THE RELATIVE VELOCITY

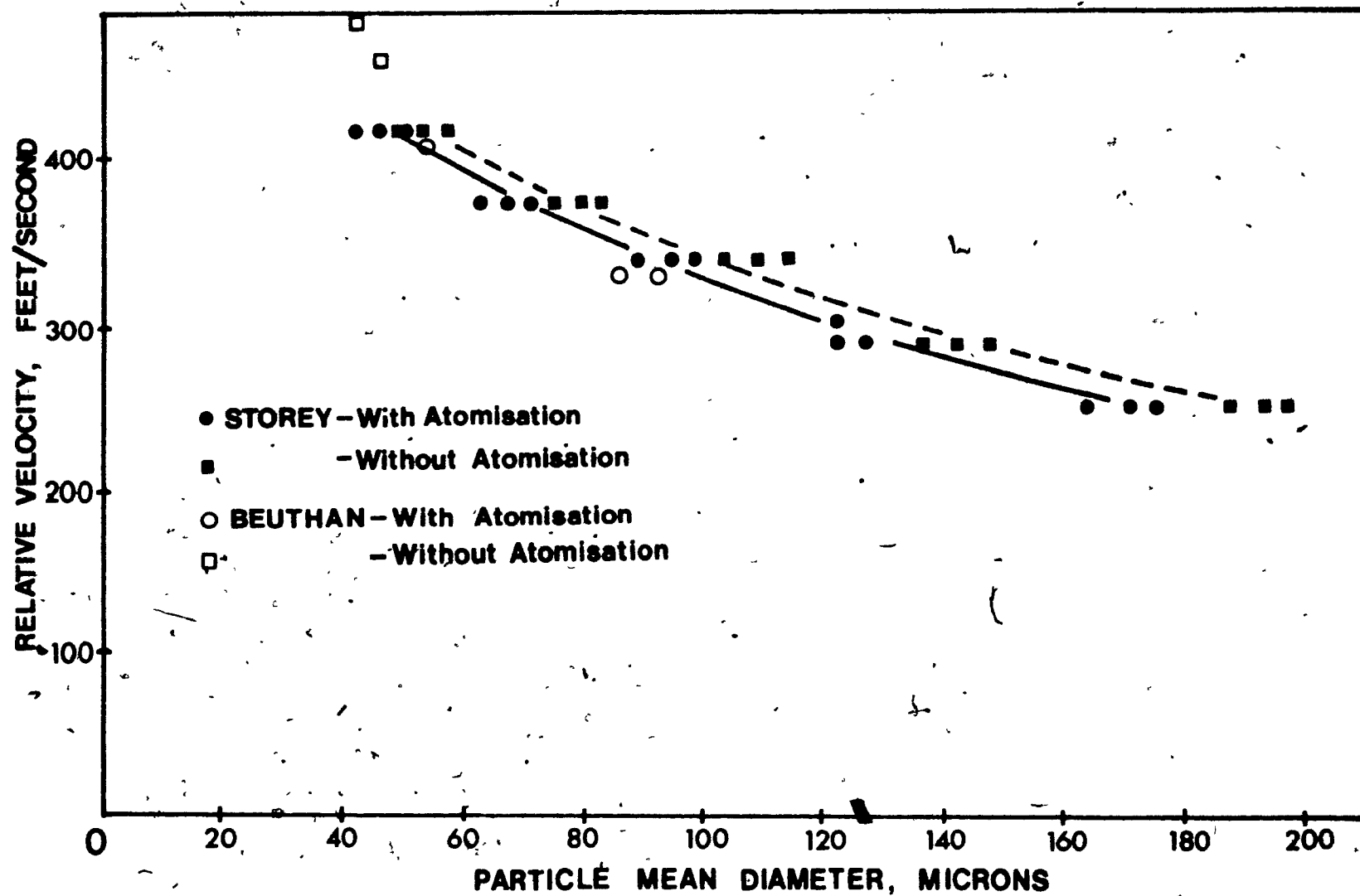


Fig. 56

SPRAY PATTERN OF INJECTED WAX ON INSERTS

- (a) 90° injection angle, simple nozzle, 300 feet/second air velocity
- (b) 90° injection angle, corkscrew nozzle, 300 feet/second air velocity



a.



b.

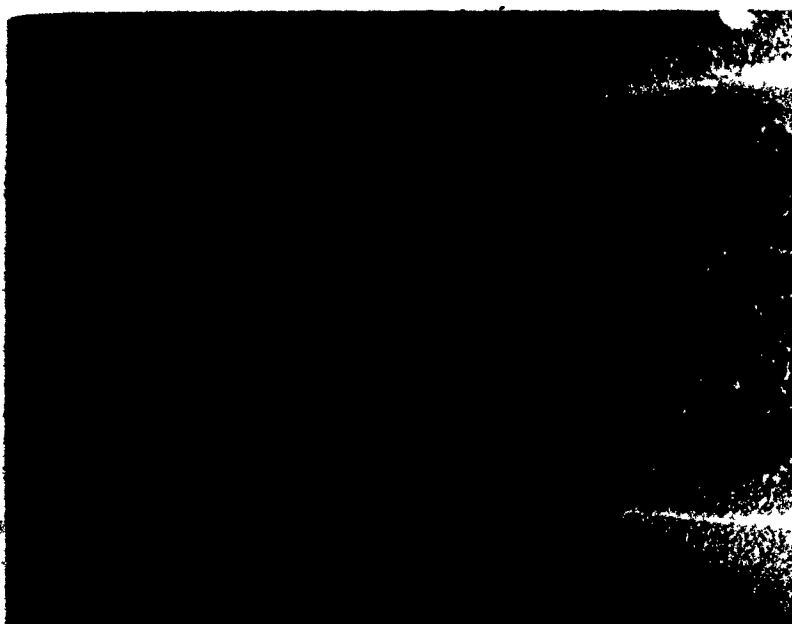
Fig. 56

(c) 90° injection angle, Simple Nozzle, 250 feet/second air velocity.

(d) 60° injection angle, Simple Nozzle, 350 feet/second air velocity.



c.



d.

Fig. 56

(e) 15° injection angle, Simple Nozzle, 350 feet/second air velocity.

(f) 15° injection angle, Corkscrew Nozzle, 350 feet/second air velocity.

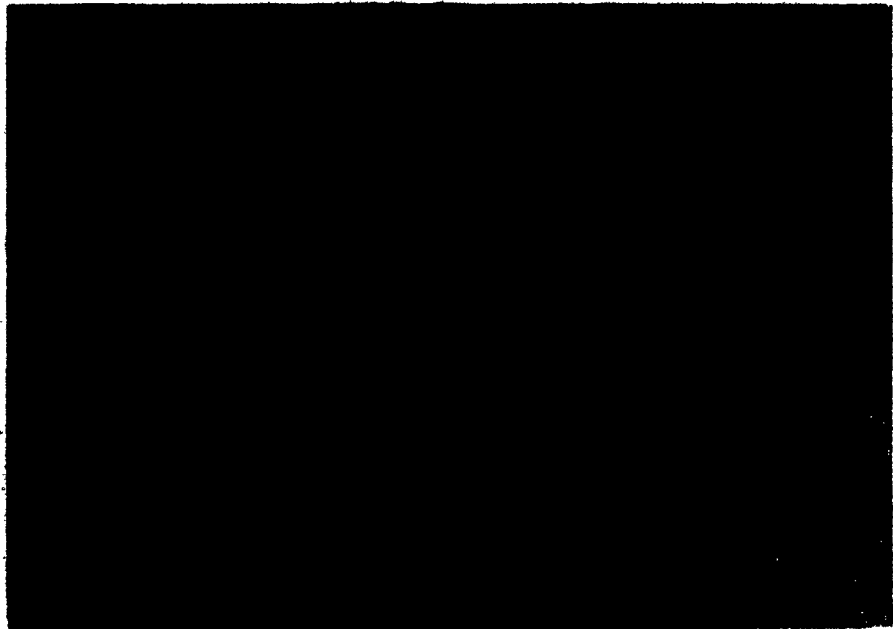
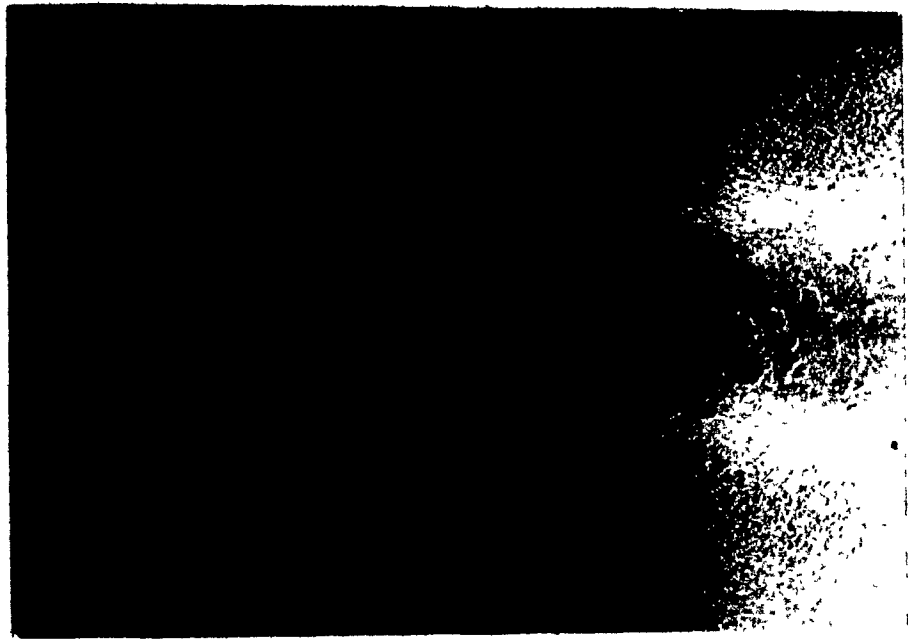


Fig. 56

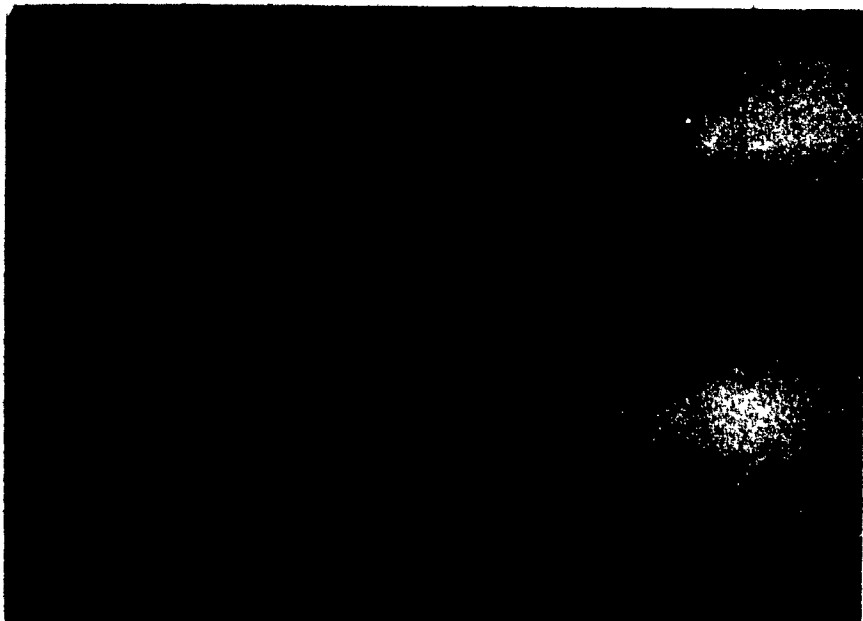
(g) 15° injection angle, Simple Nozzle, 450 feet/second air velocity.

(h) (i) 15° injection angle. Simple Nozzle, 350 feet/second
air velocity. Lance 1" off-centre towards injection port.

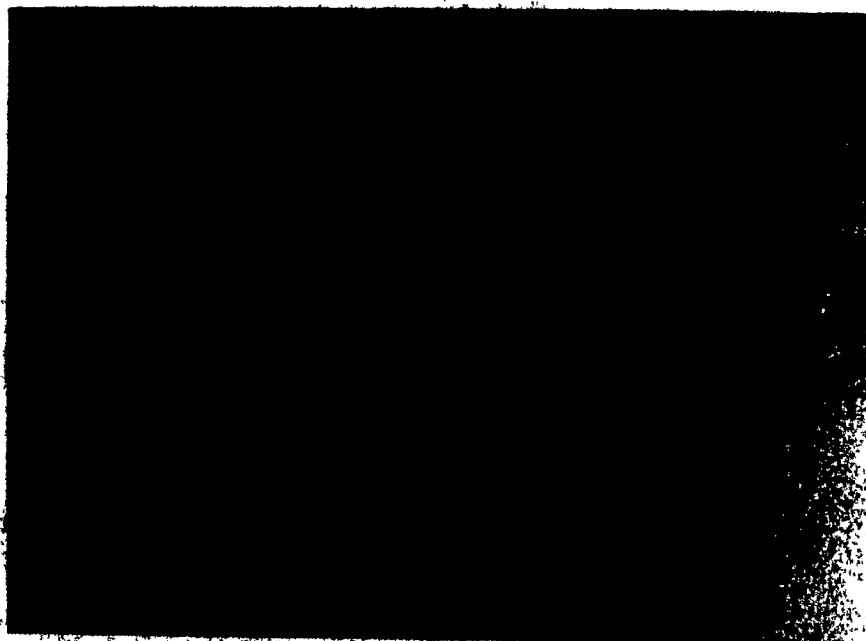
(ii) 15° injection angle, Simple Nozzle, 350 feet/second
air velocity. Lance 1" off-centre towards opposite wall.



g.



h.
(i)



h.
(ii)

Fig. 57

WEIGHT OF CROSS-SECTION OF SPRAY PATTERN OF FIG. 56c).

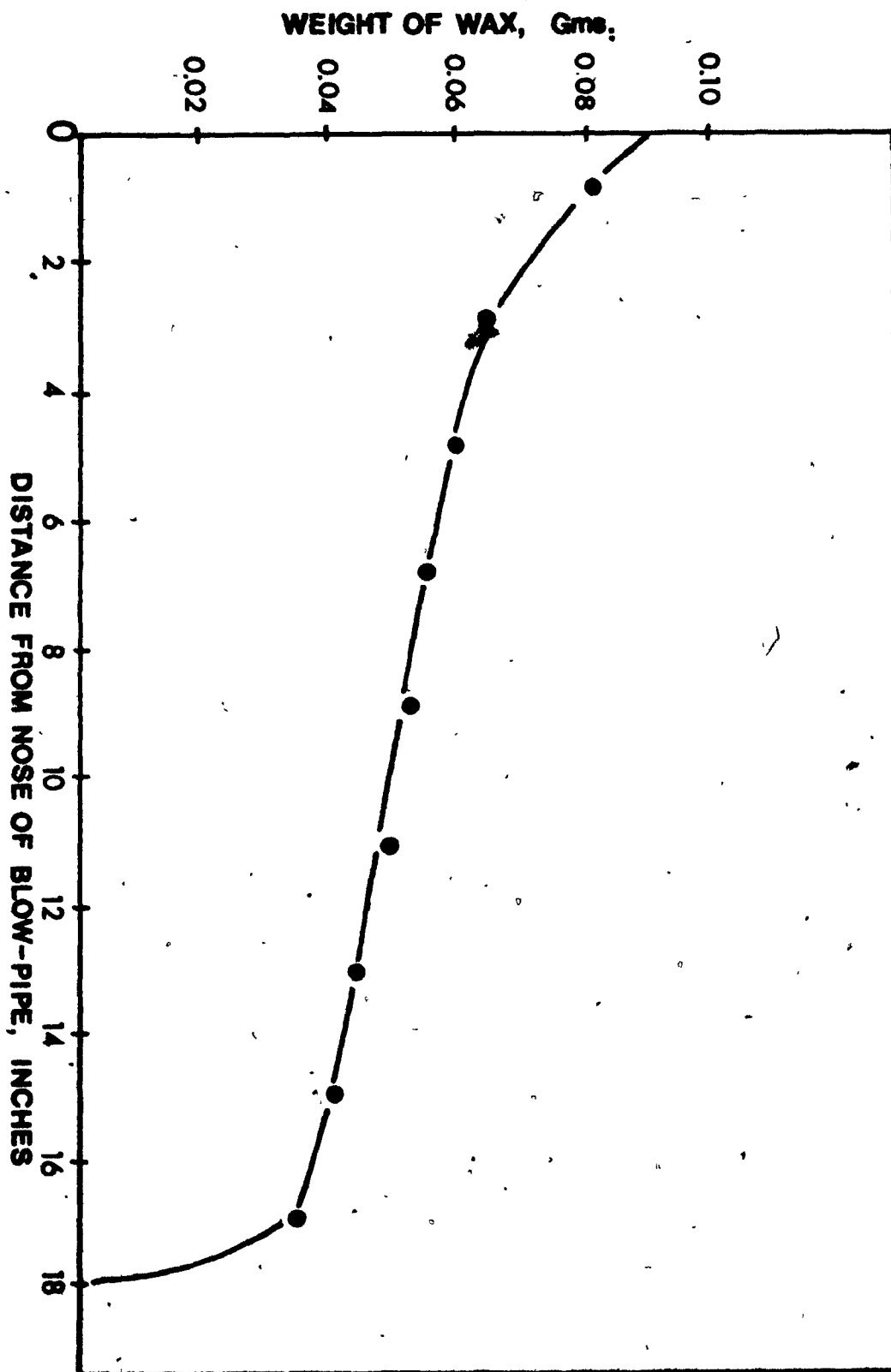


Fig. 58

WAX SPRAYED WHICH IMPACTED ON WALL VERSUS AIR VELOCITY.

3.2 gallons/minute wax flow rate

15° injection angle.

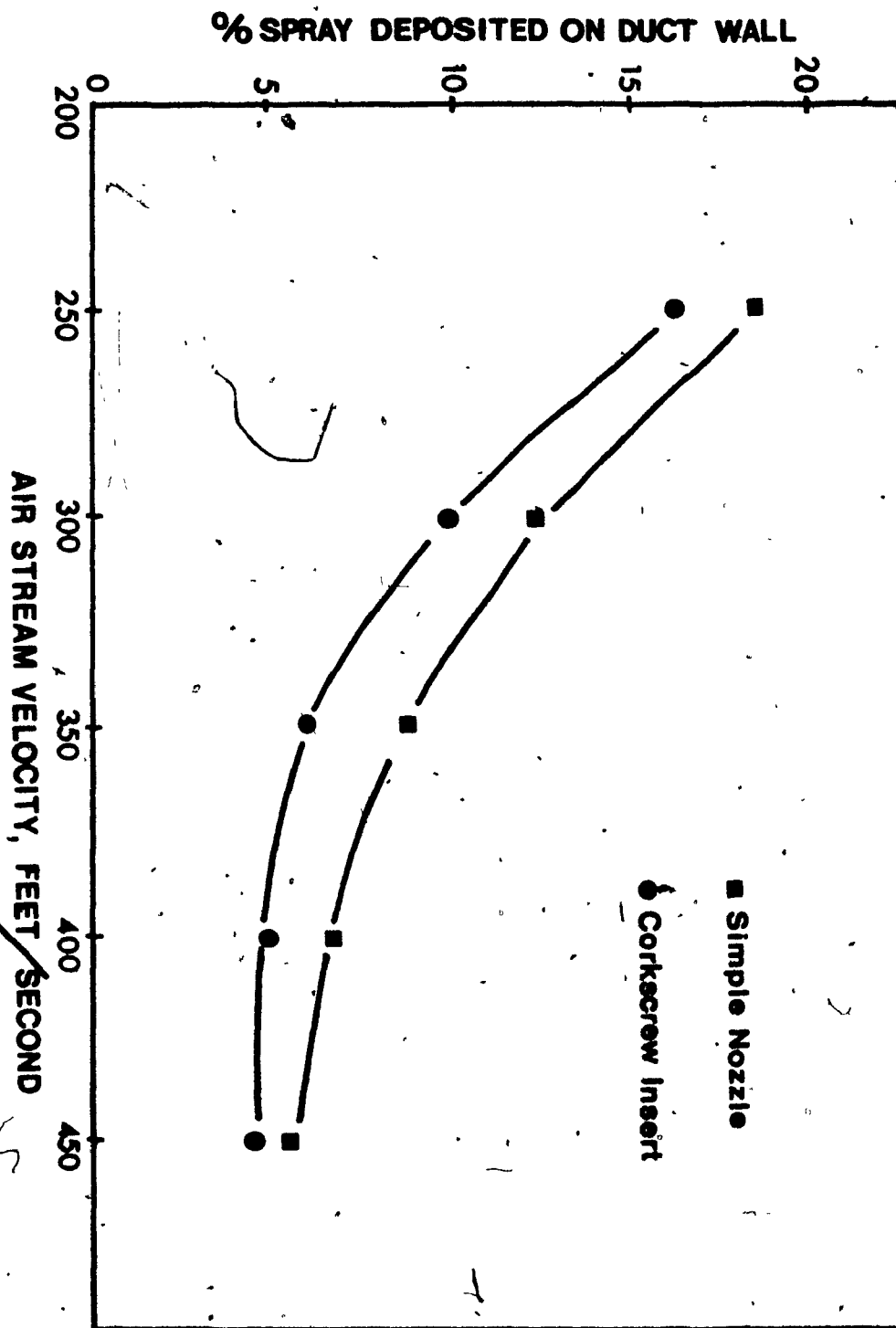


Fig. 59

NORMAL DISTRIBUTION OF WAX PARTICLES PRODUCED BY INJECTION INTO AIR STREAMS.

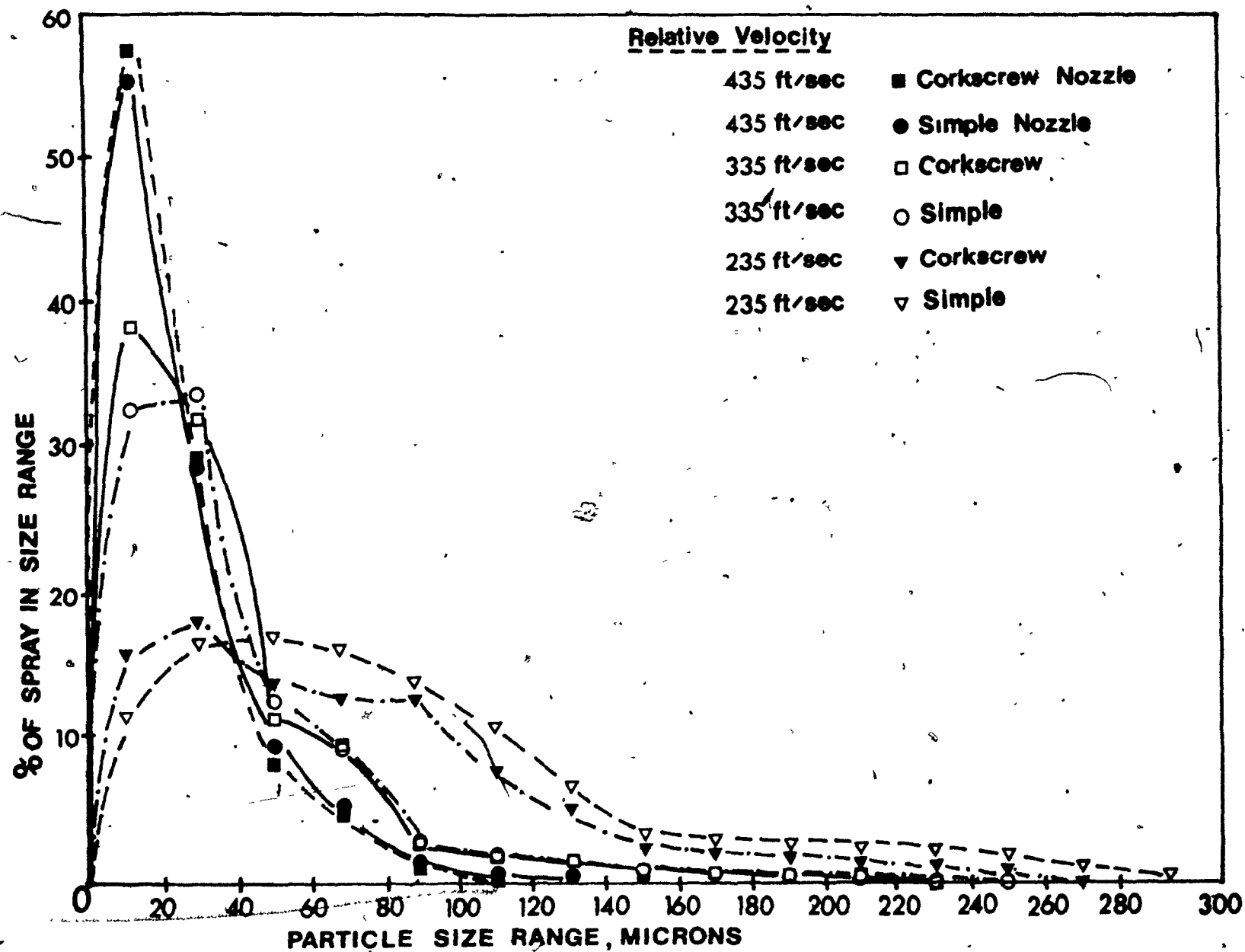


Fig. 60

COMPUTED PARTICLE TRAJECTORIES

(a) 450 feet/second air velocity, 30 feet/second sheet velocity
15° injection angle.

0.5, 0.1, 0.01 refer to particle diameters, cms.

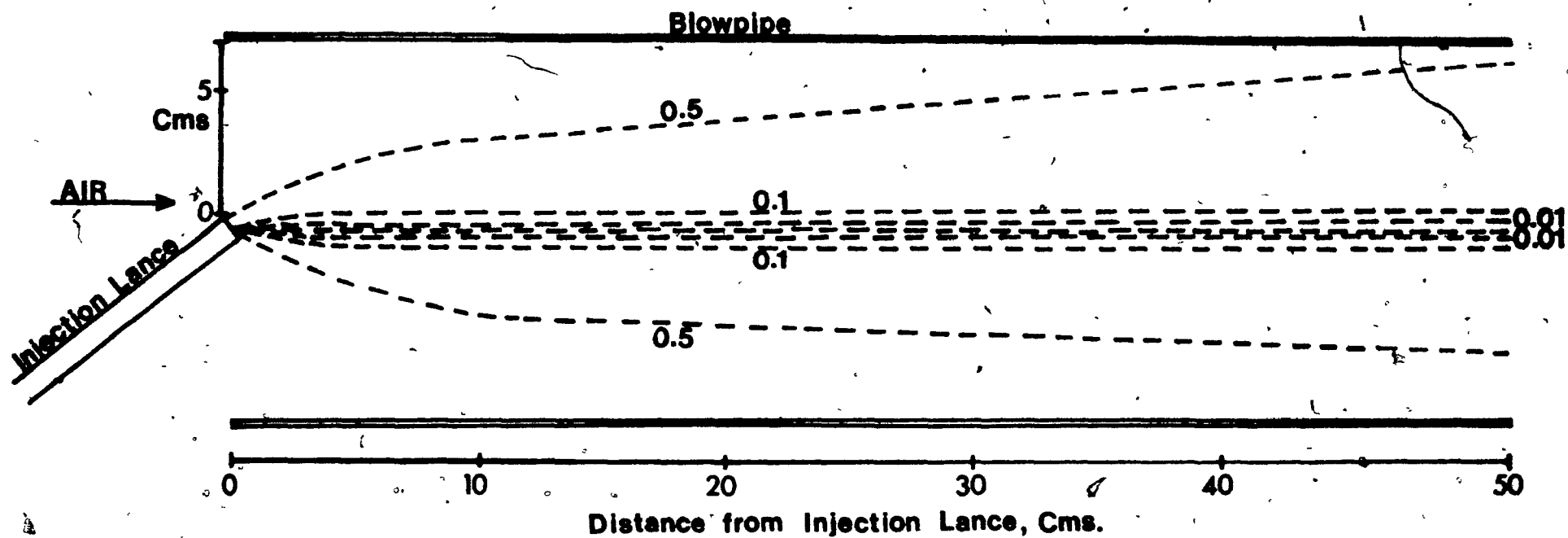
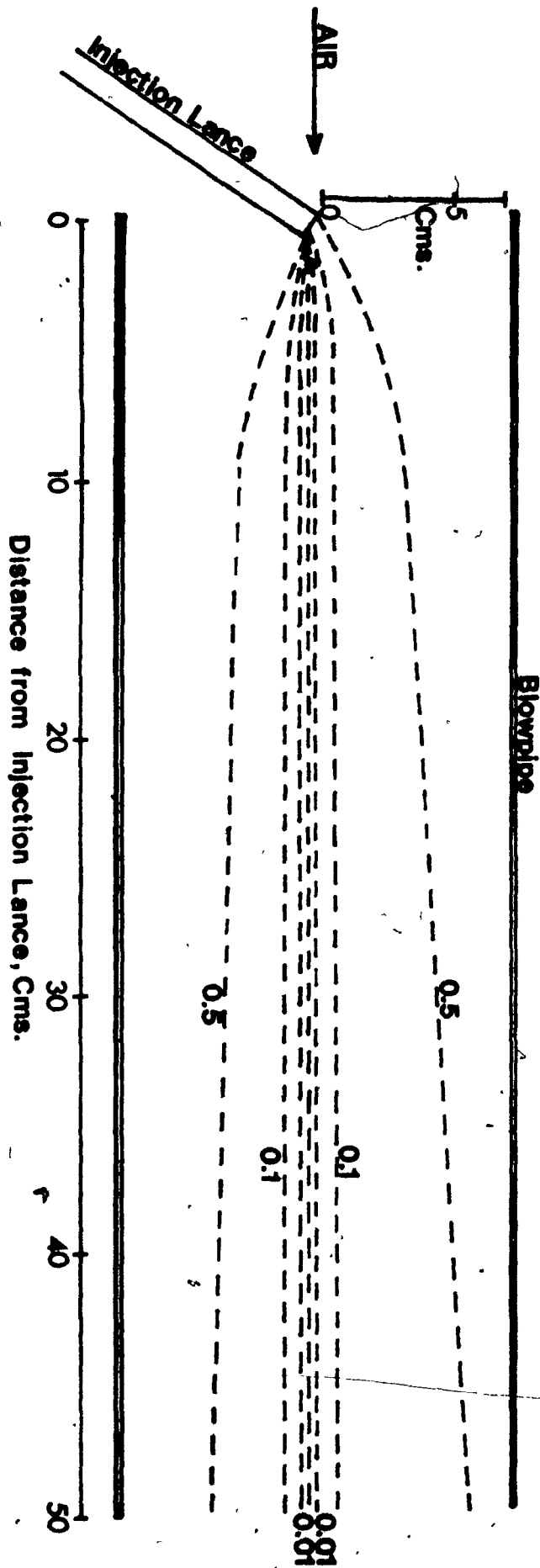


Fig. 60

(b) 450 feet/second air velocity, 30 feet/second sheet velocity,

✓ 30° injection angle.

0.5, 0.1, 0.01 refer to particle diameter, cms.



b.

Fig. 60

(c) 450 feet/second air velocity, 30 feet/second sheet velocity,
90° injection angle.

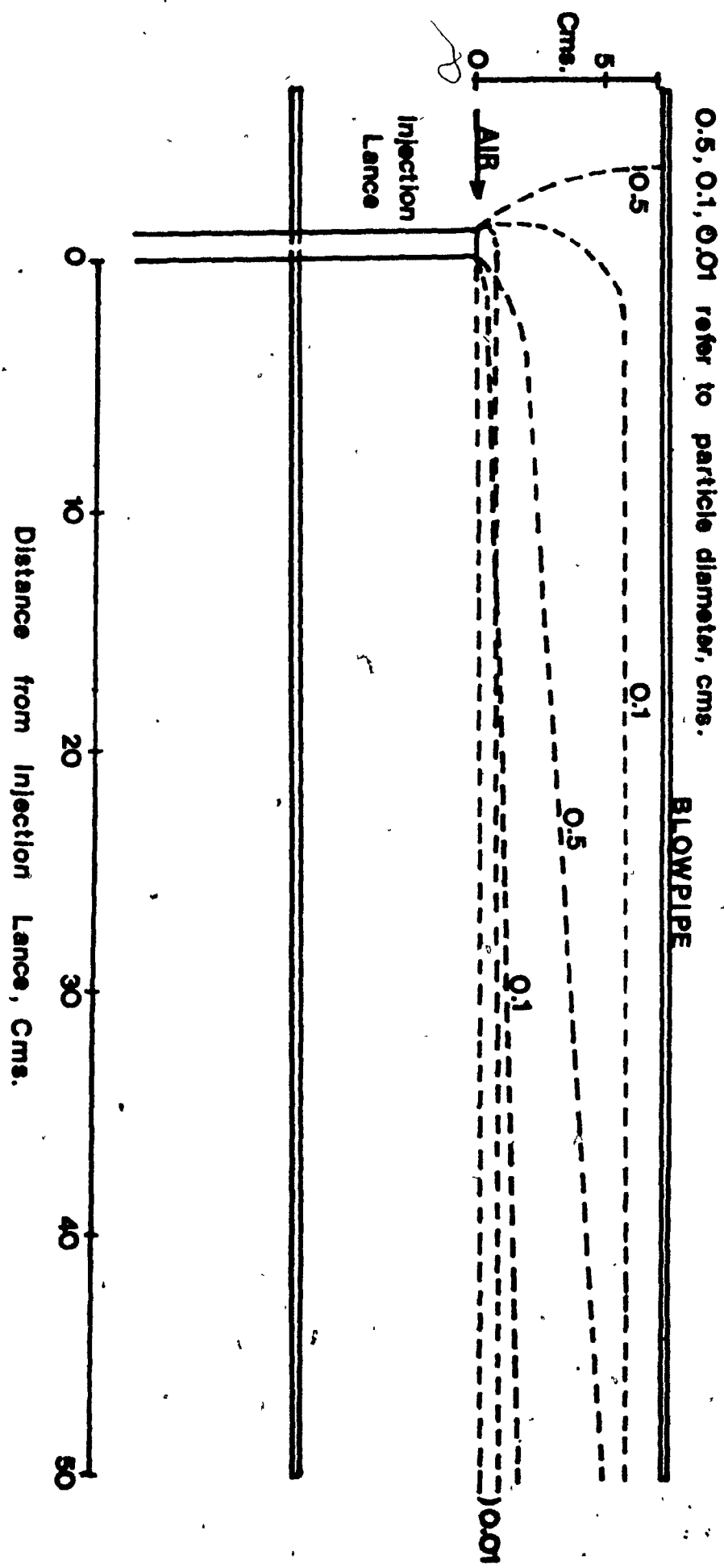




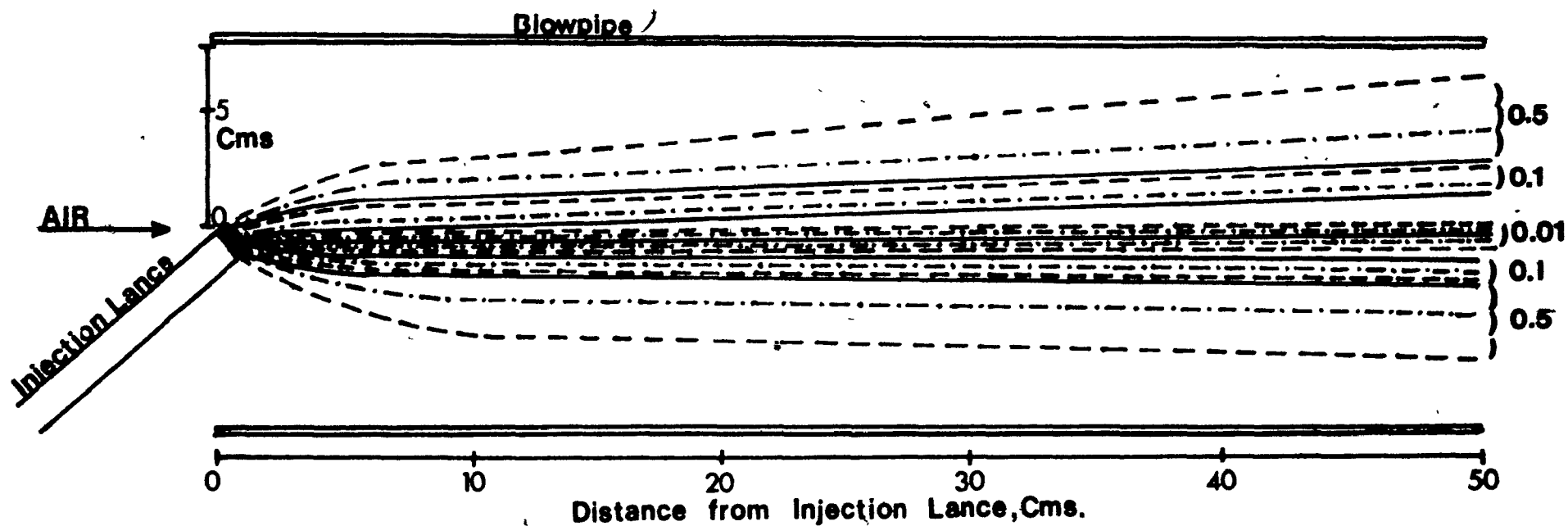
Fig. 60

(d) 450, 550, 650 feet/second air velocity, 30 feet/second sheet velocity,
15° injection angle.

0.5, 0.1, 0.01 refers to particle diameter, cms.

AIR VELOCITY

----- 450 Ft.sec⁻¹
-.-.-.- 550 Ft.sec⁻¹
_____ 650 Ft.sec⁻¹



d.

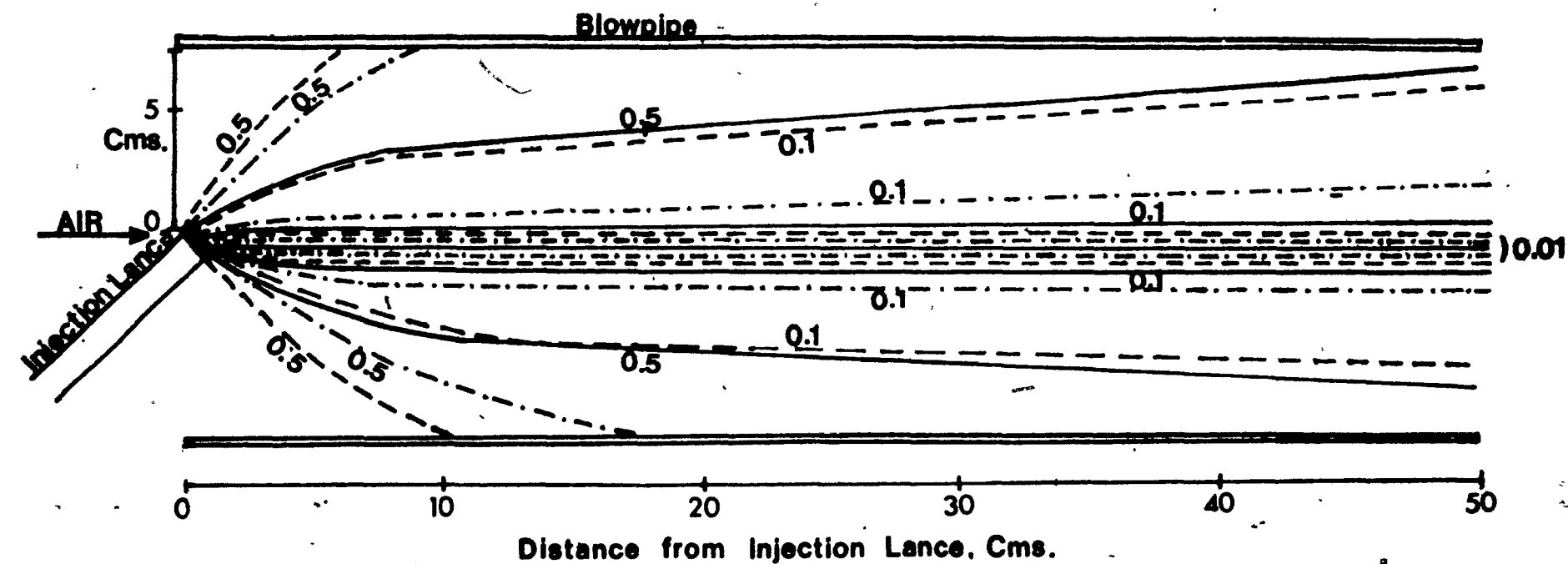
Fig. 60

(e) 450 feet/second air velocity, 30, 50, 70 feet/second sheet velocity,
15° injection angle.

SHEET VELOCITY

----- 70 Ft.sec⁻¹
 -.-.-.-.- 50 Ft.sec⁻¹
 _____ 30 Ft.sec⁻¹

0.5, 0.1, 0.01 refers to particle diameter, cms.



Chapter 7.
CONCLUSIONS.

7.0 CONCLUSIONS.

- (1) The positioning of a two-revolution corkscrew $3/4$ inch from the exit orifice of the lance caused primary atomisation of the liquid stream, the exiting liquid being in the form of a hollow cone.
- (2) The use of wax as a 'replacement liquid' for oil proved successful. The physical properties of the wax, Mobilwax 2305, were comparable to those of a Bunker 'C' oil, and no problems were associated with molten wax injection.
- (3) The effect of viscosity on the final droplet size in the still air studies was seen to be that with an increase in viscosity from 100 SUS (5 cp) to 40 SUS (2 cp) caused a decrease in the Sauter Mean Diameter of 20-25%. This is important in blast furnace oil injection, since a small particle size is a necessary criterion for efficient combustion.
- (4) Injection of water into high velocity air streams showed that with the simple nozzle, a decrease in the penetration distance resulted with increase in the air stream velocity from 250 feet per second up to 450 feet per second, for all injection angles. At 450 feet per second, secondary atomisation of the exiting stream occurred immediately on entering the air stream. With the corkscrew nozzle, since the exiting liquid was in the form of a thin sheet, disruption was immediate, at all air stream velocities greater than 300 feet per second.
- (5) Injection of wax, at varying flow rates, into air streams of constant velocity indicated that at the lower flow rates of 250-350 feet per second, injection through a simple nozzle resulted in a

smaller droplet size at lower flow rates (1.8 gallons per minute to 2.4 gallons per minute). Increase in the air stream velocity to 450 feet per second caused a uniform droplet size at all wax flow rates (from 1.8 gallons per minute up to 3.2 gallons per minute).

With injection through the corkscrew nozzle, a decrease in droplet size was noted with injection of wax into low velocity air streams (250-350 feet per second), from a flow rate of 1.8 gallons per minute up to 2.8 gallons per minute, and then further increase up to 3.2 gallons per minute caused a slight increase in the particle mean diameter. Increasing the air stream velocity to 400 feet per second resulted in a uniform particle mean diameter at all flow rates.

Consequently, from a droplet size of view, increasing present oil rates should not prove detrimental to combustion efficiency i.e. the particle mean diameter would not increase to a stage where evaporation and combustion time would be insufficient to burn the oil.

- (6) The injection angle which proved to be most successful in this study was 15° , since a more uniform spray was formed sooner. This is despite the fact that a smaller droplet size resulted with injection at 90° . However, impaction of wax was greater at 90° than at 15° .
- (7) Injection of molten wax at 3.2 gallons per minute flow rate into the air stream of varying velocities proved that injection into an air stream of 450 feet per second (435 feet per second

relative velocity) through both nozzles (simple and corkscrew) resulted in a particle mean diameter of 45 microns and 39 microns respectively. Even at the relatively low air stream velocities used in this study, both nozzles produced a droplet size which fell within the size range of 25 microns to 45 microns as specified by Heynert for satisfactory combustion. Thus, with an air stream velocity of, say, 550 feet per second, which seems to be an average wind velocity in current blast furnace practice, a droplet size suitable for good combustion is produced.

- (8) Impaction of the injected wax was seen to be greatest at the low air velocities, and increased with increase in the angle of injection from 15° up to 90° . Increasing the velocity of the air stream to 350 feet per second caused a uniform spray distribution of the injected wax from the corkscrew nozzle, at an injection angle of 15° . A uniform spray distribution of the wax was not achieved with the simple nozzle until an air stream of 450 feet per second velocity was attained.
- (9) The effect that secondary atomisation plays in the process of fuel injection can be seen from the computed trajectories of droplets within the blow pipe. With injection at 3.2 gallons per minute, the computed sheet velocity of 30 feet per second is seen to be such that at all velocities above 450 feet per second, the effective 'zone of atomisation' i.e. that between the trajectories of 100 microns particles on either side of the axis of the blow pipe, was narrow, and if no secondary atomisation were to take place, then oxygen starvation of the spray would result in soot formation.

Increasing the spray sheet velocity to 70 feet per second results in a wider 'zone of atomisation'. However, it is felt that such a spray sheet velocity is, at present, unobtainable in blast furnace practice.

- (10) In a comparison of the benefits of the corkscrew nozzle and the simple nozzle for oil injection, it can be stated immediately that based on results obtained in this study, there is no benefit to be derived for the use of the corkscrew insert if the particle mean diameter of the spray is to be the sole criterion. Where the corkscrew nozzle does have an advantage is in the formation of a uniform spray distribution within the blow pipe. Because the exiting spray is in the form of an extremely thin sheet, it is immediately disrupted by the passage of a high velocity air stream, and since the sheet of liquid is a hollow cone, the droplets are already well dispersed within the blow pipe when secondary atomisation begins. With the simple nozzle, the initial 'zone of atomisation' is narrow and it is the effects of secondary atomisation which cause dispersion of the spray.

The corkscrew nozzle is relatively simple in design and inexpensive to construct, and in plant trials, has been found to have as long an operational life as a simple lance. Because of the advantage of spray distribution, it is felt that further plant trials should be undertaken so that the full potential of the corkscrew nozzle as an aid for improved fuel oil injection can be more fully investigated.

APPENDIX 1

Computation of Spray Sheet Velocities

Consider a flow rate of 3.2 gallons per minute through the lance, the exiting sheet having a cone angle of 43° .

The initial velocity of the spray sheet can be found by the use of the relationship

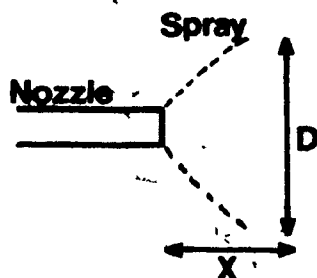
$$Q = AU$$

where

Q = Flow rate of fluid, gallons per minute

A = Area of spray

U = Velocity of sheet



D is the diameter of the hollow cone at distance X from the nozzle

Consider a horizontal distance of 0.1 cms. from the exit orifice of the lance. Therefore, the total diameter of the cone at this point is $2 \times 0.1 \tan 43 + 2.54/4$ cms., where $2.54/4$ is the inside diameter of the nozzle.

Therefore, cone diameter 0.1 cms. from the lance = 0.655 cms.

Now consider the sheet to have a thickness of 0.15 cms.

$$\begin{aligned}\text{Area of sheet} &= \frac{\pi}{4}(0.655)^2 - \frac{\pi}{4}(0.355)^2 \\ &= \underline{0.238} \text{ cms.}^2\end{aligned}$$

Now $Q = 3.2$ gallons per minute = 200.5 cms.^3 per second

$$U = \frac{200.5 \text{ cms. per second}}{0.238}$$

$$= \underline{843} \text{ cms./second}$$

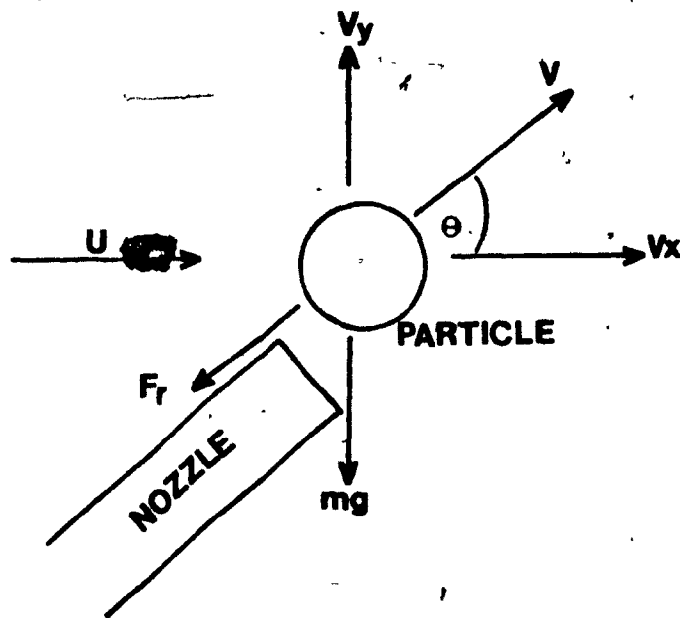
$$= \underline{28.1} \text{ feet/second}$$

Application of this relationship can be used to obtain the spray sheet velocities presented in Fig. 47.

APPENDIX 2

Computation of Particle Trajectories

Consider



where

U = Air Velocity

V = Particle Velocity

V_y = Velocity of Particle in Y -Direction

V_x = Velocity of Particle in X -Direction

F_r = Resultant Friction Force

Consider the angle of injection to be 15° , with an exiting cone angle of 43° .

Thus, $\theta = 58^\circ$

Sum of Forces in X-Direction

$$F_x = ma = -F_r \cos$$

$$V \rho_p a = -\frac{1}{2} \rho_a V_{res}^2 A f_D \cos$$

ρ_p = Density of Particle

ρ_a = Density of Air

f_D = Coefficient of Friction

V_{res} = Resultant Relative Velocity of Particle

$$\frac{\pi D^3}{6} \rho_p \frac{dU_x}{dt} = -\frac{\pi D^2}{8} \rho_a V_{res}^2 f_D \cos$$

D = Particle Diameter

$$\text{Thus, } \Delta U_x = -3/4 \frac{\rho_a \cos \theta}{\rho_p D} f_D \Delta t V_{res}^2$$

$$\text{Thus, } U'_x = U_{x_0} - 3/4 \frac{\rho_a \cos \theta}{\rho_p D} f_D \Delta t V_{res}^2$$

U_{x_0} = Wind Velocity - Initial Particle Velocity in X-Direction

$$= U - V \cos$$

$$= V_{rel} \cos$$

V_{rel} = Relative Velocity

f_D can be found from the tables presented in Ind. Eng. Chem. 1940, pages 605 - 621 (Particle Trajectories) with a knowledge of $N_{Re} = \frac{D \rho_a V_{rel}}{\mu_a}$

Sum of Forces in Y-Direction

$$F_y = ma = -mg - F_r \sin$$

Neglect Bouyancy Term

$$V \rho_p \frac{dU_y}{dt} = -V \rho_p g - \frac{\pi D^2}{8} \rho_a V_{res}^2 f_D \sin \theta$$

$$\frac{\pi D^3}{6} \rho_p \frac{dU_y}{dt} = -\frac{\pi D^3}{6} \rho_p g - \frac{\pi D^2}{8} \rho_a v_{res}^2 f_D \sin \theta$$

Thus,
$$\frac{dU_y}{dt} = U_{y_0} - g \Delta t - \frac{3}{4} \frac{\rho_a}{\rho_p} \frac{\sin \theta}{D} f_D v_{res}^2$$

$$U_{y_0} = v_{rel} \sin \theta$$

The distance travelled by a particle of diameter D, in time interval t, can be found from

$$S_x = \frac{U'_x + U_{x_0}}{2} \Delta t$$

$$S_y = \frac{U'_y + U_{y_0}}{2} \Delta t$$

Based upon these relationships, the trajectories of particles of known diameter can be computed, a typical programme being shown overleaf.

COMPUTER PROGRAMME FOR COMPUTATION OF PARTICLE TRAJECTORIES

```
0001 /LOAD WATFIV
0002 WRITE(6,7)
0003 7  FORMAT( , 'TOTAL TIME', 5X, 'X-INCREMENT', 5X, 'Y-INCREMENT')
0004 U=13500.
0005 V=900.
0006 VY=777.
0007 VX=484.
0008 THETA=1.036
0009 UX=13016.
0010 VRE=13039.
0011 F=0.45
0012 PA=0.001145
0013 PB=0.98
0014 D=0.01
0015 T=0.00001
0016 TT=0.0
0017 5  K=((3./4.*PA/PB*F/D*COS(THETA)*(VRE**2.)))*T
0018 UX=UX-K
0019 SX=((2.*VX+K)/2.)*T
0020 VX=VX+K
0021 KY=K*(SIN(THETA)/COS(THETA))
0022 SY=((2.*VY-KY)/2.)*T
0023 VY=VY-KY
0024 THETA=ATAN(SY/SX)
0025 IF(SX.GE.50.0) GO TO 6
0026 IF(SY.GE.10.0) GO TO 6
0027 IF(COS(THETA).EQ.1.0) GO TO 6
0028 TT=TT+T
0029 WRITE(6,8)TT,SX,SY
0030 8  FORMAT( , F8.5, F8.2, F8.2)
0031 GO TO 5
0032 6  STOP
0033 END
```